Sludge-derived biochar: Physicochemical characteristics for environmental remediation FREE

Neelaambhigai Mayilswamy ; Amrita Nighojkar ; Mohan Edirisinghe ; Senthilarasu Sundaram ;
Balasubramanian Kandasubramanian ✉

Check for updates

View Online

Export Citation

CrossMark

AIP Publishing

Sludge-derived biochar: Physicochemical characteristics for environmental remediation

View Online   Export Citation   CrossMark

Neelaambhigai Mayilswamy,[1] (iD) Amrita Nighojkar,[1] (iD) Mohan Edirisinghe,[2] (iD) Senthilarasu Sundaram,[3] (iD)
and Balasubramanian Kandasubramanian[1,a] (iD)

AFFILIATIONS

[1]Nano Surface Texturing Lab, Department of Metallurgical and Materials Engineering,
Defence Institute of Advanced Technology (DU), Pune, India
[2]Department of Mechanical Engineering, University College London, United Kingdom
[3]School of Engineering and the Built Environment, Edinburgh Napier University, Edinburgh, United Kingdom

[a]Author to whom correspondence should be addressed: meetkbs@gmail.com

ABSTRACT

The global production of fecal wastes is envisioned to reach a very high tonnage by 2030. Perilous handling and consequential exposition of human and animal fecal matter are inextricably linked with stunted growth, enteric diseases, inadequate cognitive skills, and zoonoses. Sludge treatment from sewage and water treatment processes accounts for a very high proportion of overall operational expenditure. Straightforward carbonization of sludges to generate biochar adsorbents or catalysts fosters a circular economy, curtailing sludge processing outlay. Biochars, carbonaceous substances synthesized via the thermochemical transformation of biomass, possess very high porosity, cation exchange capacity, specific surface area, and active functional sorption sites making them very effective as multifaceted adsorbents, promoting a negative carbon emission technology. By customizing the processing parameters and biomass feedstock, engineered biochars possess discrete physicochemical characteristics that engender greater efficaciousness for adsorbing various contaminants. This review provides explicit insight into the characteristics, environmental impact considerations, and SWOT analysis of different sludges (drinking water, fecal, and raw sewage sludge) and the contemporary biochar production, modification, characterization techniques, and physicochemical characteristics, factors influencing the properties of biochars derived from the aforestated sludges, along with the designing of chemical reactors involved in biochar production. This paper also manifests a state-of-the-art discussion of the utilization of sludge-derived biochars for the eviction of toxic metal ions, organic compounds, microplastics, toxic gases, vermicomposting approaches, and soil amelioration with an emphasis on biochar recyclability, reutilization, and toxicity. The practicability of scaling up biochar generation with multifaceted, application-accustomed functionalities should be explored to aggrandize socio-economic merits.

Published under an exclusive license by AIP Publishing. https://doi.org/10.1063/5.0137651

NOMENCLATURE

a (m^2 m^{-3})	Specific packing area
a'	1.035 (constant)
A	Filtration area
AFR	Air flow rate
Al_2O_3	Aluminum oxide
AO_7	Acid orange 7
Ar	Argon
A_T (l mg^{-1})	Equilibrium binding constant
A_t (m^2)	Area of the cooling coil
B	Slope of line
b'	Adsorption energy constant
B300	Biochar obtained by pyrolysis at 300 °C
B500–700	Biochar obtained by pyrolysis at 500–700 °C
BC	Biochar
BC-700 K	Sewage sludge-based biochar produced at 700 °C
BET	Brunauer, Emmett, and Teller analysis
BJH	Barrett, Joyner, and Halenda method
Boa	Bodenstein number (ratio of convective to diffusive fluid transport rate)
BPA	Bisphenol A
b_T	Temkin model heat adsorption constant
C	Initial concentration of adsorbate
C'	Boundary layer thickness
C''	Concentration of solids
CH_4	Methane
CIP	Ciprofloxacin

c_e (mg l^{-1})	Equilibrium adsorbate concentration
C_{BET} (l mg^{-1})	BET isotherm model correlating with the surface interaction energy
C_0 (mg l^{-1})	Initial metal ions concentration
CaO	Calcium oxide
CIP	Ciprofloxacin
CO	Carbon monoxide
CO_2	Carbon-dioxide
c_{pf} (kcal/ kg°C)	Specific heat coefficient of fluid
c_s (mg l^{-1})	Monolayer saturation adsorbate concentration
CST	Capillary suction time
d (m)	Diameter of particulate solid
D	Dosage of adsorbent
D_{ea}	Dispersion coefficient along the radial direction
DNA	Deoxyribonucleic acid
DOC	Dissolved organic carbon
DOX	Doxycycline
dH	Heat of evaporation
d_P (m)	Pellet diameter
DSS	Dewatered sewage sludge
DWS	Drinking water sludge
EDS	Energy dispersive spectroscopy
ENR	Enrofloxacin
Fe^0	Zero-valent iron
$Fe(NO_3)_3 \cdot 9H_2O$	Ferric nitrate
Fe_3O_4	Iron oxide
FiBR	Fixed bed reactor
FlBR	Fluidized bed reactor
FTIR	Fourier transform infrared spectroscopy
G (kg m^{-2} s^{-1})	Specific mass flow
g (m s^{-2})	Acceleration due to gravity
g_c [kg m (kgf s^2)$^{-1}$]	Dimensional constant
H (m)	Reactor height
H160	Hydrochar obtained by pyrolysis at 160 °C
H180–200	Hydrochar obtained by pyrolysis at 180–200 °C
H_2	Hydrogen
H_2O_2	Hydrogen peroxide
H_2S	Hydrogen sulfide
H_3PO_4	Orthophosphoric acid
HAP	Hydroxyapatite
HAZOP	Hazard and operability analysis
HC	Hydrochar
H_{loss}	Summative heat losses from the gasifying unit
HNO_3	Nitric acid
HR	Heating rate
HTC	Hydrothermal carbonization
IFR	Inflow rate
IPD	Intra-particle diffusion model
K	Compressibility coefficient
k_{fd}	Rate constant of the film diffusion model
k_i [mg (g min$^{1/2}$)$^{-1}$]	IPD model rate constant

29 August 2023 15:25:40

k_{LF}	Equilibrium heterogeneous solid constant
KOH	Potassium hydroxide
k_R (l g^{-1}), a_R (l mg^{-1})	Redlich–Peterson isotherm model constants
k_1 (g mg^{-1} min^{-1})	PFO rate constant
k_2 (min^{-1})	PSO rate constant
K_2CO_3	Potassium carbonate
L (m)	Length of reactor
La-SSBC	Lanthanum-loaded sewage sludge biochar
La-SSBC-P	Phosphate-integrated lanthanum decorated sewage sludge-based biochar
m, k_s (l mg^{-1})	Sips isotherm constant
m_0	Amount of moisture desiccated
M(g)	Mass of adsorbent
MB	Methylene blue
MBC	Magnetic biochar
MgO	Magnesium oxide
M_{LF}	Heterogeneity parameter
$MnCl_2$	Manganese (II) chloride
MnO_x	Manganese oxide
MO	Methyl orange
MOC	Material of construction
n, k_F (mg g^{-1} (l mg^{-1})$^{1/n}$)	Freundlich isotherm constants incorporating all parameters influencing the sorption intensity and efficiency, respectively
N_2	Nitrogen
NH_4OH	Ammonium hydroxide
NOR	Norfloxacin
N-SSBC	Nitrogen-doped sewage sludge biochar
NP	Nanoparticle
O_2	Oxygen
OUR_{max}	Optimum oxygen rate in activated sludge systems generating sludge for digestion
OUR_{meas}	Oxygen uptake rate estimated in sludge subjected to digestion
$P20$	Biochar sample containing 20 mg g^{-1} phosphorous
$P4$–60	Biochar sample containing 4–60 mg g^{-1} phosphorous
Pe_a	Peclet number (ratio of convective to conductive heat transfer in fluids)
PFO	Pseudo-first-order reaction
PMS	Peroxymonosulfate
PSO	Pseudo-second-order reaction
P_s	Percentage volume utilized by sludge subsequent to 30 min of settling period
P_x	Percent of solids suspended in mixed liquor specimen
Q	Heat involved in the evaporation of water or organic substances
$Q = -UA_t(T-T_c)$	Term contributes to heat transfer rate due to heat flow

q_e (mg g^{-1})	Equilibrium adsorption capacity
$q_m = q_{max}$ (mg g^{-1})	Maximum sorption capacity
q_s (mg g^{-1})	Theoretical saturation capacity
q_t (mg g^{-1})	Quantity of adsorbate adsorbed at time "t"
Q_{LFM} (mg g^{-1})	Maximal adsorption capacity
$Q_t/Q_e = F$	Fractional achievement of equilibrium at time "t"
Q_0	Adsorption efficiency constant
R	Universal gas constant
R (%)	Removal efficiency
R_A	Rate of reaction
RB	Rhodamine B
RB4	Reactive Blue 4
RB5	Reactive Black 5
R_c'	Constant describing SRF of cake for head loss $=1$
Re	Reynolds number (Used to anticipate the fluid flow patterns: Lower Re is characterized by laminar flow transiting to turbulent flow at higher Re)
R_0	SRF at $k=0$
RS	Raw sewage sludge
S3W7	Biomass comprising 30% sewage sludge and 70% pine sawdust pyrolyzed at 700 °C
Sc	Schmidt number (ratio of kinematic viscosity to mass diffusivity)
SDG	Sustainable development goal
SEM	Scanning electron microscopy
SiO_2	Silicon dioxide
SO_2	Sulfur dioxide
SRF	Specific resistance to filtration
S_s	Percent sludge stability
SS	Sewage sludge
SSBC	Sewage sludge-based biochar
SSBC-P	Phosphate-incorporated sewage sludge biochar
SVI	Sludge volume index
SWOT	Strength, weakness, opportunities, threat analysis
t	Time
t_r	Reaction time
t_s	Reactor shut-down time
T(°C)	Absolute temperature/system temperature
T_c(°C)	Cooling water temperature
TC	Tetracycline
TCE	Trichloroethylene
u (m s^{-1})	Fluid velocity
U (W/m^2°C)	Overall heat transfer coefficient
U_{mf} (m s^{-1})	Minimum fluidization velocity
UNICEF	United Nations International Children's Emergency Fund
US EPA	US Environmental Protection Agency
v (m s^{-1})	Interstitial fluid velocity
V (L)	Volume of solution

29 August 2023 15:25:40

V_b (m³)	Batch reactor volume
V_{OC}	Settled sludge volume
WCA	Water contact angle
XPS	X-ray photoelectron spectroscopy
XRD	X-ray diffraction
X_{SS}	Mixed liquor suspended solids concentration
α (mg g⁻¹ min⁻¹)	Initial sorption rate
β	Desorption constant
β' (mol² kJ⁻²)	BET isotherm model constant associated with sorption energy
ΔH_A (J/kmol)	Enthalpy change of reaction per mole of A
ΔH_R^0	Heat of reaction at standard pressure and temperature
ΔH_{out}^T	Latent and sensible heat of exit gases from ambient temperature (25 °C) to gasification temperature, T
ΔP (kPa)	Pressure drop across the reactor
ΔP	Pressure difference
ε (kJ mol⁻¹)	Adsorption potential
ε'	Dielectric constant (capability of substance to undergo polarization in an external electric field)
ε''	Dielectric loss (efficient loss that quantizes effective transformation of microwave energy into heat)
$\varepsilon*$	Complex dielectric constant
$\in$	Void fraction of bed
$\lambda_{af}, \lambda_{as}$ (kcal/ kg m°C)	Axial thermal conductivities of fluid and solid
λ_e (kcal/ kg m°C)	Effectual axial thermal conductivity of reactor
λ_f (kcal/ kg m°C)	Fluid thermal conductivity
μ (kg m⁻¹ s⁻¹	Dynamic viscosity of water
μ''	Dynamic viscosity of filtrate
ρ, ρ_s (kg m⁻³)	Specific weight of water and solid
ρ_f (kg m⁻³)	Density of fluid
$\sum m_j c_j$	Summation of heat capacities of all reactor components and the reaction mixture
$(\Sigma m_j c_j)\frac{dT}{dt}$	Heat accumulation rate
χ	Number of moles of reactant converted per unit volume
χ'	Filterability constant
ω	Mass of suspended dry solid matter obtained per unit volume of filtered sludge water
$\varnothing$	Dimensionless parameter
5S@Fe-500	Mass ratio of sludge and Fe(NO₃)₃.9H₂O–5:1 and calcined at 500 °C
$(-\Delta H_A)V_b R_A$	Accounts for heat transfer rate due to chemical reaction

I. INTRODUCTION

With accelerated urbanization and industrial expansion, enormous quantities of sludge-based waste have been engendered over the preceding decades.[1] Sludge is comprehended as comprising particulates agglomerated as flocs that function as hydrodynamically distinct particles obtained as a derivative of diverse methodologies, including agriculture, water purification plants, sand, and coal washery plants, sewage treatment plants, and on-site sanitary systems.[2] Sewage sludge generated as an ancillary product in wastewater treatment facilities comprehends over 80% water, an extensive array of transition metal ions (like nickel, iron, cobalt, etc.), biological macromolecules, inorganic (Al₂O₃, CaO, MgO, SiO₂, etc.), and organic compounds (carbohydrates, cellulose, lignin, lipids, and phenolics), pathogens, and a higher proportion of phosphorous, and nitrogen, inflicting detrimental impacts to the environmental and human health post disposal. Post-drying sewage sludge encompasses 0.5%–2.5% phosphorous, 3%–4% nitrogen, 50%–70% organic matter, and additional micronutrients like copper and zinc.[3,4] As an illustration, the greater content of heavy metal ions present in sewage sludges could induce subterranean water and soil pollution attributable to potential hazards of leaching.[5,6] The worldwide sludge generation on a diurnal basis surpasses 10 000 tonnes, and a conventional water treatment system yields around 1 00 000 tonnes of sludge annually.[7] The global production of fecal wastes (constituting human feces and animal fecal biomass) accounted for around 3.9×10^{12} kg/year in 2014 and is envisioned to reach 4.6×10^{12} kg by 2030. Perilous handling and consequential exposition of human and animal fecal matter are inextricably linked with stunted growth, enteric diseases, inadequate cognitive skills, and zoonoses, respectively.[8]

Consequently, the treatment of various sludges and their reusability recently turned into a research hotspot.[9] Progression of economic, facile, and green strategies is essential to fulfilling the stringent policy demands. Some ubiquitous sludge treatment strategies in developing nations, including incineration and landfilling, entailed inexpedient secondary pollution.[10] Sludge handling expenditures account for almost 40%–50% of the total effluent treatment outlays and is also a time-sapping process entailing the utilization of sophisticated machinery. Hence, sludge treatment, reclamation, and disposition should be administered economically, considering federal regulations. The U.S. Environmental Protection Agency's (EPA) 40 code of federal regulations aimed at ascertaining safe usage and disposal of sewage sludge innocuous to humankind and the surroundings.[11] The aforestated pernicious effects of sludges can be alleviated through reuse by employing various approaches like using them as constructional materials,[12] feedstock for cement manufacturing,[13] fabricating barrier coatings for refuse heap, and production of bio soils on amalgamation with stabile organic constituents of communal refuse,[14] the pyrolytic transformation of sludge into bio-crude, synthesis gas, and a rigid char by-product delineated as biochar[15] and sustainable materials engineering practice.[16]

Biochar is a pyretic carbonous matter acquired by the thermo-chemical transformation of biomass in an oxygen-deficient atmosphere.[17] Attributable to greater surface area and porousness, facile amendment strategies, cost-effective synthesis, and easy accessibility, biochar is used in an extensive array of applications spanning from carbon sequestration and soil amendment to effluent treatment. Biochar could be generated from various feedstock substances, including municipal refuse, factory waste, and agrarian derivatives.[18] They are bestowed with a plentitude of active sorption sites containing –COOH, –OH, -C=C–, –C–C–, mineral crystalline phases, distinct

oxygen comprising functional moieties, and aromatic carbon frameworks engendering them as multifaceted sorbents.[19] Unmodified biochars exhibit reduced adsorption efficiency toward contaminants, while modified biochars activated chemically or physically enhance various physicochemical characteristics, including functional layer moieties, surface area, and pore structure functioning as substitutes for conventional carbonous adsorbents (graphene,[20–22] activated carbon,[23] and carbon nanotubes).[18]

Generation of biochar from sludge-based biomass feedstock bequeaths to sustainable development goal 12 and expedites zero-waste and a wastewater-based circular economy through the explicit carbonization of sludges to yield biochar catalysts or adsorbents, thereby mitigating environmental liabilities. The conversion of sludges into biochar solves two key challenges synchronously by depreciating disposal costs while abetting as an asset competent for eliminating various contaminants from wastewater.[24] Additionally, biochar obtained by the thermochemical transformation of sludge-based biomass has been employed in soil amelioration in myriad ways ascribable to the adsorption of toxic metal ions, pesticides, and refinement in soil structure and quality and its biological characteristics, enhancement in agricultural produce while endowing to carbon sequestration.[25]

The world population growth is anticipated to increase to 10.4 $\times 10^9$ by 2100 in concordance with the United Nations survey[26] eliciting the requisites for water to augment by almost 60% in the forthcoming years.[27] Accruing water demand is directly congruous with a multitude of factors like economic advancement, growing population, and variable usage patterns.[28] As per the UNICEF data, in 2020, 5.8 $\times 10^9$ people had access to securely handled potable water facilities, while 771×10^6 people were devoid of the primitive standard of amenities necessitating the prospection of freshwater resources and the establishment of efficacious water conditioning and circulation mechanisms.[29] By 2025, it is envisaged that around 1.8×10^9 people will have sustenance in nations with unmitigated water deficiency and two-thirds of the globe will be subjected to water-stressed circumstances.[30] Anthropogenetic wastewater generation and the contagiousness of surface water bodies and soil expedites pernicious repercussions on ecological and human health attributable to the depletion of biodiversity and groundwater pollution contributing to the climate change crisis.[31] Traditional water treatment plants embody a multi-stage process comprising coagulation and flocculation, sedimentation, clarification, percolation, sterilization, and disinfection.[32] The characteristics and amount of sludge generated from the treatment stations rely on the water purification technique employed, quality of influent and the water desired at the consumers' end, and type and dosage of adsorbents employed, and it contains differing amounts of chemical elements, microbes, coagulants, and suspended and primal material.[7] Even though customary wastewater treatment facilities serve as an indispensable sanitation barrier, they imbibe around 3% of the global electricity, thereby serving as one of the prodigious greenhouse gas emitters and power consumers.[33,34] In this context, sludge-based biochar has sprouted as a denouement to environmental remediation; the transformation of sludge-based waste into biochar fosters the "waste to adsorbent" approach along with serving as a soil amending agent, and mass production of biochar is propitious as it generates revenue in lieu of disbursements while addressing the concerns inextricably linked to sludge management.[35]

The past five years corroborated an intensification in the number of review articles on biochar, encompassing quintessential subjects like the utilization of co-pyrolysis technique to augment the functionalism of sewage sludge based-biochar and immobilization of toxic metal ions,[36] hydrothermal carbonization of plausible biomass residue along with the environmental applications of the synthesized hydrochar,[37] degeneration of organic contaminants from the water via biochar-fostered advanced oxidation technique,[38] bioremediation of antibiotics,[39] eviction of contaminants employing advanced oxidation technique and adsorption by sludge-derived biochar,[40] the prognosis of biochar and its composites in persulfate-advanced oxidation method,[41] Fenton-like process for effluent treatment,[42] adsorbents for eliminating dyes from aqueous media[43] and soil remediation.[44] Contemporary reviews enshrouding the generation of sewage sludge and its disposition concern, the synthesis, characterization, modification, and activation strategies of sludge-derived biochar, and the utilization of the aforementioned biochar as adsorbents for the elimination of heavy metal ions, metalloids, dyes, and phenolic moieties, and in catalysis, advanced oxidation processes, solid biofuel generation, role in agronomy, toxicity assessment, and consequences on climatic variations[45–49] serve as a compendium for eventual progress in their domain; analogously this study endeavors to impart a meticulous description of methodologies that can be endorsed for environmental remediation considering the sustainable development goals employing sludge-based biochar. We have comprehensively congregated the latest advances in drinking water, fecal, and raw sewage sludge-based biochar for environmental remediation and explicated cutting-edge biochar synthesis methodologies including electron and gamma-beam irradiation against the traditional methodologies customarily employed. Advancements in engineered design and customization of chemical reactors involved in sludge-based biochar production have stimulated fresh outlooks on application-orientated effluent treatment, soil amelioration, and toxic gas adsorption, possessing varied specific necessities, entailing a review on biochar derived from the aforementioned sludges for environmental remediation. The present review is the first that analytically contemplates biochars derived from drinking water, fecal, and raw sewage sludge as a renewable means to promote a circular economy in waste management for the adsorption of heavy metal ions, antibiotics, microplastics, toxic gases, catalytic degradation of organic compounds, vermicomposting, and soil amelioration leading to enhanced plant growth. This work also recapitulates the characterization, SWOT analysis, and environmental impact considerations of the aforestated sludges comprehending the designing of various chemical reactors (fixed bed reactor, batch reactor, and fluidized bed reactor) involved in biochar production along with the factor of safety design considerations in reactors. We highlight the relationship between various physicochemical properties, biochar characterization, modification strategies, and factors implicating the characteristics of sludge-based biochar for environmental remediation. Furthermore, adsorption kinetic studies rendering details about mass transfer mechanisms, adsorption rate and performance, and categorization of isotherm models predicated on the number of parameters, and their physical meanings imparting adsorption information incorporating adsorption mechanisms involved and utmost adsorption capacities, along with their significance and corresponding mathematical equations are also presented. Finally, we articulate biochar recycling, and reutilization studies to annihilate

29 August 2023 15:25:40

secondary pollutants along with a description of its toxicity assessment.

II. GENERATION, CHARACTERISTICS, AND ENVIRONMENTAL IMPACT CONSIDERATIONS OF VARIOUS KINDS OF SLUDGES

A. Drinking water sludge

Drinking water sludge (DWS) is an entailment of flocculation and coagulation techniques employing trivalent iron (Iron (II) sulfate, Ferrous chloride, Iron trichloride hexahydrate) or aluminum-based salts (aluminum sulfate octadecahydrate) accumulated as a suspended solidified matter resulting from the precipitation reactions of humus, algal matter, colloidal and clay precipitates extant in freshwater resources.[50–52] Colloidal contaminants in the feed water are evicted through charge neutralization, sweep coagulation process, and sorption through hydroxide-based precipitates. The residual moisture level of wet sludge usually exceeds 80 wt. %.[52] The constitution of DWS differs in contingence with the type of coagulating agent employed and water resources being processed.[51] Straightforward lagoon sludge treatment involves an abatement in the total proportion of sludge being processed, succeeded by disposition as landfilling. Utilizing sand drying beds is another permissible approach that encompasses the dewatering of sludges from clarifying units or sedimentation tanks for consequential landfilling.[2] Although the aforestated techniques are economical and facile, they do not serve as persistent adequate findings owing to the plausible pollution of soil and water reserves through the chemical substances employed in the process and toxic metals (cadmium, nickel, lead, etc.) exuded through sprouting industrial manufacturing plants.[51,52] Hence, researchers are emphasizing the advancement of renewable sludge handling methodologies compliant with the strict environmental regulations focusing on the reutilization of the disposed refuse.[52]

B. Fecal sludge

Roughly around 31% of the population residing in developing nations rely on incompetent sanitary facilities and disposition of fecal sludge (FS)-derived wastes.[53] Human feces, including flushing water, urine, communal litter, and greywater, are conventionally discarded within cesspits, latrine pits, or catch basins in regions devoid of efficacious sewerage networks incorporating in-house wastewater processing facilities.[54,55] The conglomerated FS is intermittently withdrawn from the septic tanks and released into terrains and trenches in its vicinity.[55] Septage obtained from on-site sanitation systems is exemplified by a black color and tends to be obnoxious owing to the emanation of various gases like hydrogen sulfide precluding proper digestion through prolonged storage. The peculiarities of FS are surpassingly inconstant owing to the variance in sludge repository methodology, retention period, and temperature. The sludge can be subjected to desiccation within perforated beds when dispersed as fine layers; nevertheless, malodors are anticipated during the dewatering step until it undergoes proper digestion.[2] FS predominantly comprises pathogenic and organic impurities ten folds greater than that present in municipal refuse, and in order to circumvent critical health concerns like helminth disease, diarrhea, etc., and other ecological hazards, it is inexpedient for application in the irrigation field.[55,56] Conventional techniques associated with fecal sludge treatment include composting, drying beds, digestion, and developed marshlands, albeit the ecological

concerns are not addressed remuneratively.[55] Within the framework of municipal sewage, even though FS is a principal factor inducing contamination, it possesses various nutrients (magnesium, potassium, carbon, phosphorous, nitrogen, and selenium) capable of reprocessing as anthropic fertilizers by virtue of appropriate accumulation, handling, and sanitary techniques.[53,57] Researchers are exploring sustainable remedies against illegitimate disposals through thermochemical transformation techniques and the plausibility of biochar generation for efficaciously processing FS and yielding biofuel.[56]

C. Raw sewage sludge

Raw sewage sludge (RS) accounts for the sedimentary refuse comprising solubilized or particulate matter of inorganic or organic substances emanating through effluent treatment. Contingent upon the processing approaches utilized, RS can exist as a semi-fluidic or liquified substance constituting around 2–8 wt. % solids.[2] In terms of dry matter content, it comprises organic compounds spanning from 35% to 65%, while the remnants account for incombustible ash. It is acquired from immense quadrangular or circular sedimentation tanks permitting the residence of denser materials underneath, which are eventually scooped out through inbuilt sludge scrapers toward subaqueous ducts. The dense slurry deposited is then siphoned to the sludge repository and processing section for subsequent treatment. RS can also be congregated through tertiary or secondary sedimentation tanks. RS present in the sludge repository is subjected to consequential physical, biological, and chemical treatments in order to abate the total water content and annihilate the possible menaces (such as the existence of harmful pathogenic bacteria, toxic metals, and generation of obnoxious odor and volatile gases during decomposition of organic content) associated with it. Conventional RS processing methodologies encompass thermal hydrolytic approaches, prefatory treatments, thickening, stabilizing, clarification, dewatering, desiccation, and calefaction.[58]

Figure 1 elucidates the advantages, shortcomings, and opportunities for subsequent breakthrough research along with the risks associated with drinking water, fecal, and raw sewage sludges investigated via the SWOT analysis.

D. Sludge characterization criteria

Sludge processing is predominantly governed by multifarious parameters, including specific resistance to filtration, sludge stability, compressibility coefficient, capillary suction time regulating sludge settling, coagulation, dewatering properties, and sludge volume index relating to sludge digestion and stabilization. Table I enlists the prominence of various sludge characterization parameters along with their mathematical expressions.

III. SLUDGE BASED BIOCHAR

Sludge management systems entail exorbitant costs arraying from 20% to 60% of the overall operational costs associated with sewage treatment plants. Incineration or landfilling of sludge-based wastes might engender secondary pollution leading to lowered ecological sustainability. In addition to dewatering improvement, the straightforward thermochemical transformation of sludges to generate biochar adsorbents or catalysts fostering circular economy has acquired considerable attention over the decades, mitigating environmental

SWOT ANALYSIS OF SLUDGES

STRENGTHS

A-1. Contains low organic carbon and heavy metal ion content.
2. Good feedstock for synthesizing high-grade biochar and hydrochar.

B-1. Absolute annihilation of pathogens.
2. Biochar obtained from FS ameliorates soil physicochemical characteristics.

C-1. Application of sewage sludges in cropland bestows vital nutrients for plant growth and lowers the environmental impact considerations that restrain incineration or landfilling.

WEAKNESSES

A- 1. Entrapment of organic matter and microbes during coagulation covering the surface adsorption sites.
2. Odour and secondary pollution issues.
3. Reduced adsorption efficiency.

B-1. Objectionable odours expected during draining stage unless sludge is well-digested.
2. Improper management of FS - detrimental impact on human and environmental health from soil, groundwater contamination, and eutrophication.

C-1. Lower adsorption capacity constraining their functionalities and porosity, necessitating physical and chemical modification strategies.

OPPORTUNITIES

A- 1. Apart from usage as adsorbents for removal of dyes, toxic metal ions, they can be used in building and construction materials.

B- 1. FS- derived biochar can be employed in soil amendments, fuel, adsorption media, carbon sequestration.

C- 1. Sewage sludge-derived biochar can be used in catalysis, gas storage materials, adsorption and soil amelioration.

THREATS

A-1. Phosphorous deficiency, aluminium toxicity, soil acidification should be addressed.

B- 1. Long-term impact on FS-derived biochar recalcitrance on nutrient release and heavy metal ion retention should be considered.

C-1. Bioavailability of sludge-borne toxic metal ions is intensified with sustained usage.

FIG. 1. SWOT (Strengths, weakness, opportunities, and threats) analysis of A-drinking water sludge (DWS), B-fecal sludge (FS), and C-raw sewage sludge (RS).

concerns and endowing sustainable development goal 12: SDG12 (responsible production).[62]

A. Circular economy in waste management

Sludge processing and elimination approaches are crucial for ecological sustainability ascribable to organic and inorganic contaminants and pathogenic microbes engendering health concerns, thereby necessitating elimination.[63] Concurrently, they entail large amounts of energy and concomitant ecological implications, the expenditures associated with sludge management typifying proximately 50% of the overall operational-cost of wastewater treatment facilities.[64] Dumping of sludge-based wastes is liable for almost 40% of the carbon emissions from the treatment plants; this proportion could be abated by the application of circular economy principles.[65] The circular economy principle originated as a substitute for the "Take-make-dispose" (linear) economic paradigm predicated on the standards of cradle-to-grave, biomimicry, blue economy, industrial ecology, looped and performance economy, and regenerative design.[66] The circular economy is a robust industrial network that deputizes the "end of life" conception with a transposition toward the utilization of sustainable energy sources, eradicating the usage of noxious substances that debilitate reutilization, and endeavors waste disposal by employing superior design of materials, systems, etc., thereby scheming to maintain products at their unparalleled utility invariably.[67] Attributing to legislation restricting land application and landfilling as sludge disposition strategies, several investigators have assayed recycling and reutilization of sludge as conceivable sustainable ecological possibilities.[68] Commensurate with this, the European Commission (2011) contemplates that if waste is to be transformed into a resource to be looped back within the economy as a feedstock, then greater precedence must be provided toward recycling and reutilization. Utilization of sludge-derived waste as a feedstock in discrete industrial sectors epitomizes a tremendous opportunity for sludge processing and handling, envisaging the integrities of the circular economy.[69] In view of the potential risks associated with the discharge of sludges, and in concordance with the standards of circular economy, the generation of biochar from different sludges serves as an effective method for promoting

TABLE I. Sludge characterization criteria delineating the mathematical expressions.[2,59,60]

Sludge characterization parameters	Test method employed	Mathematical expressions	Significance
Specific resistance to filtration (SRF)	Buchner funnel test	$SRF = \frac{2\Delta P A^2 b}{\mu \omega}$	It serves as a pragmatic means of analyzing the dewaterability of the sludge, i.e., opposition imparted by sludge toward water removal. SRF is concurrent with the filtration rate and quantizes the sludge filterability.
Sludge stability	Aerobic digestion	$S_s = 100 a' \left[1 - \frac{OUR_{meas}}{OUR_{max}} \right]$	The stability of aerobically digested sludge is enumerated using the mathematical equation put forth by Paulsrud and Eikum.[61] Greater sludge stability results in ameliorated sludge digestion.
Compressibility coefficient	Voir filterability test	$R_c' = R_o H_L^k$	The cake compressibility coefficient is contingent upon its specific resistance, and it analyzes the capability to compress sludge components on the application of normal stresses.
Capillary suction time (CST)	CST test	$CST = \varnothing \left[\frac{\mu'' C''}{\chi'} \right]$	It is the time stipulated for a specific amount of filtrate acquired from sludges to be absorbed by a blotting sheet by virtue of capillary forces. It is utilized to evaluate the impact of sludge conditioning on filterability and to ascertain the optimal dosage of conditioners needed for dewatering.
Sludge volume index (SVI)	Settleability test	$SVI = \frac{P_S}{P_X}$ OR $SVI = (1000 V_{OC}) X_{SS}$	It connotes the settling properties of sludge subjected to the activation process with different SVI values signifying distinct kinds of settling properties described below:

SVI values	Settling properties of sludge
$SVI > 150$	Inadequate settling causing sludge bulking.
$50 < SVI < 100$	Fine settling
$100 < SVI < 150$	Good settling
$100 < SVI < 150$	Exceptional settling

carbon-dioxide sequestration and eradicating sludge-based wastes.[70] It aims to satisfy sustainable development demands through waste mitigation, recycling, and reutilization.[71] The concept of reutilizing waste in regenerated systems endeavors to culminate the material usage loop contemplating economic sustainability and value addition. The circular economy approach to waste management, as per the European Union regulations, deals with the thermochemical conversion of sludge into biochar, synthesis gas, and bio-oil.[15,72] Worldwide implementation and commercialization of biochar utilize an enormous quantity of biomass-derived waste as a regenerative raw material in a value-aggregated approach thereby facilitating a circular bioeconomy and sustainable waste management. Biochar generation is supplemented by diminishing demand for waste incineration and landfilling while yielding renewable bioenergy.[73] Integrating economic, multifaceted, and green materials like biochar in wastewater treatment techniques permits us to enhance the treatment efficacy while depreciating the carbon footprint for SDG 6 and SDG 13.

B. Biochar production techniques

Sludges being bestowed with a substantial amount of biomass can be thermochemically transformed into biochar and other entailments. This section accentuates some of the cutting-edge biochar production techniques employing ionizing radiations apart from the conventional methods appertaining to drinking water, fecal, and raw sewage sludges as enlisted below. Among varied biochar generation techniques, slow pyrolysis possessing greater commercial viability, technical maturity, and climate change mitigation epitomizes the domineering techniques for yielding biochar.

The various stages involved in biochar synthesis employing the customary approaches, namely, (a) hydrothermal carbonization, (b) traditional pyrolysis (c) updraft and (d) downdraft gasification methods, and (e) torrefaction are illustrated in Fig. 2.

1. Hydrothermal carbonization (HTC)

Hydrothermal carbonization is a thermochemical transformation technique inducted by Friedrich Bergius in 1913 while dealing with
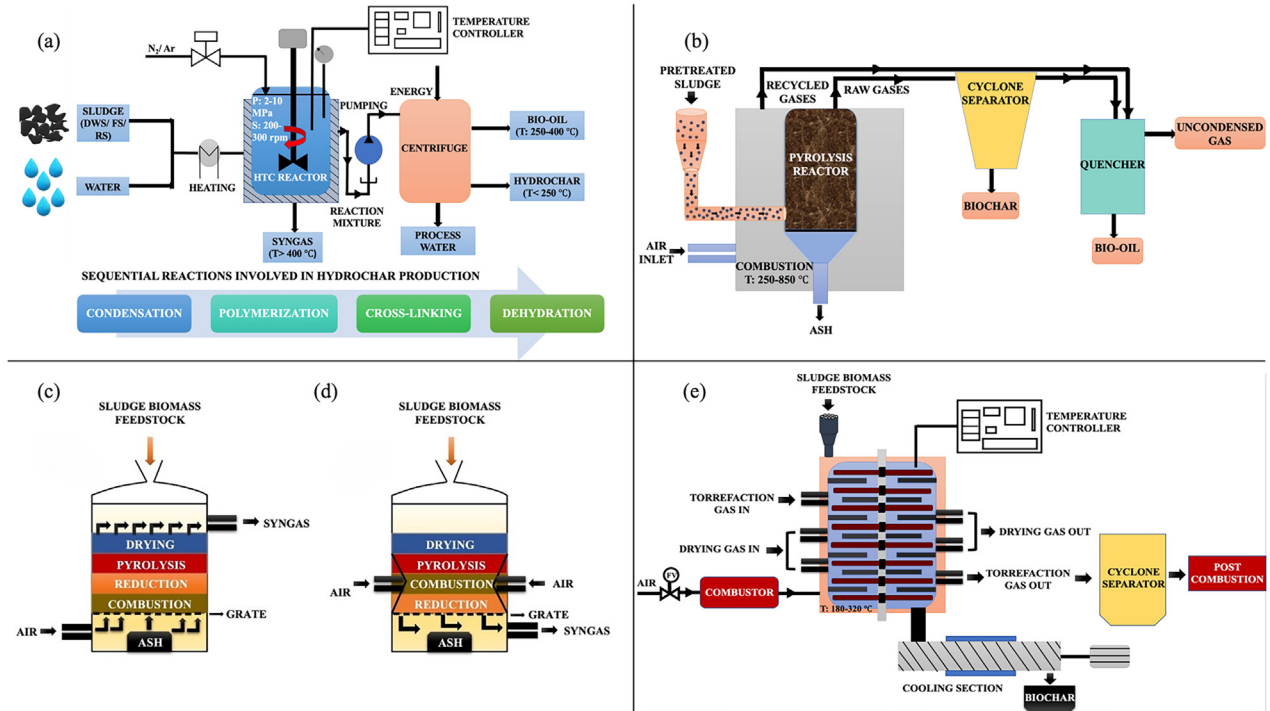
FIG. 2. Schematic illustration of various conventional biochar generation techniques: (a) Hydrothermal carbonization (HTC) process and the sequential reactions (condensation, polymerization, cross-linking, dehydration) associated with hydrochar generation, (b) conventional pyrolysis of sludge-derived biomass, (c) updraft and (d) downdraft gasification processes, and (e) various steps associated with the torrefaction of sludges.

the coalification of cellulose-based biomass.[74] It targets the conversion of biomass matter loaded within high-pressure batch reactors into hydrochar and other entailments like carbon dioxide and process water at reaction pressure and temperatures ranging from 2–10 MPa and 180–250 °C, respectively, with optimum residence time.[75] Hydrochar is obtained through sequential reactions incorporating condensation, polymerization, cross-linking, and desiccation stages of sludge-based biomass in a hydrothermal carbonization reactor.[76] This technique utilizes the benefits of greater residual moisture content of sludge-based feedstock material in the presence of water as the reaction medium at autogenic saturation pressures and subcritical temperatures, generating a reactive solvating atmosphere, thus circumventing the necessity for an energy-intensive drying step.[77] Moreover, the HTC technique is accounted to possess a greater yield (∼50%–80%) in contrast with the slow and fast pyrolysis methodologies.[78] Escala *et al.*[79] reported an abatement in the electrical and thermal energy requirements of hydrothermally carbonized sewage sludge by 65% and 60%, respectively, in contrast to the energy consumption involved in traditional drying processes.[79] The yield and characteristics of hydrochar obtained are contingent upon multitudinous factors, encompassing the type of catalysts and reaction medium employed, processing, loading parameters, and the constitution of feed material. The hydrothermal technique can be further classified at elevated temperatures into hydrothermal gasification and hydrothermal liquefaction, yielding biogas (an admixture of carbon dioxide and methane) and bio-oil.[80]

2. Pyrolysis

a. Conventional pyrolysis The conventional pyrolytic transformation of organic biomass into carbonaceous substances (biochar), biogas, and bio-fuel at elevated temperatures in a muffle furnace, fixed bed horizontal tubular reactors, or vacuum tube furnace in an oxygen deficit atmosphere with a minimal discharge of greenhouse gases antecedes to archaic Egypt. Biochar generated can enhance feedstock material properties when incorporated as a filler in building equipment and soil amelioration.[81] The quantitative and qualitative peculiarities of biochar obtained are influenced by various processing criteria, including residence time, rate of heating, raw material particulate size, and temperature. For instance, greater pyrolysis process temperature leads to an enhancement in various biochar properties, such as Brunauer–Emmett–Teller surface area, toxic metal stabilization, accessible essential nutrients, pH, and carbon content, whereas its cation exchange capacity, overall nitrogen content, total yield, and water adsorption capacity are diminished. Biochar generated at elevated temperatures ameliorates its porousness, subsequently augmenting its efficaciousness as sorbents for capturing pollutants in the soil. In contrast, at lower temperatures, it is desirable for agrarian purposes.[82] Among different types of pyrolysis, fast pyrolysis serves as a predominantly effective technique for generating bio-oil owing to a greater amount of oil produced by virtue of a lower residence time and greater heating rate. In contrast, the slow pyrolysis method is beneficial for developing biochar possessing characteristic yield values of 35% from dry biomass attributable to prolonged residence time and lower heating rates.[83]

Table II outlines various processing parameters, such as the pyrolysis type, reactor type, heating rate, pyrolysis temperature, carbonization atmosphere, and inert gas flow rate, involved in the pyrolysis of sludge-based-biochar along with the percentage yield and changes in properties after the thermochemical transformation.

b. Microwave-assisted pyrolysis The microwave region in the electromagnetic spectrum spans from 1 mm to 1m wavelengths with corresponding frequency values of 0.3–300 GHz. The practicality of the microwave-assisted pyrolysis technique is based on its ability to particularly heat substances, modify reaction pathways and expedite the conversion rate due to fast proportional heating at molecular scales. It has a considerable scope as an effective thermal source for processing and valorizing sludges. Microwave energy absorbance of substances is regulated by their dielectric characteristics, namely, dielectric loss and dielectric constant. The resultant dielectric characteristics of substances are denoted by the following equation:

$$\varepsilon^* = \varepsilon' \pm j\varepsilon''. \tag{1}$$

Dielectric heating occurs on the molecular scale activated through incident microwaves resulting in the electromagnetic coupling of dipolar organic matter in sludge and water. The predominant dielectric heating mechanisms involved include athermal effects because of ionic migration and thermal effects attributable to dipolar rotation.[88] This technique exhibits substantiated amelioration in biochar quality and yield and the ability to repudiate unwanted secondary reactions amidst evanescent substances.[78]

3. Gasification

Gasification is a thermochemical technique in which carbonous matter is transformed into inflammable gases and ash in the presence of a reducing environment.[89] Contrary to conventional pyrolysis, the gasification process necessitates the usage of gasifying agents like oxygen (oxygen gasification) or steam (steam gasification occurs at temperatures greater than 800 °C) for reorganizing molecular framework, incorporating hydrogen and stripping hydrocarbon from the feedstock employed.[78] It is typically characterized by intricate chemical and physical modifications of sludges commencing with the desiccation process leading to the generation of preliminary gaseous fuel and solid or liquid-based byproducts. The dried sludge is subjected to thermolysis followed by gasification of char, incondensable and condensable vapors, and pyrolysis derivatives, where they undergo synchronous oxidation and reduction reactions. The drying stage involves the degression of sludge within the gasification unit with subsequent moisture vaporization by heat released in the lower regions. The calorific content of gas generated is determined by various parameters like the reactor and feedstock used, while the characteristics of fuel obtained through gasification are conditional on residual moisture content, carbon content, and evanescent matter.[89] The heat of gasification involved can be expressed by an energy balance equation delineated as follows:[90]

$$-\Delta H_R^0 = \Delta H_{\text{out}}^T + H_{\text{loss}}. \tag{2}$$

The updraft gasification systems are associated with the movement of gasifying medium (steam, oxygen, or air) in the upward direction, while the fuel bed descends underneath, thereby ensuring the solid and gaseous components to be in a concurrent mode. The gasifying media penetrates the bed through the grate, where it comes in contact with the heated ash bed. On the other hand, the downdraft gasifier serves as a synchronous reactor, which involves the entry of air within the gasifier at specified distances beneath the top. The product gases surge in the downward direction and exit from the base region of the gasifying unit through a heated ash bed.[91]

4. Torrefaction

Torrefaction (mild pyrolysis) is associated with the gradual heating of biomass in rotary kilns, fluidized bed reactors, quartz tube furnaces, or fixed bed reactors at ambient pressures and temperatures spanning from 180 to 320 °C in an oxygen-deprived atmosphere. The principal purpose of the torrefaction technique is to modulate the heating rate, surface area, moisture content, and particulate size of biochar. The torrefaction process is often categorized into three classes: wet torrefaction, oxidative torrefaction, and steam torrefaction. Wet torrefaction involves the inclusion of water, and the biomass treatment is performed at residence time and processing temperatures of 5–240 min and 180–200 °C, respectively. Steam torrefaction encompasses biomass treatment in the presence of steam at temperatures not greater than 260 °C with a residence time of 10 min. Oxidative torrefaction entails biomass treatment employing oxidizing agents, involving gases customarily employed in combustion, where energy generation occurs post-completion of the process.[18] The oxygen content of the initial biomass matter is greater than that of the torrefied derivatives, while the heating value is considerably less. Torrefied derivatives are exemplified by enhanced hydrophobicity, energy density, brittleness, and resistance to microbial decomposition.[92] This process yields superior-grade biofuels for subsequent thermochemical transformation through combustion, gasification, and pyrolysis.[93] The energy prerequisites for this process are computed by quantifying the energy involved in heating the inflowing biomass from atmospheric to torrefaction temperature, latent heat of evaporation, and devolatilization contingent with the equation given as follows:[94]

$$Q = m_0 dH. \tag{3}$$

The torrefaction process at the pilot scale consists of a vertically oriented furnace encompassing numerous hearths comprising a rotating shaft. The furnace column is outfitted with multiple hearths and an interior rabbling arrangement to ascertain the translation of sludge-based biomass within the hearth.[95] Before the biomass is fed into the furnace, the system is preheated for the specified duration until the operational processing temperature is attained. The torrefied sludge egressing the oven is cooled within two sequential screw conveyors and eventually collected. Table III summarizes the processing conditions and characteristics of DWS, FS, and RS-derived biochar.

5. Ionizing radiations

Ionizing rays employing electron beams and gamma rays generated by electron accelerators and gamma irradiators are used to sterilize sludges of microbes competently, and they also find potential applications as soil conditioners in agriculture.

a. Gamma beam irradiation. High-energy gamma rays generated during the radioactive disintegration of radioisotopes like ^{60}Co and ^{137}Cs can penetrate substances and immobilize microbes by cleaving

TABLE II. Processing parameters associated with the pyrolysis technique encompassing the percent biochar yield and changes in properties of sludge-derived biochar.

Sr.No.	Sludge type	Pyrolysis type	Reactor type	Pyrolysis temperature (°C)	Heating rate (°C min^{-1})	Residence time (min)	Carbonization atmosphere	Inert gas flow rate (ml min^{-1})	Biochar yield (%)	Change in properties	Ref.
1.	SS	Slow pyrolysis	Quartz tube furnace	500, 600, and 700	25	300	Nitrogen (N$_2$)	630	40.2–54.5	- Ash content, bio aromaticity, micro, and macronutrient content, and pH were intensified at elevated pyrolysis temperatures. Moreover, molar ratios, percentages of O, N, H, biochar, crystallite size, and biochar polarity were diminished.	84
2.	SS		Electrical furnace	300, 400, 500, 600, and 700	3	120	Argon (Ar)	⋯	52.9–72.5	- Biochar yield was substantially diminished to 52.9% at 700 °C from 72.5% at 300 °C, while an enhancement in the pyrolysis temperature resulted in ameliorated gas yield. Furthermore, a depreciation in biochar bulk density and intensification of porosity and particle density were	85

TABLE II. (*Continued.*)

Sr.No.	Sludge type	Pyrolysis type	Reactor type	Pyrolysis temperature (°C)	Heating rate (°C min⁻¹)	Residence time (min)	Carbonization atmosphere	Inert gas flow rate (ml min⁻¹)	Biochar yield (%)	Change in properties	Ref.
										ascertained at higher pyrolysis temperatures.- Biochar synthesized at reduced temperatures exhibited greater total organic carbon and nitrogen content and curtailed $CaCO_3$ equivalent, C/N ratio, and K, P, and Na proportions.	
3.	Biosolid (Treated SS)	Slow pyrolysis	Fluidized bed reactor	400, 500, an 600	35	60	Nitrogen, carbon dioxide (CO_2)	7500	N_2 atmosphere: 46.2 ± 0.1 to 54.7 ± 0.3; CO_2 atmosphere: 46.2 ± 0.11 to 54.1 ± 0.1	-Elevated pyrolysis temperatures entailed greater surface area, fewer functional moieties, and reduced O/C and H/C proportions. - Biochar synthesized in CO_2 and N_2 atmospheres demonstrated greater surface area and augmented salinity, respectively.	86
4.	DWS		Horizontal rotary	300, 500, and 700	10	60	Nitrogen	$\cdots$	43.18–60.18	- Proximate analysis	81

TABLE II. (*Continued.*)

Sr.No.	Sludge type	Pyrolysis type	Reactor type	Pyrolysis temperature (°C)	Heating rate (°C min^{-1})	Residence time (min)	Carbonization atmosphere	Inert gas flow rate (ml min^{-1})	Biochar yield (%)	Change in properties	Ref.
			reactor							studies manifested that the as-prepared biochar had greater carbon stability for plausible pertinence for carbon sequestration.- Ultimate analysis studies signified that the surface hydrophobicity varied as follows: -Biochar > DWS. - Moreover, the synthesized char could be employed as adsorbents and soil culture medium ascribable to decreased metal content, greater surface area, and stimulation on germination.	
5.	FS	Slow pyrolysis	Tunnel furnace	350, 450, and 600	25 3	10, 20, 40	Nitrogen	8–33.33	57.7–70.4	- Shorter holding time (10 minutes) was sufficient for the thorough pyrolysis of FS. - The biochar synthesized in this study	87

TABLE II. (Continued.)

Sr.No.	Sludge type	Pyrolysis type	Reactor type	Pyrolysis temperature (°C)	Heating rate (°C min⁻¹)	Residence time (min)	Carbonization atmosphere	Inert gas flow rate (ml min⁻¹)	Biochar yield (%)	Change in properties	Ref.
										demonstrated several parameters analogous to chars derived from biowaste and lignocellulose-based biomass for utilization to ameliorate soil and carbon sequestration.	

the covalent linkages of microbial DNA. It is applicable under secure and regulated operating conditions, and as there is no production of moisture or heat, it is devoid of outgassing, condensate discharge, thermal stress, and residuum radioactivity post-irradiance.[99]

b. Electron beam irradiation. This technique is associated with bombarding the target with a high-energy electron beam inducing a surge of electrons impelling throughout the material. The electrons engendered in the process undergo interaction with the atoms present in the metal target, knocking out electrons from their orbitals, thereby producing free radicals. A particle accelerator is employed to accelerate the electrons produced to the relative light speed. The consequent energy typically spans from 3–10 MeV, and on conjugation with the power of the order of 1–50 kW, it can penetrate through an extensive array of materials. The electrons generated interact with the sludge, resulting in molecular dissociation, excitation, recombination, and fragmentation, as illustrated in the mechanism below (Fig. 3). The electrons engendered during irradiation with a beam of electrons can interact with genetic components or other cellular elements present in organisms, eventually affecting the capability of the cells to replicate and endure. This direct effect of radiation is known to portray an inconsiderable role in the treatment of pathogens and is found to be substantial in the elimination of more than 10% of organic compounds when the concentration of pollutants exceeds 0.1 M.[100] These same electron species liberated can also instigate ruptures in the double-helical DNA strands of the microbes, prohibiting gene replication and eventuating its ability to sterilize[99,100]

$$
\begin{aligned}
&1.\ AB + e^- \rightarrow AB^* + AB^+ + e^- \,(\text{molecular dissociation})\\
&2.\ AB^+ + e^- \rightarrow AB^* \,(\text{recombination})\\
&3.\ AB^* \rightarrow A^{\cdot} + B^{\cdot} \,(\text{fragmentation})\\
&4.\ AB^+ \rightarrow A^+ + B^{\cdot} \,(\text{fragmentation})
\end{aligned}
\tag{4}
$$
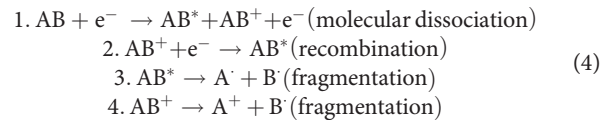
where $\cdot$: Free radical generated; $^-$: anion; $^+$: cation; $*$: excited molecule.

C. Designing reactors for biochar production

Chemical reactors are sophisticated apparatus characterized by diffusion, friction, mass transfer, or heat transfer in conjunction with regulable chemical reactions promoting the transformation of feedstock into the desired products, and its design serves as a critical milestone in the comprehensive process design.[59]

For designing chemical reactors, the following criteria should be fulfilled:

(i) Chemical factors: reaction kinetics—reactors should be designed to yield adequate residence time for the intended chemical reactions to advance to the requisite degree of conversion.

(ii) Heat transfer considerations: they should be modeled considering the heat inclusions and eliminations of the heat of the reaction.

(iii) Mass transfer considerations: the rate of heterogeneous chemical reactions can be regulated through the diffusion rate of the reacting entities in lieu of chemical kinetics.

(iv) Safety margin: reactors should constrain perilous products and reactants while regulating chemical reactions and processing parameters.

TABLE III. Biochar production techniques encompassing their characteristics and processing parameters.

Sludge type	Biochar production technique	Biochar yield (%)	Heating rate (°C/ min)	Residence time	Temperature (°C)	pH	Surface area (× 10⁴) (m² kg⁻¹)	Total pore volume (× 10⁻⁵) (m³ kg⁻¹)	Pore radius (Å)	Reference
DWS	Hydrothermal carbonization	51.19–67.19		4 h	140–200	4.32–4.50	15.69–28.58	22.1–44.7	18.20–18.25	81
	Pyrolysis	43.18–60.18	10	1 h	300–700	6.57	10.47–10.88	35.5 – 37.6	64.45–90.32	81
FS	Hydrothermal carbonization	70–73	-	5 h	250	6.8–7.2	0.44–0.56	3.5–4.9	8.6–9.2	55
	Pyrolysis	19–66.7	15	1 h	300–600	9.11–10.8	· · ·	· · ·	· · ·	96
RS	Hydrothermal carbonization	57.29–84.73	· · ·	4 h	160–250	7–8	0.29–0.12	· · ·	· · ·	97
	Pyrolysis	45	3	2 h	500	9.54		· · ·	· · ·	25
	Gasification	36–60.8	5	34–55 min	750–850	· · ·		· · ·	· · ·	98
	Torrefaction	69.1–94.9	· · ·	3–10.8 min	220–320	· · ·		· · ·	· · ·	92

The fundamental processes involved in designing chemical reactors are synopsized in the supplementary material (Fig. S1).[102]

While selecting reactor parameters, especially in design optimization and reaction conversion, the interaction of chemical reactor design with distinct processing conditions must be considered. The degree of conversion of feedstock loaded in reactors influences the expenditure and sizing of apparatus essential to segregate and reprocess untransformed components. In this context, the reactor and its corresponding equipment should undergo optimization as individual entities.[102]

The categorization of chemical reactors used in thermochemical transformation processes, namely, torrefaction (based on gas–solid mixing and heating mode employed), gasification, fast pyrolysis, and hydrothermal carbonization is represented in the supplementary material (Fig. S2).[103] Among an extensive array of reactors used in thermochemical transformation processes, fluidized bed [Fig. 4(a)], fixed bed reactors [Figs. 4(b)–4(d)], and batch reactors [Fig. 4(e)] predominantly utilized for biochar production employing drinking water, fecal, and raw sewage sludge illustrated in the figure given below will be emphasized in this section.

1. Fluidized bed reactors

Indigenous reactors of this kind include the Winkler coal gasifier patented in 1922, accompanied by the Esso cracker in 1940, which are presently being superseded by riser reactors employing zeolite-based catalytic systems.[101] The fluidization technique can be exclusively
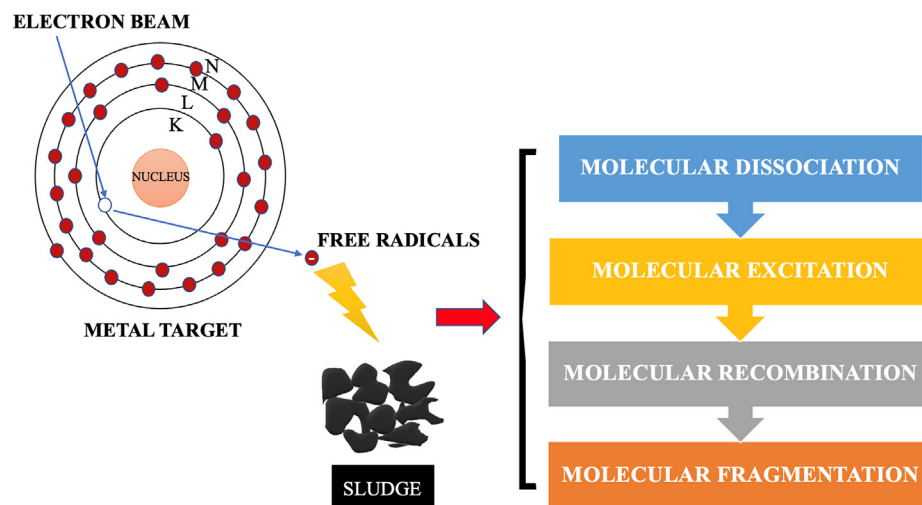
FIG. 3. Pictorial representation of different steps involved in the interaction of high energy electrons with sludge biomass matter, ensuing in the dissociation, electronic excitation, recombination, and fragmentation of molecules.
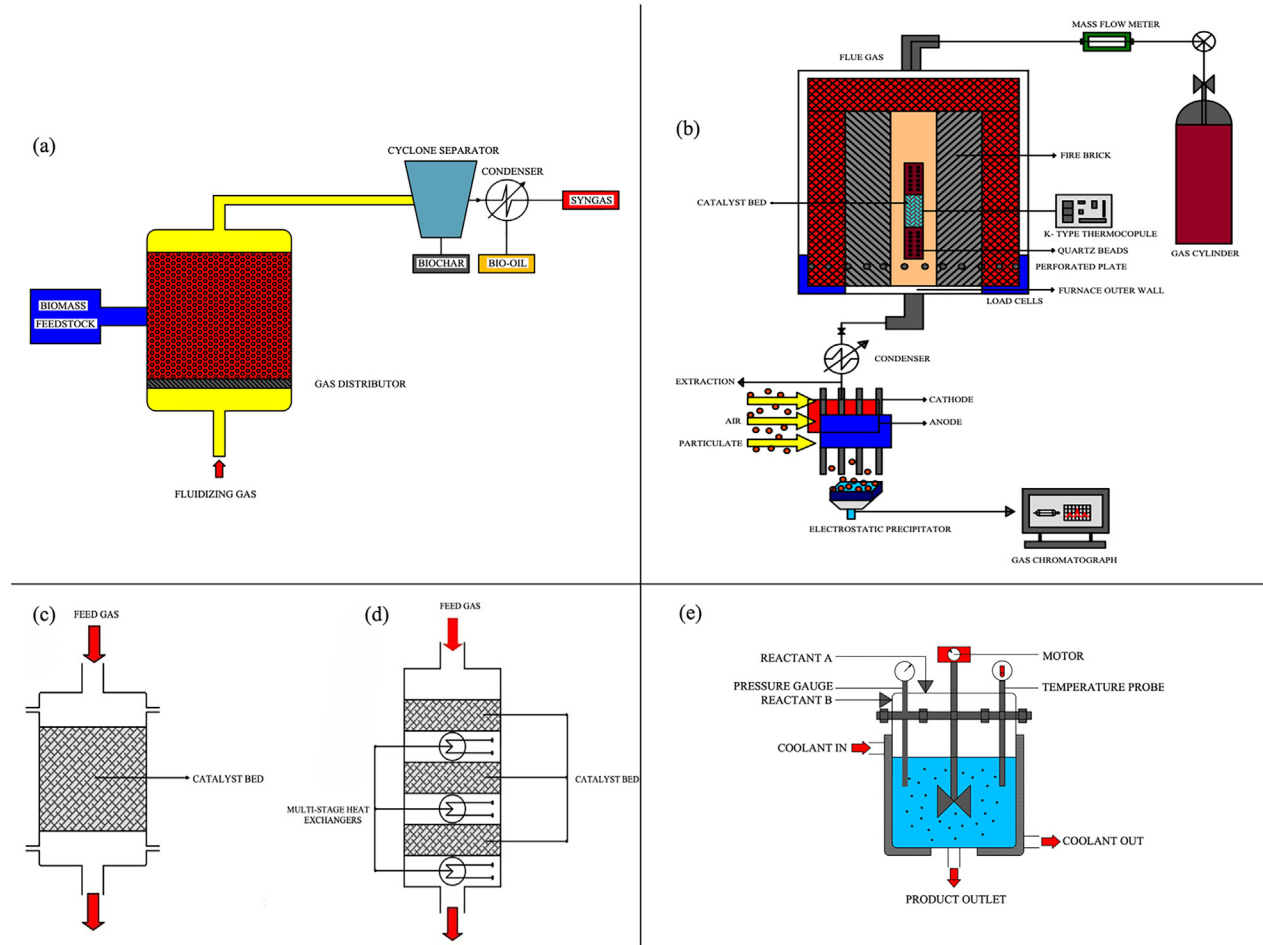
FIG. 4. Diagrammatic representation of different types of chemical reactors employed in the thermochemical transformation of sludge-based biomass into biochar: (a) Conventional fluidized bed reactor system, (b) fixed bed reactor, (c) single-bed adiabatic fixed bed reactor, and (d) multi-phase adiabatic fixed bed reactor encompassing heat exchangers between different stages, and (e) conventional batch reactor.

employed for reasonably small-sized particulate matter, less than 300 μ m for gases.[102]

The fundamental characteristics of fluidized bed reactors (FlBR) involve solid components (reactant, catalyst, or inert substances included for facilitating heat transfer) being suspended by ascending current of reacting fluid, expediting greater heat and mass transfer reaction rates and favorable mixing. At lower velocities, the fluid induced onto the static bed flows through the cavities of particulate solids, while at higher velocities, the static bed undergoes expansion till the particulate matter becomes suspended as the forces of gravity and drag forces are counterbalanced by the buoyant forces. The bed gets entirely suspended at the minimum fluidization velocity (U_{mf}) when the particulate mass corresponds to the pressure differential existing across the bed, and it can be computed using the following expression:[104]

$$U_{mf} = 16.50 \frac{d^2(\rho_s - \rho)g}{\mu}. \tag{5}$$

Commensurate with the fluidization velocity, different flow regimes like bubbling fluidization, turbulent fluidization, particulate fluidization, pneumatic conveying, and slugging fluidization are attained, and it also impacts homogeneous temperature distribution, enhanced mass transfer rates, and good particle mixing characteristics. Reactor geometry is another significant criterion influencing the particulate mixing and dispersion in fluidized bed reactors. For instance, cylindrical bed FlBR resulted in higher mixing rates in contrast with square bed reactors owing to dead zones in the latter impeding adequate mixing in the reactors.[104]

Martínez et al.[92] conducted torrefaction experiments of sewage sludge using a lab-scale fluidized bed to analyze the effect of temperature and residence time on the properties of the final product. With a maximal bed height of 0.15 m, the crushed and screened sludge particles were supplied to the reactor at a feed rate varying from 10^{-4} to 26.67×10^{-4} kg/s. The mean solid and gas residence time was modified from 216–612 and 6.17 to 5.02 s, respectively. The reactor freeboard, bed, and cyclone were subjected to heating through an electric

29 August 2023 15:25:40

kiln, and the torrefaction temperature ranged from 220 to 320 °C. A hot filter maintained at a similar temperature as the reactor bed was positioned prior to the condensate system (comprising an electrostatic precipitator and two frigid condensers) to withhold fine particulate matter with a micro chromatograph setup to analyze the composition of flue gases.[92]

2. Fixed bed reactors

Fixed bed reactors (FiBR) are extensively utilized for the thermochemical transformation of biomass matter, and they can be employed in incineration in grate-type furnaces and gasifiers for generating syngas. The major classes of fixed bed gasifiers include cross-draft fixed bed systems, co-current or downdraft fixed bed systems, and countercurrent or updraft fixed beds.[103] The fixed bed reaction mechanism involves the liberation of combustibles through pyrolysis, which is further incinerated due to heat transfer through furnace walls and existent flame. The inflamed region proliferates to the particulate matter in its proximity through heat transfer accompanied by subsequent oxidation and gasification stages of char beyond the inflammation front possessing a depreciated reaction rate. The grate-type furnaces are characterized by a specific phase involving the oxidative conversion of char, post the movement of the inflammation front toward the base of the reactor bed. The peculiarities of the reaction in a fixed bed are influenced by various parameters, including the flow rate of air, particulate size, and fuel characteristics. Air flow rate ascertains the extent of heat transfer through convection mode and the oxygen content of the fuel. Pressure drop, void ratio, and air diffusion within the bed are some factors impacting the particulate size distribution and particle size. Calorific value and volatile matter fraction of fuel ascertain the heat of the reaction and the quantity of inflammable components discharged during pyrolysis.[105]

The laboratory scale FiBR comprises a columnar reactor, air feed, load cells, and gas cleansing system. A perforated plate is located within the reactor to sustain the bed encompassing fuel particles and circulate air steadily. A k-type thermocouple was employed to estimate the temperature in the bed's interior. Load cells were ensconced beneath the reactor system to control the fuel weight. Air was dispensed through a compressor with flow rate values spanning from 74.5 to 596 kg m^{-2} h^{-1}. The fuel components were incinerated in the upper region of the bed employing kerosene. The product gases released from the reactor were transmitted across a condensing system utilizing acetone and water. Post-segregation of water and char, the incondensable gases were conveyed through an electrostatic precipitator to eliminate particulate matter. The purified gaseous components were examined to estimate the constitution of gases through an online analyzer for unremitting regulation and a gas chromatograph for comprehensive analysis of CH_4, O_2, CO_2, CO, H_2, and other bulkier hydrocarbons.[105]

a. Design considerations in adiabatic FiBRs. Adiabatic FiBRs are characterized by the presence of a catalyst as a homogeneous static bed enclosed by external insulation jackets and the dispersal effect and convective heat and mass transfer occurring along the flow direction.[106]

(i)   Pressure drop evaluation:
The differential pressure across an adiabatic FiBR is computed through the Ergun equation[106]

$$\frac{\Delta P}{L} = \left(\frac{150.(1- \in).\mu'}{d_p} + 1.75.G \right) . \frac{(1- \in)}{\in^3} . \frac{G}{d_p.\rho_f.g_c}. \qquad (6)$$

(ii)   Axial heat dispersion coefficient:
Axial heat dispersion coefficients in an adiabatic FiBR can be estimated through the Dixon and Cresswell expression[106]

$$\frac{1}{Pe_a} = \frac{\lambda_{ea}}{u.\rho_f.c_{pf}.d_p} = \frac{\lambda_{af}}{u.\rho_f.c_{pf}.d_p} + \frac{\frac{\lambda_{as}}{\lambda_f}}{Re.Pr} + \frac{u.\rho_f.c_{pf}}{ah.d_p}. \qquad (7)$$

In Eq. (7), for greater Re values, $Pe_a \approx 2$

(iii) Axial mass dispersion coefficient:
The axial mass dispersion coefficient for adiabatic FiBR is analyzed based on the correlativity proposed by Edwards and Richardson that was further investigated by Wen and Fan[107] on various empirical findings applicable in the range of $2.2 \geq Sc \geq 0.28$ and $400 \geq Re \geq 0.08$[106]

$$\frac{1}{Bo_a} = \frac{D_{ea}}{v.d_p} = \frac{0.5}{1 + {9.5. \in}/{(Re.Sc)}} + \frac{0.75. \in}{Re.Sc}. \qquad (8)$$

Table IV outlines the design parameters of various kinds of FiBRs involved in the thermochemical conversion of sewage sludge into biochar.

3. Batch reactors

Batch reactors are tanks customarily equipped with agitators and heat transfer mechanisms to sustain temperatures within reasonable limits. In such reactors, all reagents are charged simultaneously, the concentration changing over time and becoming consistent thoroughly. They are predominantly utilized for moderately slow reactions proceeding for multiple hours.[101] Batch operations differ from continuous processes in several attributes, including operating technique, the versatility of performance, low-volume manufacturing, determinate functioning duration, and initial charging parameters.[110] Small-sized-batch reactors usually necessitate fewer ancillary devices like pumps, with their regulation mechanism being less intricate and expensive. Batch reactors possess several benefits associated with heterogeneous reactions; agitation systems could be configured to permit the suspension of solids within liquid systems and the dispersion of non-miscible fluid systems. Estimating the volume requisites for batch reactors involves designating the liquid volume to be processed. The design of a reactor vessel is associated with augmenting the height by almost 10% to account for freeboard regions encompassing perturbations and waves on the liquid surface, with an auxiliary freeboard needed in the case of contemplated foaming reactions.[111]

a. Fundamental design equations associated with batch reactors.

(i)   Computation of reaction time:
Estimating the time stipulated to achieve the desired conversions is the primary objective in designing batch reactors. The reaction time (t_r) is analyzed using the generic material balance equation. For reversible reactions, the reaction time incorporating multiple reagents can be expressed as the number of moles of reactant A converted per unit volume[111]

TABLE IV. Design specifications of some FiBRs used in biochar production.

| Biochar feedstock | Reactor type and MOC | Reactor dimensions | | Bed height (m) | Air flow rate (kg m^{-2} h^{-1})/ Inflow rate (ml h^{-1}) | Heating rate (°C min^{-1}) | Operating temperature (°C) | Thermocouple type used | Reference |
		Length (l)/ height (H) (m)	Inner diameter (m)						
SS	Cylindrical quartz glass FiBR	L: 0.45	0.06	...	...	10	250, 350, 350, 500, 550, 600, 700	K-type	108
SS	Up-flow Polypropylene column FiBR	H: 0.10	0.015	0.01, 0.02, 0.03	IFR: 72, 144, 216	...	400–800	...	109
SS	Cylindrical SUS310 stainless steel FiBR	H: 0.70	0.30	0.30	AFR: 74.5 – 596	10	530	K-type (10 no.)	105

$$t_r = \int_0^{\chi_f} \frac{d\chi}{\mathcal{R}_A}. \tag{9}$$

(ii) Maximum production rate:

The maximum production rate for batch processes involving no changes in volume can be expressed as the maximum value in the following equation:

$$\frac{\chi}{t_r + t_s}, \tag{10}$$

where t_s = Reactor shut-down time.[111]

(iii) Heat balance in non-isothermal processes:

The heat balance across non-isothermal batch reactors can be estimated through the following expression:[111]

$$-UA_t(T - T_c) + (-\Delta H_A)V_b\mathcal{R}_A = (\Sigma m_j c_j)\frac{dT}{dt}. \tag{11}$$

(iv) Heat balance in adiabatic processes:

For adiabatic processes, the heat balance depicts the temperature at any step of the reaction process, and this could be explicated in terms of reaction conversion attributable to the fact that heat liberated during the reaction is restrained as sensible heat within the reactor. For adiabatic reactions at constant volume, the heat balance can be expressed as follows:[111]

$$(-\Delta H_A)V_b d\chi = (\Sigma m_j c_j)dT. \tag{12}$$

4. Design considerations (factors of safety) in chemical reactors

Chemical reactors involving exothermic reactions exemplify the most lethal operational entities in the chemical industry. Safety audits of the chemical reactors' functioning must be conducted at every design and fabrication stage.[112] Errors result from uncertainties in the design data procured and, in the approximations that are essential in design quantification. To ascertain that the design prerequisites are complied with, factors are incorporated to impart a safety margin, thereby ensuring that the equipment will function safely and not induce any hazards. Design factors are implemented in process design to render some tolerances in the design. For instance, the process stream average flows enumerated from material balance equations are intensified by 10% customarily to impart design versatility in the process operation. This factor will establish maximal flows for instrumentation, equipment, and piping design.[102]

HAZOP serves as one of the most stringent methodologies for recognizing hazards in chemical industries. This approach rigorously scrutinizes all the devices progressively, along with the deflexions from standard operating conditions, and examines the failures that are likely to occur. A typical HAZOP report comprehends all the deflections, their sources, ramifications in equipment performance, assessment of such repercussions, executed protection (passive or active), and substantial implications. In recent decades, extensive research has been committed to smart systems for automatizing HAZOP analysis through computer-generated codes. While performing HAZOP analysis of chemical reactors, pertinent deflections from standard operating parameters are generated. The fundamental objective is to analyze the causes for such deflections and deduct their implications on the performance of the reactor. Through a befitting mathematical model, the magnitude of deviations can be facilely encompassed, and the potential repercussions are explored.[112]

a. Special process hazards. The standard process hazards are factors rendering a prominent role in establishing the magnitude of loss ensuing an incident as enlisted below:

(i) Endothermic chemical reactions: A penalty of 0.2 is employed for the chemical reactors, which is further intensified to 0.4 if the reactor is subjected to heating by means of fuel combustion.

(ii) Exothermic chemical reactions: The penalty digresses from 0.3 for mild exotherms to 1.2 for extremely sensitive exotherms.

(iii) Accessibility of emergency devices: Regions not possessing admissible access are subjected to penalization. Minimum prerequisites include access from both sides.

(iv) Materials handling and transportation: This penalty contemplates the risks associated with material handling, transportation, and repositioning.

(v) Drainage and spillage regulation: This penalization is associated with the design parameters engendering massive spills of incendiary substances conterminous to the process equipment, like incompetent drainage design.[102]

  b. Basic precautionary measures. The fundamental safety measures to be comprehended in chemical process design as proposed by the Dow Chemical Company are enlisted below:

(i) Use of pressure-relief valves.

(ii) Appropriate structural design of piping, vessels, and steelwork.

(iii) Fail-safe instrumentation

(iv) Safeguarding fired devices (furnaces) against fortuitous outbursts and fire.

(v) Earthing of electrical devices.

(vi) Conformity with national standards and codes.

(vii) Appropriate and impregnable water supplies for fire management.[102]

D. Modification techniques of sludge-based biochar

  Unmodified biochars yield lower adsorption capacity toward an extensive array of contaminants, and they are afflicted by inadequate active functional moieties, diminished surface area, and pore characteristics. Biochars subjected to modification demonstrated a higher density of functional moieties and surface area, efficacious physicochemical steadiness, ameliorated porousness, and were propitious toward usage and environmental remediation.[15] The major biochar activation pathways, including physical (steam and CO_2 activation) and chemical modification techniques (metal/metal oxides impregnation, acid-alkali modification, modification using oxidizing agents, nanomaterials, and nonmetallic heteroatom doping), are presented in this subsection.[18]

1. Physical modification

  Physical modification strategies involve carbonizing precursors at higher temperatures (less than 800 °C), ensued by activation through carbon dioxide (CO_2) or steam. CO_2 activation entails the interaction of carbonaceous components of biochar with CO_2 gas leading to the generation of a microporous biochar framework and carbon monoxide (CO) gas. Steam activation encompasses the reaction of carbonaceous biochar with steam to engender evanescent substances, fixed C transformation to CO_2 and CO, and eradicating the confined substances. This activation technique aims to enhance the biochar pore volume, surface area, and morphology by curtailing its polarity and aromaticity.[18]

2. Chemical modification

  Chemical modification strategies are the most sought-after activation techniques for biochar. It can be performed as a single activation (during) or a two-step activation technique (post) carbonizing the pristine biomass feedstock employing chemical agents like oxidizing and reducing agents, alkali or acid modifiers, or impregnation with metal oxides or metallic salts.[18]

(i) Metal or metal oxides impregnation:
Chemical modification via metal oxide or metal impregnation could be achieved by the following methodologies:

(1) Thermochemical transformation of biomass to biochar followed by soaking the synthesized biochar in metal oxide or metallic salts under specific circumstances.

(2) Pyrolysis of the admixture of biomass feedstock and metal oxides or metal-based salts to obtain biochar.[114]
The predominately negatively charged ion exchange functionalities on the biochar surface are diminished during intense heat treatment during pyrolysis. Toxic metal ions present in sewage sludges, primarily existing as cations, restrain the adsorption capacity of biochar.[115] To augment biochar's adsorption capacity, researchers are modifying biochar by incorporating metal ions within it, possessing a significant amount of binding sites. Modifying sludge-based biochar via metal impregnation enhances the catalyzing activity of biochar. For instance, the concomitance of metal oxides possessing mixed valences could facilitate the degradation of hydrogen peroxide (H_2O_2) for the subsequent disintegration of organic moieties.[116] Bao *et al.*[117] reported SS-based biochar modified with different rare earth elements and transition metals (Ti, Ce, Fe, Al, and La) for enhanced catalytic activity toward the degradation of H_2O_2 for the substantial degradation of tetracycline. The degradation efficiency of tetracycline subjected to catalysis via metal ion-impregnated biochars were 58% (Ti-modified biochar), 69% (Ce-modified biochar), 90.7% (Fe-modified biochar), 58% (Al-modified biochar), and 59.9% (La-modified biochar). Fe-modified biochar exhibited excellent catalytic activity within the H_2O_2 system, and the degeneration efficacy of tetracycline reached 90.7% compared to 39% for pristine biochar, implying that Fe-modified biochar apprehended superior catalytic performance along with lowered reaction time.[117] In another study, hydrothermally synthesized iron-loaded SS-based biochar was employed to adsorb and co-adsorb doxycycline and tetracycline antibiotics selectively. The as-prepared biochar displayed adsorption capacities of 81.21 and 89.5 mg g^{-1} for doxycycline toward binary (B-) and unary (U-) systems, respectively, almost 1.6 times greater than the unmodified biochar. Contrarily, the biochar exhibited an adsorption capacity of 30.79 and 70.63 mg g^{-1} for tetracycline toward B- and U- systems, respectively, compared to 23.29 and 46.21 mg g^{-1} for pristine biochar. The substantial enhancement in biochar adsorption capacity toward antibiotics could be ascribed to abundant oxygen-possessing functional moieties, greater specific surface area, and reduced particle size compared to pristine biochar.[118]

(iv) Acid–alkali modification:

Acid modification eliminates metallic salt impurities and instills acidic functional moieties on the biochar surface. Acids commonly used for this purpose include oxalic acid, sulfuric acid, citric acid, nitric acid, hydrochloric acid, phosphoric acid, etc.[113] Contrarily, alkali modification enhances the biochar surface area, pore volume, and functional moieties possessing oxygen via alkalizing substances, such as sodium hydroxide and potassium hydroxide.[119] Sewage sludge-derived biochar generally comprises large amounts of silicon that could be eliminated through viscous hot alkaline solutions. Technically, the eradicated substances resulted in enhanced surface functionalities and porousness engendering improved adsorption capacities. The consolidated acid-alkali modification technique is a contemporary approach to intensify the adsorption characteristics efficaciously.[120]

(v)   Modification via oxidizing agents:
Employing oxidizing agents as modifiers in pristine biochar augments the amount of functional moieties possessing oxygen on the biochar surface. H_2O_2 modification could also amplify the proportion of oxygen-based functionalities, particularly the carboxyl moieties leading to improved adsorption capacities of contaminants.[121] For instance, Sun et al.[122] reported the existence of abundant carbon–oxygen functional moieties on the biochar surface subjected to the air-roasting oxidation process in contrast with the pristine biochar demonstrating an enhanced adsorption capacity of 490.2 mg g^{-1} (pH: 6, T: 25 °C) with 96% removal efficacy of U (VI) ions even at lower uranium concentrations.[122]

(vi)   Modification using nanomaterials:
Modifying pristine biochars with nanostructured components, such as manganese oxide, iron oxide, zinc sulfide, zinc oxide, graphene, and carbon nanotubes, augments the adsorption efficacy of biochars toward toxic metals. Zuo et al.[123] reported calcite nanoparticle (NP) modified SS-derived biochar for ameliorated adsorption of Cd (II) (adsorption capacity: 36.5 mg/g), almost three folds greater than that of unmodified biochar attributable to precipitation and ion-exchange mechanisms between calcite NPs, biochar, and toxic metal in the former.[123]

(vii)   Modification via nonmetallic heteroatom doping:
Nonmetallic heteroatom doping employing nitrogen, fluorine, sulfur, boron, phosphorus, etc., atoms as dopants serves as another customary approach to augment the catalytic efficacy of biochar. Heteroatom doping leads to the generation of surface defects within the carbon matrix, which is contemplated as an efficient strategy for ameliorating the transportation of electrons, across the interface existing within carbonaceous substances. In this approach, the surface characteristics of carbon can be regulated by destroying preliminary equilibrium and instigated polarization.[124] Furthermore, this methodology entails the alteration of surface and volume characteristics of carbon, in order to transform various chemical and physical characteristics including surface chemistry, magnetism, heat stability, and surface properties of carbon, thereby imparting carbonaceous substances versatile functions for environmental

technology, and catalysis.[125] Among different nonmetallic heteroatoms, nitrogen has acquired considerable emphasis. Nitrogen atoms can facilely penetrate the framework of a graphene sheet, for it exhibits a size equivalent to that of carbon atoms. Additionally, the electronegativity of carbon is lower than that of nitrogen, subsequently, the carbon atom positioned alongside nitrogen might function as the Lewis base site.[126] The electronegativity difference can also expedite the development of defects and promote the electron transportation capability, which might be favorable for the catalytic ability of carbonous substances.[127,128] Wang et al.[129] fabricated nitrogen-doped sewage sludge biochar (N-SSBC) and utilized it for activating peroxymonosulfate for the subsequent disintegration of sulfamethoxazole, contemplating the influence of calcination temperature on the degeneration mechanism. The as-prepared biochar (N-SSBC), demonstrated enhanced catalytic activities in contrast with the sewage sludge-based biochar (SSBC), signifying that nitrogen doping ameliorated the catalytic efficacy of SSBC. Moreover, N-SSBC fabricated at 800 °C, manifested increased catalytic activity toward PMS in contrast with the nitrogen doped-biochar synthesized at other temperatures.[129] Besides nitrogen heteroatom, boron heteroatom can also be doped in biochar to enhance its catalytic efficacy. A negligible proportion of boron doping demonstrated a considerable influence on the elemental constitution and active sites of sludge-derived biochar, bringing about an advancement in the electro-Fenton activity for the eviction of sulfamerazine possessing removal rates of around 95.12% within 3 hours.[130] The physicochemical characteristics of nitrogen-doped biochar can be customized by co-doping with other foreign atoms within the carbon matrix. This methodology is capable of enhancing the reactivity of nitrogen-doped biochar by establishing synergetic bonding conformations.[131] Liu et al.[132] prepared sewage sludge-derived biochar doped with sulfur and nitrogen heteroatoms employing the HTC and chemical activation methodologies. The as-prepared adsorbent displayed unparalleled properties encompassing the existence of a considerable amount of mesopores, an enormously higher degree of graphitization, and heteroatomic doping. Maximal adsorption capacities of 440.53 mg g^{-1} were reported for acid orange 7 dye at 25 °C, ascribable to π–π stacking interactions and electrostatic attractive forces between the adsorbent and adsorbate, along with unsurpassed porosity.[132]

E. Characterization and physicochemical properties of biochar

1. Characterization of sludge-derived biochar

An extensive array of morphological, structural, and chemical characteristics is known to substantially influence the eventual utilization of sludge-based biochars. Hence, the comprehensive characterization of biochar prior to its application is imperative, employing profound analytical techniques like Brunauer–Emmett–Teller (BET) analysis, Fourier transform Infrared spectroscopy (FTIR), X-ray

29 August 2023 15:25:40

photoelectron spectroscopy (XPS), X-ray diffraction (XRD), Scanning electron microscopy (SEM) coupled with X-ray energy dispersive spectrometer (EDS), ultimate and proximate analysis, etc.[133] The desired properties of sludge-based biochar for application in the effluent treatment domain are related to enhanced polarity and surface functionalities, greater specific surface area, presence of distinct minerals like magnesium, iron, and calcium, and a formulated porous framework prevailed by microporous structures.[134]

In conjunction with EDS, SEM is used to analyze the distribution of mesoporous and microporous components, morphological structures, and elemental constitution of biochar.[135]

As illustrated, pure hydroxyapatite (HAP) was observed as an uneven, slack, and poriferous nanoparticle [Fig. 5(a)], while SS-derived biochar was noticed in the form of a heap of granular flakes [Fig. 5(b)] SEM analysis of HAP-modified SS-based biochar revealed the presence of a well-dispersed composite structure consolidating the granular flakes of SS-derived biochar and non-uniform hydroxyapatite nanoparticle [Fig. 5(c)]. EDS analysis substantiated the loading of HAP onto the SS-based biochar exhibiting higher capacity of P, O, and Ca [Fig. 5(d)]. Enhanced adsorption capacities toward Cd^{2+} and Cu^{2+} were ascribed to the uniform loading and good dispersion of HAP nanoparticles in the SS-based biochar adsorbent.[136]

XPS is conducted to analyze the elemental valence states and surface chemical characteristics of biochar-based adsorbents prior to and post-adsorption experiments. For instance, Liu et al.[135] denounced prominent peaks of chromium post-adsorption reaction, indicating that chromium could be effectually bonded on the magnetic biochar surface [Fig. 5(e)]. Figure 5(f) depicts chromium adsorption on the biochar surface at two characteristic valence states, notably at 576 and 585 eV for Cr (III) and at 577 and 587 eV for Cr (VI), respectively. Figures 5(g) and 5(h) illustrate a diminishment in the number of major peaks from 5 to 4. This peak elimination is attributable to Fe_3O_4 facilitating the reduction of Cr ions in the +6 oxidation state.[135]

FTIR spectroscopic studies ascertain the characterization of different functional moieties on the biochar-based adsorbent surface. FTIR spectrum of magnetic biochar (attained via the co-pyrolysis of SS and Fe^0) revealed pristine peaks of higher intensity at wavenumbers of about $2400 \, cm^{-1}$ post-adsorption attributable to the generation of hydroxyl functionalities on the biochar surface. Additionally, it was ascertained that post adsorption, the intensities of several peaks corresponding to 500, 800, 1050, 1400, 1650, 3100, and $3400 \, cm^{-1}$ wavenumbers were substantially lowered, signifying the involvement of Fe–O vibrations, –C–H– deformations, C=O stretching, CH_2/CH_3 functionalities, N–H groups, C–O–C stretching, and O–H stretching in the reduction process of Cr (VI) ions.[135]

BET analysis helps to evaluate the specific surface area (SSA) of biochar-based adsorbents. Agrafioti et al.[82] denounced enhanced BET surface area values for SS-derived biochar ascribable to augmentation of pyrolysis temperature. Biochar chemically modified with K_2CO_3 at ratios of 0.5 exhibited four times greater surface area at a pyrolysis temperature of 500 °C (SSA of K_2CO_3 modified biochar at 500 °C, $8.99 \times 10^4 \, m^2 \, kg^{-1}$) in contrast with that at 300 °C (SSA of K_2CO_3 modified biochar at 300 °C, $1.8 \times 10^4 \, m^2 \, kg^{-1}$) while the SSA of pristine biochar was increased to $1.39 \times 10^4 \, m^2 \, kg^{-1}$ with an enhancement in the pyrolysis temperature from 300 to 500 °C.[82]

XRD analysis provides information about the composition and crystalline components present in the biochar-based adsorbent. Major

diffraction peaks before and after adsorption studies were noticed in the proximity of $2\theta = 26.4°$ ascribable to quartz in magnetic biochars. Quartz served as the predominant crystalline component in biochar pre and post-adsorption. Post-adsorption peaks at $2\theta = 51°$ attributable to Fe^0 or Fe_3O_4 were observed, indicating that Fe^0 or Fe_3O_4 conceivably functioned as the electron donor for the reduction reactions associated with Cr (VI). New peaks corresponding to $2\theta = 31.1°$ were noticed from the XRD spectra imputable to the chemisorption of chromium ions.[135]

2. Physical and chemical characteristics of sludge-based biochar

Multifarious operational parameters associated with the synthesis of biochar possess diverse reaction mechanisms, chemistry, and physics, often resulting in end products with variegated physicochemical characteristics. The distinct features of the obtained end products are significant for multifarious applications, including effluent treatment, soil amelioration, energy conservation, catalysts for obtaining specific chemical conversions, precursor materials for catalysts, etc.[137] The predominant physical (surface area, porosity, pore volume, hydrophobicity, water retention) and chemical characteristics (ash content, pH, elemental composition, cation exchange capacity) of sludge-derived biochar are described in this subsection.

a. Physical characteristics.

(i)   Surface area:

Biochar surface area is enumerated using the BET method, contingent on the nitrogen adsorption statistics employing gas adsorption analyzers.[82] Greater surface area values inextricably linked to several additional characteristics like the cation exchange capacity is a fundamental requisite for various biochar applications. Biochar synthesized through the conventional pyrolysis technique is characterized by higher surface areas, while the residuals obtained through the HTC process possess lower surface area values.[138] Biochar surface area is augmented with higher pyrolysis temperature ascribable to the chemical compositional transformations associated with preliminary feedstock during pyrolysis. Enhanced pyrolysis temperature enhances the aromaticity of biochar and, consequently, the production of mesoporous and microporous structures accompanying greater biochar surface areas. For instance, Zhang et al.[81] reported an amplification in freshwater sludge-derived hydrochar and biochar surface areas from 15.69×10^4 to 28.58×10^4 and 9.65×10^4 to $10.5 \times 10^4 \, m^2 \, kg^{-1}$ at 140–180 and 300–500 °C, respectively. However, a minor reduction in biochar surface area was ascertained at a pyrolysis temperature of 700 °C, while the hydrochar surface area was lowered to $19.76 \times 10^4 \, m^2 \, kg^{-1}$ at 200 °C. This could be ascribed to the elimination of organic matter within the biochar surface and pores eventuating in greater surface area values and hydrochar pore wall deterioration subjected to greater pressures in the HTC process.[81]

(ii)   Porosity and pore volume:

Biochar porosity comprising zones of particulate matter devoid of solids is deduced from three predominant sources, namely, micropores (pore diameter: 0.1–50 nm), mesopores (pore diameter: 2–50 nm), and macropores (pore diameter:
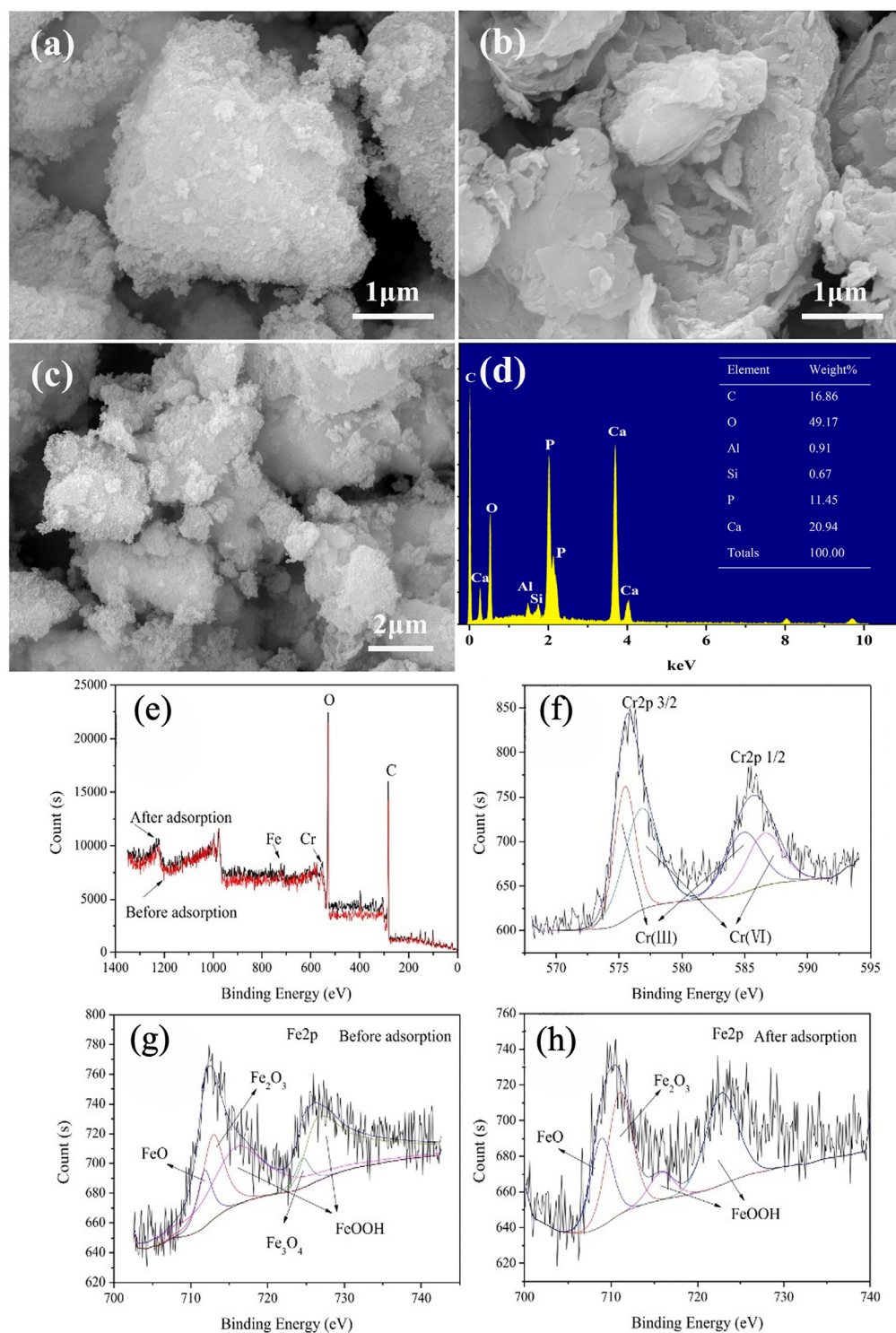
FIG. 5. Morphological characterization of (a) hydroxyapatite, (b) sewage sludge-based biochar, (c) hydroxyapatite modified sewage sludge-based biochar (H-SSB) using SEM, and (d) EDS spectrum of (H-SSB). Reprinted with permission from Chen *et al.*, Bioresour. Technol. **321**, 124413 (2021). Copyright 2020 Elsevier.[136] (e)–(h) XPS spectrum of magnetic biochar prior to and post-adsorption studies. Reprinted with permission from Liu *et al.*, J. Cleaner Prod. **257**, 120562 (2020). Copyright 2020 Elsevier.[135]

29 August 2023 15:25:40

50–10^6 nm).[18,139] Microporous components originating from gas vesicles generated during pyrolysis are substantial for greater adsorption capacities to retain organic contaminants, toxic metal ions, nutrients, and gases, while macropores emerge from the vascular framework of the biomass employed.[18] Biochar porosity is assessed using nitrogen adsorption-desorption isotherms employing automated surface area analyzers. The specimens are subjected to degassing for a specific duration prior to testing, followed by transference to the analysis station for nitrogen filling at −196.15 °C.[140] Micropore statistics and pore size distribution of biochar are customarily analyzed using the t-plot and Barrett–Joyner–Halenda (BJH) methods, respectively.[141] Méndez *et al.*[142] reported an enhancement in microporosity with intensified pyrolysis temperature from 400–600 °C accompanied by a diminishment of microporous volume for sewage sludge-derived biochar.[142] The total pore volume of freshwater sludge-derived biochar followed a rising trend from 0.31–0.36 cm^3 g^{-1} from 300 up to 500 °C, with a subsequent reduction in pore volume.[81]

(iii) Hydrophobicity:
Surfaces with static water contact angle (WCA) values < 90° having an affinity toward water are said to be hydrophilic, while the ones with WCA > 90° repelling water are referred to as hydrophobic substances.[143] Hydrophilic substances are characterized by polarity and are held together by intense hydrogen bonding interaction with water molecules. In contrast, hydrophobic substances are apolar and demonstrate weaker interactions with water molecules and more robust interactions with apolar liquids.[144] Biochar pyrolyzed at higher temperatures manifests an exceptionally hydrophobic structure inclusive of methodical carbon layers ascribable to the depletion of oxygenated functionalities and water content, engendering the as-prepared biochar to possess lesser hydrogen and oxygen-based functional moieties. Subsequently, the surface functionalities can function as electron acceptors or donors, causing the production of suitable domains with properties spanning from hydrophilic to hydrophobic and acidic to alkaline.[18] Owing to the pyrolysis processing parameters, various functionalities like –CH$_2$, –CH$_3$, O–H, CO=, and CC= present in biochar could be modified, fostering hydrophobic interactions in biochar.[145] Hydrophobic biochars promote the sorption of insolvable adsorbates, while hydrophilic biochars exhibit lower efficaciousness imputable to water adsorption; the existence of oxygen-based functionalities on the surface of hydrophilic biochars permits water permeation through hydrogen bonding, contributing to competitivity for the accessible biochar sites between the adsorbate and water molecules.[146]

(iv) Water retention:
The principal process during pyrolysis that regulates the hydrological characteristics of biochar includes enhancement in porosity that modifies its water adsorption capacity. The water retention capacity of biochar, i.e., its capability to withhold water, is inextricably associated with the porosity and interconnectedness within the porous framework.[147]

Biochars synthesized at elevated temperatures are known to retain a significant amount of water within the pores.[148] Although biochars prepared at lower temperatures possess a porous framework, they may not be facilely approachable owing to lower pore size, interconnectedness within pores, and the residual tar constituents blocking the pores.[149]

b. Chemical characteristics.

(i) Ash content:
Determining the ash content of biochars is essential as the kind and quantity of inorganic matter produced help in ascertaining the plausible end-use application. Ash content of sludge-derived biochars is computed using the ASTM D3176 standard by combusting the desiccated specimens at specified durations and temperatures and evaluating the residuals present post-heat treatment. The ash contents of hydrochars and biochars are inversely and directly related to the processing temperatures.[150] The reduced ash content of hydrochars with processing temperatures is accredited to ameliorated demineralization of mineral components in the super and sub-critical water regions.[151] Sewage sludge-based biochars exhibited higher ash content values spanning from 64.1%–79.1%, in contrast with the feedstock matter (ash content of SS: 55.8%–61.3%) at enhanced pyrolytic temperatures. This is inextricably linked to the nonvolatile mineral content constituting ash and the elimination of inflammable organic degradation products.[84] The ash content of freshwater sludge was around 38.6% and that of the synthesized hydrochars and biochars followed an ascending trend with an increment in the thermochemical transformation processing temperatures. The restrained minerals and detriment of volatile constituents could account for a greater ash content (> 51%).[81]

(ii) pH value:
Biochar pH is a significant characteristic to be considered for environmental remediation applications. The characteristics of biochars synthesized through the HTC process and pyrolysis vary substantially. Hydrochars synthesized through the HTC technique encompass the generation of organic acids engendering them to be acidic.[138] Various functional moieties in biochar, such as the formyl, hydroxyl, or carboxyl groups dissociated during the pyrolysis process, are principally acidic, and the residual solid becomes more alkaline as other functionalities are liberated. Enhanced pH values are explicitly associated with intensifying degree of carbonization.[138,152] The pH of the freshwater sludge was neutral at 6.57. Contrarily, the pH of the synthesized biochar was augmented from 4.91 to 7.78 with enhanced biochar temperatures from 300 to 700 °C, while hydrochar exhibited acidic pH values spanning from 4.32 to 4.50, and an inconsiderable diminishment in pH values was noticed at elevated HTC processing temperatures. The rise in pH values of biochar was elucidated by ash amelioration and condensation/polymerization reactions associated with the elimination of hydroxyl and carboxyl functional moieties occurring during pyrolysis.[81]

(iii) Elemental composition:
Biochar synthesis is often associated with modifications in its chemical constitution leading to an enhancement in

carbon content in comparison with the unprocessed biomass feedstock. This could be accredited to the dissociation of oxygen and hydrogen-based functionalities. The predominant elemental compositions of biochars include hydrogen (H), carbon (C), and oxygen (O), with minor quantities of phosphorous (P), silicon (Si), iron (Fe), sulfur (S), and nitrogen (N) with amounts lesser than that in hydrochars that are ascribable to the dissolution and the flushing out of inorganic components with subcritical water. The overall elemental composition of sewage sludge-derived biochars comprised 3.5%–5.7%, 3.8%–5.1%, 4.4%–14.8%, and 21.6%–26.2% of N, H, O, and C, respectively. A substantial diminishment in the O, H, and N proportions was ascertained in the biochars post pyrolysis against the primary sewage sludge.[84]

(iv)   Cation exchange capacity:

Cation exchange capacity refers to the quantity of exchangeable cations like Mg^{2+}, NH_4^+, Na^+, K^+, and Ca^{2+} that the substance can retain.[153] It is the consequence of negative surface charges enticing cationic entities and is often utilized to expound soil fertility (since all the nutrients utilized by microorganisms and plants are absorbed in the form of ionic matter).[154] The cation exchange capacity is explicitly contingent upon various parameters, including surface morphology, functional moieties imparting the necessary surface area, and charges rendering the surface charges accessible.[155] The estimation of cation exchange capacity is unequivocally reliant on the pH values at which the solutions are prepared employing various solvents.[156] The cation exchange capacity values are augmented with an enhancement in pH values.[153] Moreover, biochars synthesized at lower pyrolysis temperatures in which the surface area was substantially ameliorated and adequate functional moieties were present, exhibited superior cation exchange values.[157]

F. Factors influencing the properties of sludge-derived biochars

Processing conditions involved in the thermochemical transformation of sludges are known to substantially impact the characteristics of the synthesized biochar. Some preeminent parameters encompassing temperature, residence time, feedstock type, and heating rate, influencing biochar characteristics are delineated here.

(i)   Temperature:

Pyrolysis process temperature affects the structural framework and various physicochemical characteristics of biochar, such as surface area, pore structure, elemental constituents, and functional moieties.[158] Biochar obtained through fast pyrolysis (pyrolysis temperature > 500 °C) comprises a conjugated aromatic framework. At elevated temperatures, the hydrophobicity of biochars is enhanced due to the elimination of surface functional moieties. The microporous network of biochars and their surface areas are intensified with enhanced pyrolysis temperatures imputable to the degasification of the biomass feedstock in the process. Fast pyrolysis is characterized by a lower degree of carbonization, signifying a lesser amount of fixed carbon matter. Consequently, the biochar yield in the case of fast pyrolysis is comparatively lower, spanning from around 10%–20%, while the biochar yield ranges from 30%–60% in the slow pyrolysis technique.[18] The oxygen–carbon and hydrogen–carbon molar proportions of sewage sludge-based biochar substantially diminished with enhanced pyrolysis temperature resulting in increased aromatic condensation and carbonization reactions.[159]

Chen et al.[160] analyzed the impact of pyrolysis temperatures on the properties and adsorptive characteristics of municipal sludge-based biochar. With an enhancement in pyrolysis temperature from 500 to 900 °C, the microstructure development and ash content were expedited, while the biochar yield was reduced. The as-prepared biochar demonstrated favorable thermal stability, and the leaching toxicity of biochar was maintained within secure limits. 900 °C was considered the optimum pyrolysis temperature for energy recovery and toxic metal ion adsorption.[160]

(ii)   Residence time:

Amplifying the biochar residence time at higher pyrolysis temperatures can considerably influence the biochar pH and yield, whereas extending the residence time at depreciated pyrolysis temperatures resulted in an abatement of the biochar yield and considerable augmentation in its iodine adsorption number and pH.[161]

(iii)   Heating rate:

Heating rate values significantly influence the biochar yield, with lower heating rates being beneficial. Lower heating rates can induce a considerable duration for the domineering impact of pyrolysis temperature on biochar stability at elevated temperatures.[162] Furthermore, lower heating rates can enhance the aromaticity and retain the structural intricacy of biochars, while greater heating rates produce enormous amounts of liquid portions decreasing the biochar yield as a consequence of hemi cellulosic and lignocellulosic depolymerization of biomass, phase transformation, local melting, and inflammation of cells.[18] Insignificant ring clusters were ascertained in biochars synthesized at greater heating rates with some biomass feedstocks subsisting unvaried.[163] Heating rates spanning from 5 to 20 °C min⁻¹ during the pyrolytic transformation process had no statistical impact on the stable volatile constituents, fixed carbon, and O/C and C proportion.[164] Taking into account both biochar stability and yield, lower heating rates are preferable even though it is a cumbersome process.

(iv)   Feedstock type:

Biomass feedstock is a significant parameter regulating the physicochemical properties of the as-prepared biochars, eventually determining its end-use application.[165] An extensive array of waste biomass, including woody residue and sludges, has been employed as the feedstock for different thermochemical conversion methods. Among various types of sludges, freshwater sludge being deduced from coagulating agents and originating from drinking water processing plants is bestowed with lower amounts of noxious elements owing to its pure water ingression (predominantly

29 August 2023 15:25:40

underground water, repositories, etc.), engendering it to be a virtuous biomass feedstock for generating superior quality biochars and hydrochars as against other types of sludges.[81]

(v)　Carbonization atmosphere:

The carbonization process is carried out in oxygen/air-deficient atmospheres or inert gas conditions. The inert gases employed must be non-reactive and stable and should possess the capability of bringing about the decomposition of the substance without oxidation.[166] Moderate to considerable amounts of vapors are generated during the pyrolysis of sludge-based biomass feedstock and these vapors if not purged, will entail themselves in secondary reactions capable of altering the constitution and nature of the pyrolysis by-products. Argon, carbon dioxide helium, nitrogen, ammonia, and water vapors can be utilized as the carrier gas for pyrolysis, but nitrogen is the most prevalent carrier gas for purging vapors generated during the thermochemical transformation process ascribable to its convenient accessibility, inertness, and cost-efficiency in contrast with the other inert gases.[167] Besides the customarily employed argon and nitrogen carrier gases, incipient injected gases are capable of altering the physicochemical characteristics of sludge-based biochar. For instance, carbon dioxide is known to intensify the defective framework of biochar,[168] while the utilization of ammonia serves as an effectual methodology for doping nitrogen on biochar surface.[169]

Aktar et al.[86] examined the effect of various carrier gases on the yield, physicochemical, and structural characteristics of biochar. Biochar synthesized in a nitrogen atmosphere possessed greater alkalinity and exhibited enhanced salinity, while the biochar prepared in a carbon-dioxide environment displayed greater surface area. The FTIR spectrum of biochar synthesized in an inert atmosphere of carbon dioxide evinced a reduction in functional moieties including C=C, C=O, –OH, and –CONH– with rising pyrolysis temperature. Conversely, the band intensity for Si–O–C or Si–O–Si and hetero-aromatic and aromatic frameworks were more substantial in biochar produced in the carbon dioxide atmosphere compared to the nitrogen atmosphere. Substituting an exorbitant inert gas (nitrogen) with carbon dioxide is intriguing ascribable to the abatement in operational expenses and attainment of equivalent biochar yields with ameliorated porosity and some analogous physicochemical characteristics.[86] In another study, Guo et al.[170] assessed the impact of the atmosphere (100% N_2, 100% CO_2, or 10% CO_2/90% N_2) on the pyrolysis of municipal sludge in a horizontal tube furnace. The carbon-dioxide environment displayed a considerable influence on carbon content. At lower pyrolysis temperatures (<600 °C), carbon dioxide functioned as an inert gas, restraining deterioration of the carbonous framework, while at greater temperatures (>600 °C), carbon dioxide operated as a reactive gas, fostering the volatilization of carbonous matter. The total pore volume and S_{BET} of the as-prepared biochar were augmented with an increment in the pyrolysis temperatures from 300 to 500 °C, with the values apprehended for carbon dioxide surpassing that of nitrogen. Furthermore, the employment of CO_2 during the pyrolysis technique could ameliorate the porous framework of biochar and impart a keystone for utilization as an adsorbent in the future.[170]

The utilization of CO_2 as the carrier gas along with a mixed feedstock for the pyrolysis process could reduce the toxicity of SS-derived biochar. Co-pyrolysis of sewage sludge with willow extracts substantially decreased the toxicity of SS based-biochar toward L. Sativum. The amendment of carrier gas from nitrogen to carbon dioxide, irrespective of the biomass feedstock employed, in a majority of the instances decreased the toxicity and positively impacted the test organisms.[171]

IV. APPLICATION OF SLUDGE-DERIVED BIOCHAR IN ENVIRONMENTAL REMEDIATION

Sludge-based biochar is extensively utilized in environmental remediation as a soil ameliorating agent, serving propitious for crops and mitigating climatic fluctuations, promoting carbon sequestration, and facilitating renewable energy production. Biochar is bestowed with greater specific surface area, tunable porosity, and functionalities, active functional sorption sites like –OH, –COOH-, –C=C–, –C–C–, aromatic carbon frameworks, and mineral crystalline phases, effectuating them as multifaceted adsorbents for capturing a diverse array of toxic metals ions, antibiotics, microplastics, dyes, microbial and organic contaminants from wastewater and soil.[19] The efficacy of biochar in adsorbing organic and inorganic pollutants is contingent on its affinity for non-polar functional moieties, cation exchange capacity, greater surface area to volume ratio, and intrinsic characteristics of adsorbate, adsorbent, and ecological conditions.[71] Biochars modified with various elements or co-pyrolyzed with other biomass feedstock matter exhibit enhanced adsorption performance.

This section focuses on drinking water, fecal, and raw sewage sludge-derived adsorbents for evicting toxic metal ions, antibiotics, microplastics, and the catalytic degeneration of organic pollutants from wastewater, emphasizing the predominant adsorption mechanisms involved and the adsorption kinetic models and isotherms customarily employed. The adsorption of toxic gases, vermicomposting approach, and soil amelioration employing sludge-based biochar are also accentuated here.

A. Adsorption of various contaminants from wastewater

Sludge-derived biochars have been substantiated to be efficacious adsorbents for eliminating toxic metal ions, microplastics, and antibiotics along with the catalytic degradation of organic compounds which is outlined below.

1. Toxic metal ions

Heavy metals categorized as a class of trace elements (metalloids or metals) possessing atomic densities higher than 4 ± 1 g/cc [e.g., Zinc (Zn), Lead (Pb), Silver (Ag), Cadmium (Cd), Iron (Fe), Astatine (As), Nickel (Ni), Chromium (Cr), Aluminum (Al), Copper (Cu), etc.] are usually regarded as pervasive noxious water and soil pollutants. The primary sources of heavy metal ions in effluent could be anthropogenetic, like landfilling, manufacturing processes, agrarian activities, metal plating, ore processing, etc. or natural, like soil-run off, the disintegration of minerals and rocks, volcano eruption, etc. Owing to the durability, greater expatriation, and solubility of toxic metal ions in water, unprocessed wastewater comprising metallic pollutants leads to diverse ecological and health consequences when discharged into water streams. The toxic metal ions are thereby assimilated in the plants, ingressing humans, and organisms via food cycles,

29 August 2023 15:25:40

detrimentally impacting their health and biological functioning.[172] The maximum permissible level of contaminants in freshwater resources laid down by the US EPA, along with their pernicious impacts on human health, is enumerated in Table V.

Toxic metal ions can be eliminated from wastewater[174–185] through an extensive array of techniques like solvent extraction, ion exchange, membrane filtration,[186] chemical precipitation, coagulation, flocculation, electrochemical removal, etc. Nevertheless, these methodologies pose some drawbacks associated with greater energy consumption, lower efficacy, incomplete removal, expensive disposition, and susceptible operational parameters. The adsorption technique[20,187–196] is usually preferred over the aforestated wastewater treatment strategies owing to its inherent advantages like cost-effectiveness, convenient operation, and a considerable influence on toxicity, transfer, and bioavailability of metal ions in the hydrous medium. Some prominent conditions impacting the efficacy of adsorbents for eliminating toxic metals from effluent include temperature, the dosage of adsorbent, contact time, initial adsorbate concentration, stirring speed, and pH.[172]

Investigators are exploring the adsorption of a broad spectrum of heavy metal ions from effluent, inclusive of Cu, As, Cd, Pb, Cr, Ni, and Zn, through sludge-derived biochar.[82,135,136,197–200] The predominant adsorption mechanisms in unmodified biochar include chemisorption through ion exchange, electrostatic attraction, surface complexation, redox reactions, precipitation, inner sphere complexation, and physisorption (based on the porous framework and specific surface area of biochar) through plentiful functional moieties like –OH, –COOH, and oxygen comprising groups existent on the biochar surface. Multifarious mechanisms associated with the interaction of toxic metal ions with biochar in the adsorption phenomenon[201] are illustrated in the supplementary material (Fig. S3).

The adsorptivity of heavy metals from water can be ameliorated through various chemical and physical modification strategies executed post or pre-pyrolysis of biochar for optimizing surface characteristics. Physical modification of biochar involves steam activation or CO_2 activation, which enhances the biochar surface area, while chemical modification techniques typically include treating biochar with bases, acids, organic substances, carbonaceous material, nanomaterials, metals, and metal oxides.[202]

Zhang et al.[197] analyzed the adsorption mechanisms of hydrochar and biochar obtained through HTC and pyrolysis of DWS for efficient removal of Pb prevalent in swine wastewater employing microstructural analysis and batch adsorption studies. The utmost adsorption capacities (Q_0) for Pb spanned in the range of H180–200: $6 \, mg \, g^{-1}$ < H140–160: $13 \, mg \, g^{-1}$ < B300: $37 \, mg \, g^{-1}$ < B500–700: $71 \, mg \, g^{-1}$ signifying that Pb uptake through biochar was a

heterogeneous approach and fitted well with the Freundlich adsorption model while hydrochar exhibited monolayer adsorption delineated by the Langmuir model. The predominant adsorption mechanisms involved were electrostatic interaction and surface precipitation of lead hydroxide and lead carbonate.[197] The influence of various pyrolysis parameters, namely, residence time, chemical impregnation of SS, and temperature, on the yield of biochar generation was analyzed by Agrafioti et al.[82] Maximum biochar yield was obtained when SS was subjected to a pyrolysis temperature of $300\,°C$ while SS modification using K_2CO_3 eventuated in enhanced surface area, five times greater than the biochar specimen at $500\,°C$. The unmodified biochar employed in batch kinetic experimental studies was capable of adsorbing 30% and 70% of As (V) and Cr (III), respectively, signifying that biochar adsorbent was highly efficacious in eliminating cations compared to anions from water.[82] Magnetic biochar fabricated via the co-pyrolysis of SS and nano-zero-valent iron (Fe^0) for the withdrawal of Cr (VI) from synthetic wastewater was denounced by Liu et al.[135] The elimination of Cr (VI) [adsorption capacity of Cr (VI): $11.56 \, mg \, g^{-1}$] was greater than that of Cr_{Total} (adsorption capacity of Cr_{Total}: $9.840 \, mg \, g^{-1}$) at all reaction conditions demonstrating a selective reduction of Cr (VI) to Cr (III) with subsequent removal by adsorption. The elimination of Cr_{Total} and Cr (VI) could be expounded through the Freundlich and Langmuir adsorption isotherms, respectively, while favorable kinetic fitting data of the pseudo-second order model indicated that the removal of Cr could be ascribed to chemisorption. The rate-regulating steps associated with Cr removal included liquid-film and intra-particle diffusion processes. Characterization of biochar pre and post-adsorption studies indicated that the electron donors favoring the reduction of Cr (VI) could be Fe^0, Fe^{2+}, or organic matter present in biochar.[135]

In a separate investigation, Chen et al.[136] delineated SS-based biochar subjected to chemical modifications with hydroxyapatite (HAP) for the efficacious eviction of Cd (II) and Cu (II) from water. The adsorption capacities and removal efficacies (in percentage) of the targeted metal ions were examined through the following equations:

Adsorption capacity:

$$q_e = \frac{V}{M} \times (C_0 - C_e). \quad (13)$$

Removal efficiency (%):

$$R\,(\%) = \frac{(C_0 - C_e)}{C_0} \times 100. \quad (14)$$

Batch adsorption studies demonstrated greater adsorptivity for HAP-modified SS [adsorptivity of Cd (II): 114.68 and Cu (II): $89.98 \, mg \, g^{-1}$]

TABLE V. Maximum permissible limit of heavy metals in freshwater along with their detrimental impacts on human health.[172,173]

Toxic metal ion	Adverse health effects	Maximum permissible level of pollutant ($mg \, l^{-1}$)
Lead	Neurotoxic and cerebral effects, circulatory and renal diseases	0.006
Cadmium	Renal, respiratory, and cardiovascular disorders	0.01
Astatine	Visceral cancer, vascular, and skin disorders	0.05
Chromium	Hyperkeratosis, diarrhea, mental retardation, and cancer	0.05
Nickel	Lung fibrosis, dermatitis, and cardiovascular disorders	0.20
Zinc	Anaemia, nausea, lethargy, abdominal pain, and neurological disorders	0.80

in contrast with the raw sludge-derived biochar attributable to chemisorption. Characterization studies through X-ray photoelectron spectroscopy (XPS), Fourier transform infrared spectroscopy (FTIR), and X-ray diffraction (XRD) substantiated the predominant mechanisms involved: ion-exchange with calcium cation, complexation with carboxylic acid and hydroxyl functional moieties, and the generation of π-π binding sites between the targeted metallic pollutant and aromatic alkene functionalities on the adsorbent surface.[136] Table VI summarizes various kinds of sludge-based biochar employed in the eviction of toxic metal ions from wastewater, along with their processing parameters, adsorption isotherms, and kinetic models.

a. Adsorption kinetics and isotherms.

(i)   Adsorption kinetics models
      Adsorption kinetics models render explicit data about the reaction and diffusion rates while ascertaining the time needed for the sorption process to attain equilibrium. Greater reaction rates manifest rapid sorption of adsorbates. Adsorption kinetics parameters deduced from batch experiments are essential in prophesying the transmission of adsorbates through perforated medium and fixed bed sorption efficiency. To acquire in-depth apprehension about the manner of adsorption, fitting empirical information obtained through batch kinetic studies into various kinetic models is imperative, along with other methodologies encompassing the analysis of adsorption isotherms, surface properties characterization, and thermodynamics to explicate the intrinsic adsorption mechanism (such as physisorption and covalent bonding).[205] Some of the commonly used mathematical models to examine the kinetic data derived through batch adsorption experiments have been outlined in Table VII.

(ii) Adsorption isotherm models
      Adsorption isotherms are quantitative approaches employed for the characterization of adsorbate equilibria associated with solid and liquid phases at persistent atmospheric temperatures. The data derived from adsorption isotherms is utilized for acquiring details pertaining to the maximal adsorption capacity of sorbents, and sorption phenomena, which is substantial in assessing the efficacy of adsorbents while catering to optimizing adsorption mechanisms and designing efficient and cost-effective treatment strategies. Some of the extensively used adsorption isotherm models for sludge-based biochar adsorbents characterized and predicated on the number of adsorption model parameters are summarized in Table VIII.

2. Catalytic degradation of organic compounds

The catalytic degeneration of organic contaminants engendered by biochar has been denounced by several researchers appertaining to various characteristics, including (i) the presence of ubisemiquinone and graphitizing frameworks functioning as electron donors and acceptors and (ii) persistent free radicals engendered in the process of biochar synthesis with a lifespan ranging from several days to months.[213] Sludge-based biochar as catalytic materials exhibited very promising catalytic activity toward an extensive array of organic

contaminants through various catalytic mechanisms, including percarbonate, peroxymonosulfate, hydrogen peroxide activation, and heterogeneous Fenton oxidation.

For instance, Hung *et al.*[214] reported freshwater sludge-based biochar comprising ferromanganese prepared via single-stage pyrolysis to facilitate the Fenton-like reaction for disinfecting phthalate ester (PAEs) based organic pollutants. Maximal PAE degeneration of 90% was observed within 12 h with 1.7 g/l of biochar (pyrolyzed at 900 °C) at pH 6. The remarkably efficient PAE degeneration was accredited to the synergistic interactions between MnO_x and FeO_x, intensifying the catalytic activation of percarbonate functionalities through the transfer of electrons, the inclusion of hydroxyl moieties, abstraction of hydrogen atoms via non-radical and radical oxidative pathway and the PAE oxidation mechanism fitted well with the pseudo-first-order kinetics model.[214]

In another investigation, Luo *et al.*[213] synthesized biochar through the pyrolytic transformation of SS for activating hydrogen peroxide (H_2O_2) for subsequent degeneration of ciprofloxacin (CIP) in aqueous solutions. Experimental analysis revealed that biochar subjected to chemical modification with HNO_3 demonstrated ameliorated catalytic activity for the activation of H_2O_2 compared to unmodified biochar. Catalytic oxidative reactions engendered by persistent free radicals attributed to 70.19% and 61.69% of the unmodified and chemically treated biochar, respectively, connoting the fundamental contribution of PFRs associated with the decontamination of CIP. The plausible mechanism significantly correlated with the catalytic activation of H_2O_2 by sludge-based biochar encompassing the following stages is depicted in the supplementary material (Fig. S4):

(i)   Biochar possesses enormous defects and is bestowed with abundant oxygen comprising functional moieties.
(ii) The prominent reactive centers catering to the catalytic activation of H_2O_2 include C=O, sp^2 hybridized C=C, pyridinic, and pyridonic nitrogen.
(iii) Hydroxyl free radicals ($\cdot OH$) are liberated during the transmission of a single electron from the aforementioned prominent reactive centers of PFRs present in biochar to hydrogen peroxide.[213]

Huang *et al.*[215] denounced the disintegration of Trichloroethylene (TCE) employing the heterogeneous Fenton oxidation process catalyzed by SS-based biochar. The maximal TCE removal efficacy of 83% was ascertained at a pH of 3.1 through the catalytically activated 300 W biochar with the most negligible environmental implications. SS subjected to microwave pyrolysis at 300 and 400 W power levels, respectively, demonstrated ameliorated catalytic activities in contrast with the biochar synthesized at 200 W microwave power owing to the plausibly greater specific areas and iron content in the former.[215]

The fabrication of SS-based carbon-supported MnO_x catalytic material via ammonium hydroxide activation and pyrolytic transformation to foster the degradation of peroxymonosulfate (PMS) and consequent decomposition of Acid orange 7 (AO7) and Rhodamine B dyes were denounced by Mian *et al.*[216] Characterization studies revealed the generation of Mn (manganese) oxides of different valences on the hybrid SS-derived catalyst, while NH_4OH treatment augmented the surface area, porousness, and nitrogen atoms. The aforestated catalyst could activate PMS for the complete degradation

29 August 2023 15:25:40

TABLE VI. Different sludge-derived biochar adsorbents for capturing heavy metal ions encompassing process parameters, adsorption kinetics models, and adsorption.

Sludge type	Modification	Biochar production method—processing parameters	Heavy metal ion targeted (adsorbate)	Adsorption process parameters	Adsorption capacity (q) (mg g^{-1})	Removal efficiency	Adsorption isotherm	Kinetics model	Reference
DWS	$\cdots$	Pyrolysis: T: 300, 500, and 700 $^\circ C$, t: 1 h, HR: 10 $^\circ C$ min^{-1}HTC:T: 140, 160, 180, and 200 $^\circ C$, t: 4 h	Pb (II)	C: 20.7, 41.4, 62.1, 103.5, 207, 414, 621, 1035 mg l^{-1}, pH: 4–8	H180-200: 6, H160: 13, B300: 37, B500-700: 71	$\cdots$	BC: Langmuir – (R^2: 0.8–0.9), HC: Freundlich – (R^2: 0.86–0.98)	$\cdots$	197
SS	Pre-treatment with K$_2$CO$_3$ and H$_3$PO$_4$	Pyrolysis:T: 300, 400, and 500 $^\circ C$, t: 30 min, HR: 17 $^\circ C$ min^{-1}	Cr (III), As (V)	C: 0.05 mg l^{-1} [As (V)], 0.2 mg l^{-1} (Cr (III), D: 4 g l^{-1}		Cr (III): 70%, As (V): 30%	$\cdots$	Pseudo second order: R^2: 0.99 [Cr (III)], 0.95 (As^{5+})	83
SS	Co-pyrolyzed with Fe^0	Co-pyrolysis:T: 500 $^\circ C$, t: 1 h, HR: 5 $^\circ C$ min^{-1}	Cr (VI), Cr$_{Total}$	C: 20–60 mg l^{-1}, T = 14.85–44.85 $^\circ C$, t = 24 h, pH: 2–6	Cr (VI): 11.56, Cr$_{Total}$: 9.40	$\cdots$	Cr (VI) removal—Langmuir, Cr$_{Total}$ removal—Freundlich	Pseudo-second order (R^2 > 0.999)	135
SS	Co-precipitation with HAP	Pyrolysis: T = 500 $^\circ C$, t: 2 h, HR: 5 $^\circ C$ min^{-1}	Cu (II), Cd (II)	C: 100 mg l^{-1}, D: 1 g l^{-1}, t = 24 h, T = 25 $^\circ C$, pH: 3–6 [Cu (II)], 3–8 [Cd (II)]	Cu (II): 89.98, Cd (II): 114.68	$\cdots$	Langmuir	Pseudo second order: R^2: 0.9997 [Cu (II)], 0.9998 [Cd (II)]	136
FS	Chemical modification with KOH	HTC:T = 200 -, t: 5 h	Cu (II)	D: 0.25, 0.5, 1, 2 g l^{-1}, C: 40 mg l^{-1}, t = 1440 min, T = 27 $^\circ C$, pH: 5	Cu (II): 18.6	Cu (II): 93%	Freundlich (R^2: 0.872), Langmuir (R^2: 0.958)	Pseudo second order (R^2: 0.9997), intra-particle diffusion (R^2: 0.8225)	203
SS with phosphorous content varying from 4–60 mg g^{-1}	$\cdots$	Pyrolysis: T = 700 $^\circ C$, t = 1 h	Cr (VI)	C: 200 mg l^{-1}, T: 25 ± 1 $^\circ C$, t = 24 h, pH: 4	Cr (VI): 6.29 for P20	$\cdots$	Langmuir (R^2: 0.9764–0.9972) for P4-P60	Pseudo second order (R^2: 0.999-1) for P4-P60	204

TABLE VII. Customarily employed adsorption kinetic models encompassing their significance and mathematical equations for fitting empirical data.[135,136,206–208]

Kinetic model	Significance	Equation
Pseudo-first order (PFO)	PFO kinetic model, also referred to as the Lagergren model, delineates adsorption rates in solid–liquid systems contingent on the adsorption capacity obeying the first-order mechanism.	$\ln(q_e - q_t) = lnq_e - k_1 t$
Pseudo-second order (PSO)	PSO relies on the presumption that the solute adsorption is proportionate to the accessible adsorbent sites, and the reaction rate is contingent on the proportion of solute on the adsorbent surface—the driving force for the reaction is proportional to the number of available active adsorbent sites.	$\frac{t}{q_t} = \frac{1}{k_2 q_e^2} + \frac{t}{q_e}$
Elovich model	The Elovich model formulated by Zeldowitsch is used to ascertain the chemisorption manner of adsorption. It is used to comprehend the nature of adsorption and envisage deactivation–activation energies and surface and mass diffusion of systems.	$q_t = \frac{1}{\beta}\ln(\alpha\beta) + \frac{1}{\beta} lnt$
Intra-particle diffusion (IPD) model	The IPD model contemplated by investigating the Weber and Morris model is extensively utilized to analyze the rate-limiting phase of the adsorption process. The adsorption of solute within a solution is associated with film diffusion (mass transfer of adsorbate), accompanied by surface and pore diffusion steps.	$q_t = {}_i t^{1/2} + C'$
Liquid film diffusion model	Boyd et al. first reported this adsorption kinetic model to ascertain whether the practical rate-determining step occurs due to pore diffusion or film diffusion. Adsorption is evaluated as a regulated film diffusion mechanism.	$\ln\left(1 - {}^{Q_t}/_{Q_e}\right) = -k_{fd}t$

of acid orange 7 dye within 40 min in a broad pH range. In contrast, the pristine SS-derived biochar displayed a removal efficacy of only 16%. Secondary (radical) as well as primary (non-radical) processes regulated the activation mechanism of PMS, followed by the eventual decomposition of AO7, while N-carbon and MnO_x functioned as the major sites and the carbonyl moieties and oxygen defects served as the secondary reaction sites in the disintegration process. Owing to the existence of surface functional moieties, PMS and AO7 molecules that underwent ionization reactions could be embedded on the catalyst surface for activation. The phases involved in the Mn^{3+}/Mn^{4+} and Mn^{2+}/Mn^{3+} redox cycle of the MnO_x component of the catalyst for the generation of hydroxyl ($\cdot OH$) and sulfate ($SO4\cdot^-$) free radicals are depicted in the reactions given as follows:[216]-

$$Mn^{2+} + HSO_5^- \rightarrow Mn^{3+} + SO_4^{\cdot -} + OH^-$$
$$Mn^{3+} + HSO_5^- \rightarrow Mn^{4+} + SO_4^{\cdot -} + OH^-$$
$$Mn^{4+} + HSO_5^- \rightarrow Mn^{3+} + SO_5^{\cdot -} + H^+$$
$$SO_4^{\cdot -} + H_2O \rightarrow \cdot OH + SO_4^{2-} + H^+$$

$$(15)$$
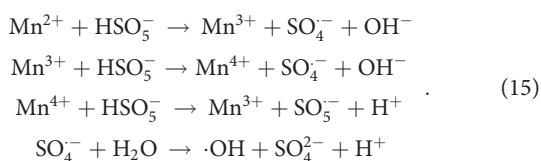
In another study, SS-derived biochar doped with nitrogen was synthesized via single-stage pyrolytic transformation and utilized for the catalytic activation of PMS by Mian et al.[217] The nitrogen content of the as-prepared biochar was modified by incorporating varying proportions of melamine with precursors. At the optimal dosage, 20 mg/l Rhodamine B was eliminated by 99.4% within 20 min employing 250 and 200 mg/l of PMS and catalyst, respectively. Moreover, absolute decoloration of a mixture of seven anionic and cationic dyes was attained within 50 min through 350 and 200 mg/l of PMS and

catalyst, respectively, denoting the efficacy of the catalyst in processing a mixture of organic contaminants. The predominant degradation mechanisms involved in this study were non-radical processes effectuated through the pyridine nitrogen-governed oxidative decomposition of contaminants in lieu of the hydroxyl and sulfate free radical processes influenced via surface metal oxides, graphitic nitrogen, and carbonyl functional moieties.[217]

Huang et al. reported sewage sludge-based biochar as an efficacious catalytic material activating peroxymonosulfate to disintegrate Bisphenol-A (BPA) pollutants. An average pollutant removal rate of 3.21 mol BPA^{-1} mol oxidant^{-1} h was attained by peroxymonosulfate across a diverse range of pH spanning from 4 to 10 at adsorbent dosage values of 0.2 g l^{-1}. A superior mineralization efficacy of around 80% (total organic carbon elimination) was achieved within 30 min. Subsequent studies of catalytic degradation mechanisms revealed that dioxidene catalytically generated by the ketonic framework within the biochar served as the primary reactive species accountable for the disintegration of bisphenol-A.[218] In another study, SS-derived biochar modified with nano-Fe_3O_4 was utilized as a catalytic material to activate peroxymonosulfate for the subsequent degradation of rhodamine-B from effluent. The as-prepared biochar catalyst (5S@Fe-500: mass ratio of sludge and $Fe(NO_3)_3 \cdot 9H_2O$—5:1 and calcined at 500 °C) demonstrated exceptional permeance and catalytic activity in the disintegration of rhodamine-B (50 mg l^{-1} could be disintegrated within 10 min) ascribable to the porous structure, appropriate iron content, and optimal dispersion of iron on the catalytic surface.[219] Table IX designates sludge-based biochar utilized for the catalytic degradation of various organic compounds comprising the catalysis mechanism and processing parameters employed.

TABLE VIII. Adsorption isotherm models (categorized based on the number of model parameters) representing their significance and mathematical expressions involved.[209–212]

Type of adsorption isotherm	Adsorption isotherm model	Significance	Equation
Two-parameter model	Langmuir adsorption isotherm	As per the Langmuir theory, the adsorption phenomenon onto solid surfaces is predicated on a kinetic principle that involves the unremitting bombardment of molecules onto the surface with the evaporation or desorption of the correspondent molecules from the surface with a zero-aggregation rate at the surface. It is predicated on the presumption that single-layer adsorption eventuates at distinct homogeneous adsorbent sites, with each molecular entity possessing constant enthalpies and sorption activation energies. Once an adsorbed molecular entity penetrates the site, no subsequent adsorption occurs, thereby attaining equilibrium, and the saturated monolayer curve can be explicated based on the Langmuir model equation.	$\frac{c_e}{q_e} = \frac{c_e}{Q_0} + \frac{1}{b'Q_0}$
Two-parameter model	Freundlich adsorption isotherm	The sorption process is characterized by multi-layered adsorption on heterogeneous sites. In this isotherm model, adsorption affinities and heat need not be disseminated consonantly on the heterogeneous surface. The exponential distribution of functional sites and the energies of the active sites, along with the surface heterogeneity, is described using the expression for the Freundlich adsorption isotherm. It is pertinent with systems possessing heterogeneous surfaces in the gaseous phase.	$\log q_e = \log k_F + \frac{1}{n} \log c_e$
Two-parameter model	Langmuir–Freundlich adsorption isotherm	This adsorption isotherm model depicts the dissemination of sorption energy upon heterogeneous sites of the absorbent. At lower adsorbate concentrations, this isotherm befits the Freundlich model, while at elevated adsorbate concentrations, it transposes to the Langmuir model.	$q_e = \frac{Q_{LFM}(k_{LF}c_e)^{M_{LF}}}{1+(k_{LF}c_e)^{M_{LF}}}$
Two-parameter model	Temkin model	This adsorption isotherm primitively employed for hydrogen adsorption onto platinum electrode system in acidic medium, contemplated as a chemisorption system, scrutinizes adsorbate-adsorbent interaction neglecting extraordinarily lower and higher concentrations. The sorption heat associated with all the layers undergoes a linear decrement with exposure as a result of adsorbent-adsorbate interactions. Additionally, it presupposes that the heat depletion in adsorption is linear in lieu of logarithmical as delineated by the Freundlich isotherm.	$q_e = \frac{RT}{b_T} \ln A_T + \frac{RT}{b} \ln c_e$
Two-parameter model	Brunauer–Emmett–Teller (BET) model	BET model is a conceptual adsorption isotherm pertinent to gas-solid equilibrium systems. Multilayered sorption processes	$q_e = \frac{q_s c_{BET} c_e}{(c_s - c_e)\left[1+(c_{BET}-1)\left(^{c_e}/_{c_s}\right)\right]}$

TABLE VIII. (*Continued.*)

Type of adsorption isotherm	Adsorption isotherm model	Significance	Equation
		possessing approximate pressure values spanning from 0.05–0.30 congruent with monolayered coverage values of 0.5–1.50 were deduced from this adsorption model. Typical applications of this isotherm include ascertaining the surface area of the adsorbent appertaining to nitrogen sorption data.	
Two-parameter model	Dubinin–Radushkevich (D–R) isotherm model	D–R adsorption isotherm originated to describe the impact of the poriferous framework of adsorbents. It was utilized to enunciate the sorption mechanism with Gaussian energy distribution within heterogeneous surfaces. It was predicated on the adsorption potential theory and hypothesized that the sorption phenomenon was associated with microporous volume filling against the layer-by-layer adsorption on porous walls.	$q_e = q_{max} e^{(-\beta' \varepsilon^2)}$
Three-parameter model	Redlich Peterson model	This is an experiential isotherm involving the consolidation of Freundlich and Langmuir adsorption isotherm models, and it does not conform with the exemplary monolayer sorption. It is a multifaceted adsorption isotherm model utilized in homogeneous or heterogeneous systems. The numerator of the mathematical expression is from the Langmuir model, and at infinite dilutions, the system can approximate the Henry region.	$q_e = \frac{k_R c_e}{1 + a_R c_e^g}$
Three-parameter model	Sips isotherm model	It involves the association of Freundlich and Langmuir adsorption isotherm models, presumed to overcome the shortcomings concomitant with greater concentrations of adsorbate in the Freundlich model, and anticipates the heterogeneity of sorption systems. It results in generating a mathematical equation possessing finite limits at greater concentrations. This isotherm effectively constrains adsorption, devoid of any interactions among the adsorbates. This isotherm model does not obey Henry's law owing to the reduction to the Freundlich model at lower adsorbate concentrations. Nevertheless, the single-layer adsorption properties signifying the Langmuir model can be prognosticated at higher adsorbate concentrations.	$q_e = \frac{q_m(k_s c_e)^m}{(1 + (k_s c_e)^m)}$

3. Microplastics

Microplastics, referred to as plastic-based debris with particle sizes spanning lower than 5 mm, have been discerned all around the globe, encompassing marine, freshwater reserves, soil as well as the Antarctic.[220,221] Being copiously attainable, microplastics manifest a greater proclivity for interconnecting with the environment, consequently hindering the biota. They can conglomerate deleterious contaminants, including polychlorinated biphenyls, toxic metals, and polycyclic aromatic hydrocarbons, from the environment functioning as transport vectors, and can concomitantly percolate additives.[222,223] Microplastics can penetrate the ecological system and terrestrial

29 August 2023 15:25:40

TABLE IX. Sludge-based biochar utilized for the catalytic degeneration of various organic compounds comprising the catalysis mechanism and processing parameters employed.

Sludge type	Modification	Biochar production method—processing parameters	Catalysis mechanism	Organic contaminant targeted	Degradation process parameters	Removal efficiency	Removal rate	Kinetics model	Reference
SS	⋯	Microwave pyrolysis: single mode irradiation at 2.45 GHz, Power: 200, 300, and 400 W	Heterogeneous Fenton oxidation	TCE	pH: 3.1, 4.8, 6.8, t = 12 min, T = 25 °C	83%	⋯	⋯	216
SS	Chemical modification with HNO_3	Pyrolysis: T = 500 °C, t = 4 h	H_2O_2 activation	CIP	pH: 3, 5, 7, and 9, D: 0.4 g l^{-1}, T = 25 °C, t = 24 h	HNO_3 modified biochar/H_2O_2: 93%, Biochar/H_2O_2: 70.6%	⋯	Pseudo first order (R^2: 0.9753 – Unmodified biochar, R^2: 0.9506 – modified biochar)	214
DWS	⋯	Pyrolysis: T = 300–900 °C, t = 4 h	Percarbonate activation	Phthalate esters	pH: 3–11, t = 12 h, D: 0.8–3.3 g l^{-1}, Molar ratio of PC:PAE = 1:10	SDB300: 30%, SDB3 = 500: 54%, SDB700: 45%, SDB900: 65%	⋯	Pseudo first order	215
SS	⋯	Pyrolysis:T =- 400–800 °C, t = 6 h	Peroxymonosulfate activation	Bisphenol-A	pH: 4–10, D: 0.2 g l^{-1}	⋯	Average removal rate: 3.21 mol BPA/ mol oxidant/h	Pseudo first order	219
SS	Nitrogen-rich sludge blended with melamine	Single-step pyrolysis: T = 800 °C, t = 3 h	Peroxymonosulfate activation	RB, RB5, MO, AO7, RB4, MB	pH: 3–9, D: 200 mg l^{-1}, T = 27 °C, Molar ration of DSS:melamine - 0:1, 0.5:1, 1:0, 1:0.5	AO7: 98.2% (5 min), RB: 98.8% (5 min), RB5: 99.4% (20 min), MB: 82.9% (30 min), MO: 99.2% (5 min), RB4: 98.8% (5 min), RB5: 99.4% (20 min)	⋯	Pseudo first order	218
SS	Integrated with agar-$MnCl_2$ and treated with NH_4OH	Single-step pyrolysis: T = 800 °C, t = 1 h	Peroxymonosulfate activation	AO7	pH: 6–12, Catalyst: 0.2 g l^{-1}, AO7: 20 mg l^{-1}, T = 25 °C	91.4% (20 min), 100% (40 min)	⋯	Pseudo first order	217

habitat by means of atmospheric deposition, wastewater sludges, and irrigation through unprocessed biosolids.[224,225] Sewage sludge is a preliminary plight and channel for the microplastics to get into the terrene personating detrimental consequences on the aquatic and soil environment.[226,227] As an illustration, a passable estimate of around 7.2×10^9 day of microplastics was emitted into streams from water treatment plants worldwide.[228] Some marine species possess microparticular matter rapidly accrued by invertebrates or plankton. Pollutants being bestowed with greater surface area values, smaller particle size, and hydrophobicity can be readily adsorbed onto the surface of microplastics, thereby engendering microplastics to function as carrier agents for various noxious contaminants, including persistent organic pollutants. Plastic debris often comprises chemical additives and plasticizing agents, such as Phthalates, Bisphenol-A, and Polybrominated diphenyl ethers, capable of inducing lethal after-effects post ingestion by living entities, instigating hazards to the ecological as well as human health.[229–232] Moreover, these microplastics are also competent enough to adsorb heavy metal ions, such as iron, cadmium, lead, arsenic, and copper, evoking endocrine disruptor implications and cellular apoptosis attributable to their interactivity with DNA molecules.[232,233] There exists an indispensable necessity to pay heed to the sludge-derived microplastic pollution and the plausible detrimental menaces associated with human health and explore effectual curbing measures.

Preliminary surveys exhibited microplastic removal efficacies of around 64.4% from conventional water treatment plant sludges through customary activated sludge methodologies posing conceivable ecological risks.[234] Different progressive strategies are employed to eliminate microplastics in sludges, including bioremediation,[235] adsorption using graphene, biochar, activated carbon-based adsorbents, etc.[225,236] Biochar serves as an efficacious adsorbent for the eviction of microplastics from aqueous environments owing to its inherent advantages, such as greater surface area, porousness, and ecological versatility.[237] Wang et al.[238] reported magnetically modified biochar adsorbents for the eviction of microplastics from aqueous systems. Magnetic biochar modified with Zn, Mg, and Fe demonstrated removal efficacies of 99.46%, 98.75%, and 94.81%, respectively, for polystyrene microspheres. The incorporation of metal nanoparticles substantially enhanced the removal efficiencies attributable to the electrostatic attractive forces and chemical bonding between microplastics and functional moieties of magnetic biochar. Microplastic disintegration and regeneration of biochar-based adsorbents were achieved by thermal treatment synchronously. The deterioration of microplastics was fostered by catalytically active sites emanating from Zn, Mg, and Fe liberating sorption sites. Even post five adsorption-pyrolysis regeneration cycles, the as-prepared adsorbents exhibited superior removal efficacies of 95.79%, 94.6%, and 95.02% for Zn, Mg modified magnetic biochar and magnetic biochar adsorbents devoid of any metal nanoparticles, respectively, thereby corroborating economic and environment-friendly Zn/Mg-magnetic biochars as potent and efficacious adsorbents for the elimination and deterioration of microplastics.[238]

4. Antibiotics

Antibiotics have extensively been utilized in inhibiting bacterial diseases while ameliorating livestock and human health.[239]

Nevertheless, a multitude of antibiotics are inadequately metabolized and are consequently defecated into the surroundings via the excreta of animals and human beings. Antibiotics discharged into the ecosystem lead to short-term and long-term prohibitory repercussions owing to their noxiousness.[239] Moreover, their existence in the surroundings might engender the preponderance of resistive bacterial strains. As an illustration, fluoroquinolone compounds, being essentially exuded invariably (undergoing less than 25% metabolism), can penetrate the ecological system through the expulsion of unprocessed swine wastewater upon agrarian soil as manure.[197] Hence, it is imperative to seek cost-efficient, expedient, and effectual strategies to eradicate antibiotics from aqueous systems. Biochar-based adsorbents derived from various sludges are endowed with greater specific surface area, mesoporosity, surface reactiveness, and polarity, consequently inducing the sorption of various antibiotics from distinct ecological systems.[240] For instance, Ma et al.[239] reported municipal sludge-based biochar subjected to activation with zinc chloride, utilized as the base material for hydrothermal production of magnetically modified sludge-based biochar to eliminate ciprofloxacin (CIP) and tetracycline (TC). The aforestated adsorbent demonstrated maximal adsorption capacities of 74.2 and 145 mg g^{-1} for CIP and TC at 25 °C, respectively. Adsorption kinetic data studies and isotherm models revealed that the sorption phenomenon was predominated by π–π conjugation, pore filling, hydrogen bonding, and complexation of oxygen possessing functional moieties. Moreover, the adsorbent displayed greater selectivity toward CIP and TC at higher ionic strength across a diverse spectrum of pH values. In another study, Wei et al.[118] proclaimed hydrothermally synthesized sewage sludge-based biochar loaded with iron to remove doxycycline (DOX) and tetracycline (TC) antibiotics. The as-prepared biochar adsorbents manifested the selective eviction of two types of antibiotics. The unary antibiotic system exhibited maximal adsorption capacity values of 129.98 and 104.86 mg g^{-1} for DOX and TC at 20 °C, respectively. The manner of adsorption of antibiotics onto the sludge-derived biochar adsorbent was regulated by a multistage comprehensive adsorption phenomenon encompassing complexation, electrostatic interactions, π–π interactions between acceptor and donor, and hydrogen bonding. Contrarily, the binary antibiotics system exemplified an antagonistic effect between DOX and TC, and the sorption of TC was more restrained compared to DOX, owing to greater steric hindrance displayed by the molecular framework of TC.[118] Zhang et al.[197] reported freshwater sludge-derived hydrochar and biochar to eliminate enrofloxacin (ENR) from swine wastewater. The adsorption of ENR was least impacted by the solution pH attributed to preeminent physisorption evinced by an appropriate fit obtained with BET adsorption isotherm model (R^2:0.95) and the sorption mechanism for hydrochar best fitted with the Freundlich adsorption isotherm.[197]

The adsorption of various contaminants from wastewater employing biochar involves an intricate relationship between the physicochemical characteristics of the adsorbent, biomass feedstock type, thermochemical conversion technique employed, and processing conditions. Various parameters encompassing particle size, heating rate, residence time, and pyrolysis temperature are known to impact the biochar quality and yield.[241] Analogously, it is discernible that these factors might exhibit a prominent effect on the adsorption efficacy toward an extensive array of contaminants, out of which temperature purportedly serves as a fundamental criterion. It was ascertained that the pyrolytic temperature demonstrated supreme leverage on the

29 August 2023 15:25:40

isotherm shapes and structural properties compared to the biomass feedstock employed.[242] The pyrolytic temperature impacted the biochars' degree of carbonization; at greater pyrolysis temperatures, the surface area was substantially augmented, and a greater amount of nanoporous structures were formed, with a diminution in the amount of nitrogen, sulfur, hydrogen, and oxygen-containing functional moieties and cation exchange capacity, thereby ensuing in precipitously ameliorated adsorption rates toward organic contaminants.[243,244] Studies reported in the literature revealed that at greater pyrolytic temperatures, alkalinity, pore structure, and specific surface area were increased, which is efficacious for capturing inorganic contaminants. Furthermore, the heating rate is known to impact the biochar yield, while the pyrolysis time impacts the porous framework, specific surface area, and constitution of biochar.[244] These parameters on integration with the carbonization atmosphere and activation techniques employed are known to demonstrate a considerable influence on the biochar adsorption performance.

B. Adsorption of toxic gases

Acidic gases, such as hydrogen sulfide (H_2S) and carbon dioxide (CO_2), are released during the anaerobic digestion of organic components, extrication of naphtha, combustion and production gases, powerhouse exhausts, etc. H_2S is a mephitic, lethal, and erosive gas that generates sulfur dioxide (SO_2) during combustion, eventuating acid rain and is often discharged in landfill sites, sewage treatment plants, etc.[245,246] Restraining the release of CO_2 is essential from the stance of climate mitigation and global warming, as CO_2 transmission induced by fossil fuel combustion is the principal forerunner of climate crisis recounting for 40% of the carbon emanations.[247] Among various adsorbents[248] employed for eliminating toxic gases, biochar is an economic and sustained alternative possessing exceptional adsorption characteristics that can be expedited through surface functionalization or activation. Biochar acquired from the fast pyrolysis technique comprehends functional moieties that effectuate it as an exemplary substance to adsorb acidic gases.[247] CO_2 eviction potential through the industries employing biochar is projected to span from 1.8 to 3.3 gigatonnes of CO_2 emissions per year. A sewage treatment facility that engenders 100 dry tonnes of SS is conjectured to produce 65 tonnes of biochar, presuming a median yield of 65% and ~20 kt of CO_2 emissions could be captured annually contingent on greenhouse gas emissions of 0.9 kg CO_2 emissions per kg of biochar.[249]

KOH-modified biochar acquired from the pyrolysis of an admixture of pine sawdust and sewage sludge (S3W7) demonstrated a greater propensity for CO_2 capture with adsorption capacity values of 177.1 mg g^{-1} at 700 °C attributable to greater micropore volume (0.68 cm^3 g^{-1}) and surface area (2623 m^2 g^{-1}). Additionally, biochar's aromaticity, hydrophobic nature, surface functionalities, and nitrogen heteroatoms were strenuously associated with CO_2 adsorption by biochar.[247] In another study, greater CO_2 adsorption capacities of 136.7–182 mg g^{-1} were ascertained for an admixture of pine sawdust and sewage sludge-derived biochar activated with KOH in contrast with the unmodified biochar (35.5–42.9 mg g^{-1}) imputable to the occurrence of micropores following KOH activation, substantially expediting the CO_2 adsorption capacity. The as-prepared biochar (BC-700K) demonstrated a recyclability of 97% within ten sequential adsorption-desorption cycles at 1 bar pressure and 25 °C temperature.[250] Sewage sludge-derived biochar manifested enhanced removal

of H_2S by 1.04 and 3.3 folds at 25 and 100 wt. % moisture content, respectively, appertaining to the catalytic transformation to elemental SO_4^{2-} and S^0 serving as the significant pathway of H_2S elimination. Sludge-based waste could be transformed into value-aggregated biochar as an adsorbent for capturing H_2S remarkably at greater moisture contents, thereby facilitating the thorough oxidation of H_2S to SO_4^{2-}.[246]

The toxic gas adsorption capacity of biochar, which is equivalent to the capacity of gas adsorbed per unit mass of biochar, predominantly relies on the physicochemical characteristics of biochar including surface basicity, hydrophobicity, pore volume, surface area, pore size, aromaticity, polarity and the existence of alkaline and alkali earth metals and other surface functionalities.[251] These physicochemical characteristics of biochar are in turn intricately linked with thermochemical parameters involved in biochar synthesis and biomass feedstock type.[252,253] The chemical and physical modifications of biochar to augment the surface properties would substantially enhance the ability of biochar to eliminate toxic gases. However, large-scale implementation of biochar for capturing toxic gases must be emphasized in the near future, along with the advancement of contemporary approaches for the reutilization of the adsorbed gas or its transformation into viable products.

C. Vermicomposting of sludges

Vermicomposting of sludges serves as a substitute to transform sludge-derived waste into value-aggregated products.[254] Vermicomposting is a decomposition technique that enables the modification of organic matter by virtue of microbes and worms into stabilized humus-like substances ascertained as vermicompost.[255] The earthworms will assimilate, pulverize, and digest the organic matter with the aid of microflora in their gut, subsequently amending the chemical, physical, and biological constitution of the organic matter.[256] This technique manifests a broad spectrum of perquisites for sustainable and expedient utilization of sludges generated by water treatment plants.[257] In the interim of the vermicomposting method, heavy metals existing within sewage sludges could impede the activities of earthworms, eventuating in lowered growth, reproduction, and death and, consequently, the efficacy of transforming sludge into vermicompost. Hence, vermicomposting of sludges shall demand the inclusion of supplemental substances to ascertain optimum characteristics for the growth and reproduction of the earthworms and, consequently, ameliorate the transformation rate and attributes of the derived vermicompost. These subsidiary substances incorporate bulking agent components such as various types of crop straw, phosphate rock, fly ash, wood chips, soil, biochar, etc.[258]

Biochar consists of comparatively recalcitrant carbon, leachable ash, and carbon, and it exhibits notable sorption characteristics and stableness, and consequently, retentivity of nutrients, water, and other compounds. Biochar can minimize the bioaccumulation of toxic metal ions in sludges and can also comprehend micro and macronutrients, thereby serving as an invaluable source of nutriment for soil macrofaunae like earthworms and other soil microbes.[259] Krystyna et al.[258] studied the utilization of SS-based biochar employed as an ancillary component for wood chips and municipal SS processed by consolidated vermicomposting and composting techniques. Incorporating SS-based biochar into the mixture prior to composting resulted in substantially greater reproduction rates; the proportion of cocoons was

enhanced by 213% in the fourth week, in contrast with the mixture devoid of biochar. The average ratio of juveniles was intensified by 11 folds in the admixture possessing biochar incorporated prior to composting and five folds in the admixtures containing biochar included post composting process in contrast with the combinations devoid of biochar. Biochar included prior to composting lowered the bioaccumulation of cadmium and zinc toward *E. fetida*. The biochar-incorporated vermicompost exhibited favorable fertilizing characteristics exclusive of higher concentrations of chromium. The as-prepared vermicompost could be employed as a cultivation substrate for ameliorating calciferous soils or horticultural applications.[258] In another study, Malińska *et al.*[257] reported the impact of biochar on the activity of *E. fetida* during vermicomposting of precomposed SS integrated with wheat straw and modified with biochar. The modification of SS and wheat straw admixtures incorporating 4% and 8% biochar expedited the reproduction rate of *E. fetida* during vermicomposting, and the maximum yield of cocoons was discerned post 4 weeks. The greater reproduction rate contemplated ensued from the decreased concentration of toxic metal ions in the admixtures possessing 4 and 8% biochar. Incorporating biochar into the SS and wheat straw admixtures during pre-composting induced greater potassium concentrations. Furthermore, the produced vermicompost and compost demonstrated reduced pH values serving as an appropriate criterion for prospective use as a horticulture growth substrate.[257]

Vermicomposting and biochar were recognized to be credible solutions to promote crop yields.[260] Nevertheless, soil emissions of nitrous oxide were intensified by the activities of earthworms.[261] The existing literature insinuated that vermicomposting is a cost-effective substitute for chemical fertilizers, as it enhanced soil fertility, nutrients (specifically N), enzymes, and microbial biodiversity while diminishing the heavy metal content and soil pathogens. Furthermore, vermicomposting augmented the nitrogen content and withheld it in the soils for longer durations. A decrement in carbon content, pH, and C/N ratio as discernible from the literature manifested the positive repercussions of vermicomposting.

D. Soil amelioration and enhancement in plant growth

Biochar possesses greater nutrient content and porosity, efficacious water retention capacity, and an extensive microstructure for plausible use as soil ameliorating agents.[262] It provides an extensive array of merits for soil amelioration, like enhancement in pH values, physicochemical characteristics, nutrient levels, curtailment of carbon emissions, minimization of soil erosion and refinement of soil structure, and immobilization of heavy metals, including zinc, cadmium, arsenic, etc.

The cation exchange mechanism contemplated for the immobilization of potentially noxious metal ions onto biochar is explained (Fig. 6).[263,264]

The toxic metal ions interchange with different cations, such as magnesium and calcium, additionally ascribed to the co-precipitation of toxic metal ions and their inner sphere complexation with the intricate mineral oxides and humus substances present in biochar. Initially, the strength of toxic metal ion adsorption onto the biochar surface is lower owing to the existence of water molecules circumscribing the metal ion (oscillation across the length of electrostatic interactive forces). Eventually, water molecules are discharged, and the propensity toward complexation augments, contingent on the structure and composition of the reactive biochar surface, consequently generating a robust inner-sphere complex depreciating the emancipation of toxic metal ions back to the soil solution.[264]
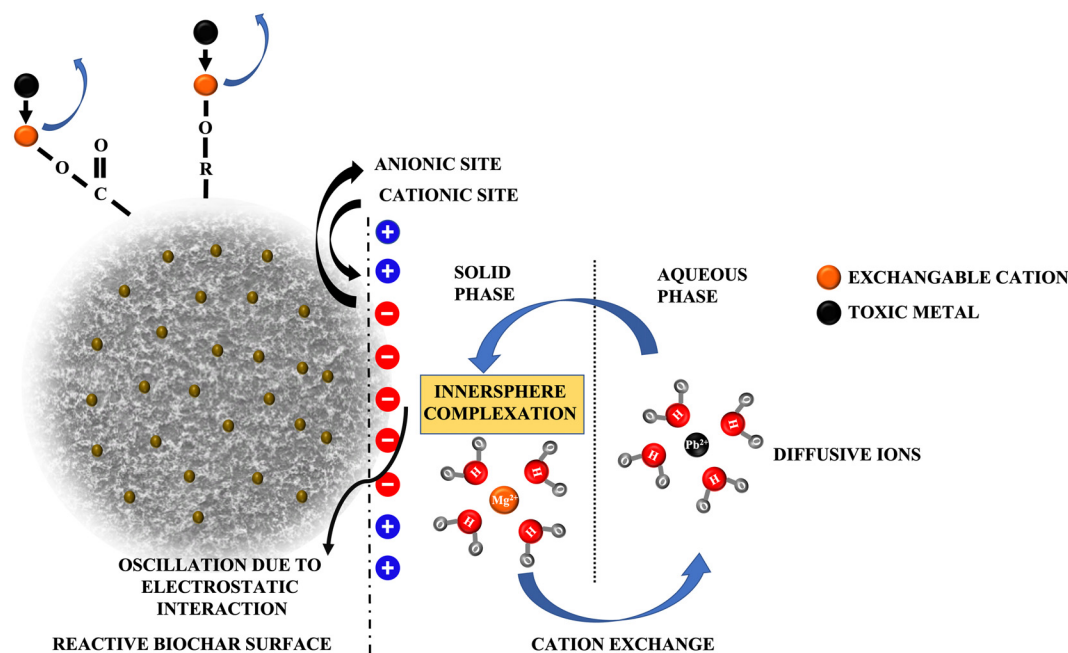
FIG. 6. Graphical illustration of the cation exchange mechanism between plausibly toxic metal ions dissolved in soil solution and the positively charged ions present on the reactive biochar surface via co-precipitation and inner sphere complexation.

The utilization of biochar as a fertilizer can enrich the productive capacity of crops with a mean increment of 10% while lowering the nutrient losses via leaching.[265–268] Sousa *et al.*[265] examined the effect of varying dosages of sewage sludge-based biochar on the soil prolificacy and agricultural growth of radish (*Raphanus sativus* L.). The experimental analysis was performed in a greenhouse and was comprehensively indiscriminate, with six treatments and four replicas. Soil characteristics assessing pre- and post-culturing of radish demonstrated that the test variables reciprocated effectively to the increment in biochar dosage from 10 to $30 \, g \, kg^{-1}$, and a negligible diminution in the test parameters was ascertained after biochar dosages of $30 \, g \, kg^{-1}$. The aforestated biochar facilitated higher ratios of foliar nutrients besides zinc and potassium, fostering additional plant growth with rising plant height, leaf number, and aboveground dry weight. It could furnish nutrients to plants within a brief interval with a subsequent improvement in radish production.[265]

In another study, Elkhlifi *et al.*[269] analyzed the efficiency of different phosphate-lanthanum coated sewage sludge-based biochars (SSBC, SSBC-P, La-SSBC, and La-SSBC-P) on the phosphate retention in soil and the growth of ryegrass (*Lolium perenne* L.) in a basic soil environment. The test results demonstrated amelioration in plant height, plant dry biomass, germination percentage, and aggregate phosphorous content in ryegrass leaves when treated with La-SSBC-P in contrast with other biochars. La-SSBC-P treatment substantially modified some chemical properties of the alkaline soil post-harvesting, such as the soil organic matter, cation exchange capacity, pH, limestone, lanthanum, and phosphate contents. The soil-accessible phosphorus content was augmented by 6.7 folds after coating biochar with La and P (La-SSBC-P). The implementation of La-SSBC-P considerably enriched the growth of ryegrass plant and soil characteristics when subjected to an alkaline soil environment, thereby serving as a prospective alternative for phosphorus-based fertilizers for agrarian implications.[269]

While assessing the effect of biochar on soil biological characteristics, community configuration, and microbial functional activities could be contemplated as efficacious indicators. The utilization of biochar can impact microbial growth by ameliorating soil characteristics, including water-holding capability, nutrients (Ca, K, N, C, Mg, and P), soil porosity, and pH. Estimation of the biome configuration in soil post the inclusion of biochar, evidenced that soil and biochar feedstock type were crucial factors.[270] The large-scale employment of biochar in soil media would ineluctably influence the constitution and amount of soil organic carbon. Biochar stability in the soil is afflicted by chemical, physical, and biological decomposition.[271] Furthermore, the mineralization rate of biochar in the soil was found to decline with an elevation in pyrolysis temperatures, inextricably linked with enhancement in the aromatic condensation of biochar.[272] The impact of biochar on carbon footprint reduction was strongly associated with the C/N, H/C ratio, and porosity.

V. REGENERATION AND REUTILIZATION OF SLUDGE-DERIVED BIOCHAR

Biochar regeneration is an indispensable criterion for practically implementing the adsorbent and is essential for the adsorption phenomenon and pecuniary sustainability. Regeneration of biochar is a reversal adsorption phenomenon predicated on two fundamental integrities: adsorbate decomposition and desorption. A competent adsorbent must demonstrate exceptional recyclability for commercial use and be capable of curtailing the expenditures associated with the adsorbent as recurrent sorption–desorption cycles. Regeneration, along with being economical, also eradicates secondary pollutants. Various regeneration strategies, inclusive of solvent, ultrasonic, thermal, electrochemical, supercritical fluid regeneration, and microwave irradiation, were denounced, but the customarily employed economic methodology for wastewater treatment is thermal regeneration.[18] Recyclable magnetic biochar derived from dewatered sludge was employed to activate PMS to disintegrate tetracycline antibiotics. The catalytic efficacy of the magnetic biochar (MBC) was higher than that of pristine biochar, and an elimination rate of 89.05% was attained for tetracycline within 120 min, accountable to the substantial enhancement in the specific surface area and pore volume of magnetic biochar and the activation of PMS through the magnetic media of Fe_3O_4. Four recycling tests performed for tetracycline disintegration to remove magnetic biochar demonstrated removal rates of 79.89% and 54.91% at the first and fourth regeneration cycles, respectively. The degradation efficacy of the antibiotic retained stability from the second to fourth cycle, manifesting the recyclability of MBC.[273]

Disposing of depleted adsorbents comprising adsorbed toxic metal ions demands considerable emphasis as the inappropriate discarding of exhausted adsorbents might engender environmental pollution. Even though the depleted adsorbents could be desorbed through chemical regeneration methodologies, reprocessing the used eluate possessing greater concentrations of heavy metal ions is nevertheless a taxing liability. Landfilling is the customarily utilized approach in disposing of depleted adsorbents; however, it still poses a risk to public health owing to the reservoir of metal ion-loaded solid debris,[274] exhilarating investigators to discern conceivable utilization of the exhausted adsorbents while catering to the requisites of circular economy and ecological integrity. Spent magnetic biochar containing adsorbed Cu^{2+} ions (Cu-Fe@BC) could be explicitly utilized as a catalyst for activating permonosulfate (PMS) for the subsequent disintegration of norfloxacin (NOR), a class of fluoroquinolone antibiotics. Density functional theory studies and electrochemical analysis elucidated that the presence of copper ions in the adsorbent ameliorated PMS activation and the deterioration efficacy of norfloxacin by upgrading the adsorption capacity of PMS and rendering the transmittance of electrons. Around 91.47% of the antibiotic was expeditiously disintegrated in the Cu-Fe@BC–PMS system along with lower leaching of Cu ($<56 \, \mu g$) and Fe ions ($<33 \, \mu g$), respectively, in the acidic media. A comprehensive mechanistic analysis performed through radical capturing, scavenging, and solvent exchange divulged that the adsorbed copper ions promoted the generation of non-radical as well as radical entities for the deterioration of NOR. The adsorbent retained a stabilized operation for a protracted period, and by sufficing the catalytic activity in complex water purification systems, it could be promptly segregated for recycling. This study bestows an optimistic approach regarding the value aggregated usage of spent adsorbent as an economically efficient catalytic material that shapes a persuasive oxidative system for treating wastewater contaminated with NOR.[275]

VI. TOXICITY OF SLUDGE-BASED BIOCHAR

The subsistence of minerals and toxic metals within sludges and their prospective bioaccumulation in food chains impersonates a severe menace to human health and impediments to their utilization

29 August 2023 15:25:40

in the agrarian domain.[276] Polycyclic aromatic hydrocarbons (PAHs), reported carcinogenic agents, are generally present in sludges, thereby necessitating the scrutinization of the variations encountered in PAHs post-transformation to biochar.[277] Phytotoxicity assessment and risk estimation of the thermochemically transformed sludges have been assayed by investigators to examine the toxicological impacts of sludge-based biochar.[278] The toxicity of biochar is inextricably linked with toxic metals, nevertheless, dissolved organic carbon (DOC) discharged from biochar ameliorated fields into freshwater reserves during sporadic precipitation with consequent generation of disinfection entailments serve as some other resources of potentially dangerous substances present in biochar.[279,280] DOC content in biochar can be curtailed by elevating the pyrolysis process temperatures above 500 °C, which augments the biochar stability befitting them for soil-based carbon sequestration.[159] The toxicity of sludges can also be ascribed to the existence of different pharmaceutical compounds that can be efficaciously evicted through the hydrothermal carbonization of sludges into biochar as a substance with upgraded characteristics for agricultural usage with the concentration of carbamazepine being diminished by almost 97% along with lowered concentrations of other micropollutants.[281]

Biochar could display positive as well as negative repercussions on flora, fauna, and microbes. The implications of biochar can be its explicit effect on organisms owing to the presence of inorganic and organic contaminants.[282] Biochar synthesized using a fast pyrolysis technique at temperatures below 500 °C possessing a more significant proportion of nutrients can be employed in agricultural applications while the sludge-derived biochar containing greater porousness and reduced nutrient values can be utilized for the remediation of degraded soil.[262,271,283] Furthermore, biochar could display toxicological effects as certain species of plants are responsive to some elements (Cl, Mn, Na, P, B, and Zn), and under such circumstances, the phytotoxicity of biochar persists, and it will differ based on the application dosages employed.[284] In addition, the implementation of biological tests permits the interpretation of plausible interactions between various pollutants and establishes the predominant substantiation of the presence or absence of toxicological repercussions on organisms.[285]

VII. CONCLUSIONS AND FUTURE PROSPECTIVES

This review analytically renders a conspectus of drinking water, fecal, and raw sewage sludge-derived biochars for environmental remediation, explicitly as adsorbents for capturing toxic metal ions, microplastics, antibiotics, and toxic gases; for the catalytic degeneration of organic pollutants, as soil ameliorating agents; and in vermicomposting approach. Transforming sludge-derived wastes into biochar is a sustainable approach to fostering a circular economy while curtailing the exorbitant costs associated with conventional sludge management systems. Chemical reactors characterized by diffusion, friction, mass, or heat transfer, including tunable chemical reactions promoting the transformation of biomass feedstock into the desired end products (biochar), served as a decisive milestone in the comprehensive process design. The predominant mechanisms in biochar liable for adsorbing a diverse array of contaminants comprehend chemisorption through ion exchange, inner sphere complexation, precipitation, surface complexation, electrostatic interactions, physisorption, and redox reactions through abundant functional moieties like –OH, –COOH, and oxygen-based groups present on biochar surfaces.

DWS and SS-derived biochars demonstrated exquisite catalytic activity toward various organic pollutants through multifarious catalytic mechanisms encompassing peroxymonosulfate, percarbonate, heterogeneous Fenton oxidation, and hydrogen peroxide activation owing to the presence of ubisemiquinone and graphitizing structures in biochar capable of functioning as electron donors or acceptors and persistent free radicals generated during biochar production. Biochar acquired from the fast pyrolysis technique comprehends functional moieties effectuating it as an exemplary substance to adsorb acidic gases. They are also capable of curtailing the bioavailability of toxic metal ions in sludges and comprising macro and micronutrients, they could serve as an invaluable source of nutriment for macrofaunae and other soil microbes. The resultant biochar properties were predominantly affected by the particle size, residence time, biomass feedstock, pyrolysis temperature, carbonization atmosphere, and heating rate. The adsorption efficacy of the synthesized biochar toward various pollutants was inextricably linked with the sludge type and physicochemical characteristics of sludge-based biochar contingent on the processing parameters. For enhanced removal efficacies, the pyrolysis processing parameters associated with sludges must be selected methodically based on the adsorbate characteristics. Apart from generating a microporous framework and specific surface area for biochars, incorporating nanomaterials and tailored functional moieties has acquired tremendous interest. Customarily, greater pyrolysis temperatures ameliorated the adsorption properties and physicochemical characteristics of sludge-derived biochars. Nevertheless, biochar modification through chemical and physical activation techniques was enormously beneficial in garnering intensified sorption capacities for different inorganic and organic contaminants ascribable to the higher density of functional groups and efficacious physicochemical stability and porousness. Diverse research domains contemplating the valorization of DWS, FS, and RS-derived biochars as potent, moderate-cost adsorbents for effluent treatment should be reconnoitered in the near future, surmounting the following outlooks:

(i) Commercialization and scaling up of sludge-derived biochars are essential to channel myriad sustainable development goals by 2030.

(ii) Computational studies coupled with big-data mining of the present scientific literature, like machine learning studies, can assist in discovering the physicochemical characteristics associated with varied biochar designs.

(iii) Wastewater purification plants possessing discrete processing techniques entail industry-centric biochar designs, thereby necessitating the generation of biochar production systems with varied modification facilities.

(iv) Besides the regeneration of expended biochar, their secondary usage as viable alternatives is a conceivable strategy for broadening the scope of the end uses of biochar as distinct applications generally rely on varied properties and functional moieties. For instance, following the recovery of different contaminants from effluents, biochar could exemplify the role of metal-immobilizing agents or soil fertilizers. Moreover, the hazards associated with the expended biochar must be thoroughly contemplated before plausible use. Low-risk biochars could be subsequently employed as soil ameliorating agents or adsorbents, while the high-risk biochars must be stabilized or reutilized in cementitious

29 August 2023 15:25:40

substances capable of attaining immobilization of contaminants and carbon sequestration. Optimizing the sorption phenomenon of sludge-derived biochars implementing contemporary approximations like the response surface methodology can prove beneficial.

(v) To scrutinize the stability of sludge-derived biochars by releasing toxic metal ions and polycyclic aromatic hydrocarbon compounds.

(vi) An integrated approach examining the pros and cons of synthesizing and using sludge-based biochars in terms of an overall life cycle analysis is imperative.

(vii) Exploring the efficiency of sludge-derived biochars in treating realistic wastewater and emphasizing the commercialization of biochars considering their stability, post-processing of expended biochar, and scaled-up applications are needed.

(viii) Extensive research should be performed to potentially convert the impurities in the sludge-derived biochars to less extirpative derivatives.

(ix) Fabrication of nanocomposites incorporating sludge-derived biochars as an additive using contemporary processing techniques for efficacious sorption of toxic metal ions and their ameliorated disintegration and chemical reduction is necessary.

SUPPLEMENTARY MATERIAL

See the supplementary material for epitomization of various steps associated with the designing of chemical reactors (Fig. S1); classification of reactors involved in biochar generation employing torrefaction (based on the heating mode and gas–solid mixing), gasification, fast pyrolysis, and HTC processes (Fig. S2); predominant mechanisms associated with the adsorption of toxic metal ions onto biochar (Fig. S3); and mechanism involved in the catalytic activation of hydrogen peroxide through biochar (Fig. S4).

ACKNOWLEDGMENTS

AUTHOR DECLARATIONS
Conflict of Interest

The authors have no conflicts to disclose.

Author Contributions

Neelaambhigai Mayilswamy: Writing – original draft (lead). **Amrita Nighojkar:** Writing – review & editing (supporting). **Mohan Edirisinghe:** Methodology (supporting); Writing – review & editing (equal). **Senthilarasu Sundaram:** Writing – review & editing (equal).

Balasubramanian Kandasubramanian: Conceptualization (lead); Methodology (lead); Supervision (lead); Writing – review & editing (equal).

DATA AVAILABILITY

Data sharing is not applicable to this article as no new data were created or analyzed in this study.

REFERENCES

[1] S. S. A. Syed-Hassan, Y. Wang, S. Hu, S. Su, and J. Xiang, Renewable Sustainable Energy Rev. **80**, 888–913 (2017).

[2] B. R. Gurjar and V. K. Tyagi, *Sludge Management* (CRC Press/Balkema, Boca Raton, 2017).

[3] W. Zhang, Y. Mo, J. Yang, J. Zhou, Y. Lin, A. Isabwe, J. Zhang, X. Gao, and Z. Yu, Cont. Shelf Res. **164**, 1–9 (2018).

[4] C. Rutgersson, S. Ebmeyer, S. B. Lassen, A. Karkman, J. Fick, E. Kristiansson, K. K. Brandt, C.-F. Flach, and D. G. J. Larsson, Environ. Int. **137**, 105339 (2020).

[5] X.-Z. Meng, A. K. Venkatesan, Y.-L. Ni, J. C. Steele, L.-L. Wu, A. Bignert, Å. Bergman, and R. U. Halden, Environ. Sci. Technol. **50**(11), 5454–5466 (2016).

[6] Q. Wu, X. Bao, W. Guo, B. Wang, Y. Li, H. Luo, H. Wang, and N. Ren, Biotechnol. Adv. **37**(5), 599–615 (2019).

[7] T. Ahmad, K. Ahmad, and M. Alam, Environ. Monit. Assess. **189**(9), 453 (2017).

[8] D. M. Berendes, P. J. Yang, A. Lai, D. Hu, and J. Brown, Nat. Sustainability **1**(11), 679–685 (2018).

[9] Y. Chen, S.-H. Ho, D. Nagarajan, N. Ren, and J.-S. Chang, Curr. Opin. Biotechnol. **50**, 101–110 (2018).

[10] T. Shen, Y. Tang, X.-Y. Lu, and Z. Meng, J. Cleaner Prod. **193**, 185–193 (2018).

[11] I. S. Turovskiĭ and P. K. Mathai, *Wastewater Sludge Processing* (Wiley-Interscience, Hoboken, NJ, 2006).

[12] J. Balasubramanian, P. C. Sabumon, J. U. Lazar, and R. Ilangovan, Waste Manage. **26**(1), 22–28 (2006).

[13] H. Chen, X. Ma, and H. Dai, Cem. Concr. Compos. **32**(6), 436–439 (2010).

[14] D. Caniani, S. Masi, I. M. Mancini, and E. Trulli, Waste Manage. **33**(6), 1461–1468 (2013).

[15] J. Racek, J. Sevcik, T. Chorazy, J. Kucerik, and P. Hlavinek, Waste Biomass Valor. **11**(7), 3677–3709 (2020).

[16] B. Chen, S. S. Ray, and M. Edirisinghe, Macro Mater. Eng. **307**(6), 2200242 (2022).

[17] M. I. Inyang, B. Gao, Y. Yao, Y. Xue, A. Zimmerman, A. Mosa, P. Pullammanappallil, Y. S. Ok, and X. Cao, Crit. Rev. Environ. Sci. Technol. **46**(4), 406–433 (2016).

[18] A. I. Abd-Elhamid and M. Emran, in *Biochar and Its Application in Bioremediation*, edited by R. Thapar Kapoor, H. Treichel, and M. P. Shah (Springer Nature Singapore, Singapore, 2021), pp. 1–26.

[19] M. Hassan, Y. Liu, R. Naidu, S. J. Parikh, J. Du, F. Qi, and I. R. Willett, Sci. Total Environ. **744**, 140714 (2020).

[20] P. D. Bhalara, K. Balasubramanian, and B. S. Banerjee, Mater. Focus **4**(2), 154–163 (2015).

[21] A. Purabgola, N. Mayilswamy, and B. Kandasubramanian, Environ. Sci. Pollut. Res. **29**, 32305–32325 (2022).

[22] K. Thakur and B. Kandasubramanian, J. Chem. Eng. Data **64**(3), 833–867 (2019).

[23] A. Pillai and B. Kandasubramanian, J. Chem. Eng. Data **65**(5), 2255–2270 (2020).

[24] Q. Hu, J. Jung, D. Chen, K. Leong, S. Song, F. Li, B. C. Mohan, Z. Yao, A. K. Prabhakar, X. H. Lin, E. Y. Lim, L. Zhang, G. Souradeep, Y. S. Ok, H. W. Kua, S. F. Y. Li, H. T. W. Tan, Y. Dai, Y. W. Tong, Y. Peng, S. Joseph, and C.-H. Wang, Sci. Total Environ. **757**, 143820 (2021).

[25] A. Méndez, A. Gómez, J. Paz-Ferreiro, and G. Gascó, Chemosphere **89**(11), 1354–1359 (2012).

[26]See https://www.un.org/development/desa/pd/content/World-Population-Prospects-2022 for "United Nations World Population Prospects 2022: Summary of Results."

[27]L. Lin, F. Xu, X. Ge, and Y. Li, Renewable Sustainable Energy Rev. **89**, 151–167 (2018).

[28]A. Boretti and L. Rosa, Npj Clean Water **2**(1), 15 (2019).

[29]See https://data.unicef.org/topic/water-and-sanitation/drinking-water/ for "Access to Drinking Water-UNICEF DATA."

[30]See https://www.un.org/waterforlifedecade/scarcity.shtml for "International Decade for Action 'Water for Life' 2005–2015. Focus Areas."

[31]See https://www.unwater.org/publications/summary-progress-update-2021-sdg-6-water-and-sanitation-all for "Summary Progress Update 2021: SDG 6—Water and Sanitation for All | UN-Water."

[32]C. M. Chew, M. K. Aroua, M. A. Hussain, and W. M. Z. W. Ismail, J. Cleaner Prod. **112**, 3152–3163 (2016).

[33]P. L. McCarty, J. Bae, and J. Kim, Environ. Sci. Technol. **45**(17), 7100–7106 (2011).

[34]W.-W. Li, H.-Q. Yu, and B. E. Rittmann, Nature **528**(7580), 29–31 (2015).

[35]S. Shackley, J. Hammond, J. Gaunt, and R. Ibarrola, Carbon Manage. **2**(3), 335–356 (2011).

[36]Z. Fan, Z. Zhou, Z. Peng, S. Wan, Z. F. Gao, S. Deng, L. Tong, W. Han, and X. Chen, Chemosphere **317**, 137929 (2023).

[37]M. Cavali, N. Libardi Junior, J. D. De Sena, A. L. Woiciechowski, C. R. Soccol, P. Belli Filho, R. Bayard, H. Benbelkacem, and A. B. De Castilhos, Jr., Sci. Total Environ. **857**, 159627 (2023).

[38]T. Jiang, B. Wang, B. Gao, N. Cheng, Q. Feng, M. Chen, and S. Wang, J. Hazard. Mater. **442**, 130075 (2023).

[39]A. K. Patel, R. Katiyar, C.-W. Chen, R. R. Singhania, M. K. Awasthi, S. Bhatia, T. Bhaskar, and C.-D. Dong, Bioresour. Technol. **358**, 127384 (2022).

[40]J. Ji, X. Yuan, Y. Zhao, L. Jiang, and H. Wang, J. Hazard. Mater. **430**, 128375 (2022).

[41]Y. Zhao, X. Yuan, X. Li, L. Jiang, and H. Wang, J. Hazard. Mater. **409**, 124893 (2021).

[42]X. Pan, Z. Gu, W. Chen, and Q. Li, Sci. Total Environ. **754**, 142104 (2021).

[43]P. Srivatsav, B. S. Bhargav, V. Shanmugasundaram, J. Arun, K. P. Gopinath, and A. Bhatnagar, Water **12**(12), 3561 (2020).

[44]M. Ji, X. Wang, M. Usman, F. Liu, Y. Dan, L. Zhou, S. Campanaro, G. Luo, and W. Sang, Environ. Pollut. **294**, 118655 (2022).

[45]A. Gopinath, G. Divyapriya, V. Srivastava, A. R. Laiju, P. V. Nidheesh, and M. S. Kumar, Environ. Res. **194**, 110656 (2021).

[46]S. Jellali, B. Khiari, M. Usman, H. Hamdi, Y. Charabi, and M. Jeguirim, Renewable Sustainable Energy Rev. **144**, 111068 (2021).

[47]Z. Liu, S. Singer, Y. Tong, L. Kimbell, E. Anderson, M. Hughes, D. Zitomer, and P. McNamara, Renewable Sustainable Energy Rev. **90**, 650–664 (2018).

[48]Y. Xiao, A. Raheem, L. Ding, W.-H. Chen, X. Chen, F. Wang, and S.-L. Lin, Chemosphere **287**, 131969 (2022).

[49]S. Singh, V. Kumar, D. S. Dhanjal, S. Datta, D. Bhatia, J. Dhiman, J. Samuel, R. Prasad, and J. Singh, J. Cleaner Prod. **269**, 122259 (2020).

[50]Y. Liu, Y. Zhuge, C. W. K. Chow, A. Keegan, P. N. Pham, D. Li, J.-A. Oh, and R. Siddique, Resour., Conserv. Recycl. **168**, 105291 (2021).

[51]S. A. Abo-El-Enein, A. Shebl, and S. A. Abo El-Dahab, Appl. Clay Sci. **146**, 343–349 (2017).

[52]T. Ahmad, K. Ahmad, and M. Alam, Procedia Environ. Sci. **35**, 950–955 (2016).

[53]E. A. Odey, Z. Li, X. Zhou, and L. Kalakodio, Environ. Sci. Pollut. Res. **24**(30), 23441–23452 (2017).

[54]R. Penn, B. J. Ward, L. Strande, and M. Maurer, Water Res. **132**, 222–240 (2018).

[55]K. Fakkaew, T. Koottatep, and C. Polprasert, J. Environ. Manage. **216**, 421–426 (2018).

[56]B. C. Krueger, G. D. Fowler, M. R. Templeton, and B. Moya, Water Res. **169**, 115253 (2020).

[57]R. Harder, R. Wielemaker, T. A. Larsen, G. Zeeman, and G. Öberg, Crit. Rev. Environ. Sci. Technol. **49**(8), 695–743 (2019).

[58]A. Hamood, J. M. Khatib, and C. Williams, Constr. Build. Mater. **147**, 27–34 (2017).

[59]Z. Xu, J. Zhou, Y. Liu, L. Gu, X. Wu, and X. Zhang, RSC Adv. **8**(67), 38574–38581 (2018).

[60]Y. Qi, K. B. Thapa, and A. F. A. Hoadley, Chem. Eng. J. **171**(2), 373–384 (2011).

[61]B. Paulsrud and A. S. Eikum, Water Res. **9**(3), 297–305 (1975).

[62]M. He, Z. Xu, D. Hou, B. Gao, X. Cao, Y. S. Ok, J. Rinklebe, N. S. Bolan, and D. C. W. Tsang, Nat. Rev. Earth Environ. **3**(7), 444–460 (2022).

[63]M. Anjum, N. H. Al-Makishah, and M. A. Barakat, Process Saf. Environ. Prot. **102**, 615–632 (2016).

[64]L. Qian, S. Wang, D. Xu, Y. Guo, X. Tang, and L. Wang, Water Res. **89**, 118–131 (2016).

[65]S. Pilli, Y. Yan, R. D. Tyagi, and R. Y. Surampalli, Rev. Environ. Sci. Biotechnol. **14**(3), 453–472 (2015).

[66]M. Geissdoerfer, P. Savaget, N. M. P. Bocken, and E. J. Hultink, J. Cleaner Prod. **143**, 757–768 (2017).

[67]A. Gherghel, C. Teodosiu, and S. De Gisi, J. Cleaner Prod. **228**, 244–263 (2019).

[68]M. Smol, J. Kulczycka, A. Henclik, K. Gorazda, and Z. Wzorek, J. Cleaner Prod. **95**, 45–54 (2015).

[69]D. Eliche-Quesada, C. Martínez-García, M. L. Martínez-Cartas, M. T. Cotes-Palomino, L. Pérez-Villarejo, N. Cruz-Pérez, and F. A. Corpas-Iglesias, Appl. Clay Sci. **52**(3), 270–276 (2011).

[70]R. R. Pahunang, A. Buonerba, V. Senatore, G. Oliva, M. Ouda, T. Zarra, R. Muñoz, S. Puig, F. C. Ballesteros, C.-W. Li, S. W. Hasan, V. Belgiorno, and V. Naddeo, Sci. Total Environ. **792**, 148479 (2021).

[71]P. R. Yaashikaa, P. S. Kumar, S. Varjani, and A. Saravanan, Biotechnol. Rep. **28**, e00570 (2020).

[72]S. Bolognesi, G. Bernardi, A. Callegari, D. Dondi, and A. G. Capodaglio, Biomass Convers. Biorefin. **11**(2), 289–299 (2021).

[73]Q. Yang, H. Zhou, P. Bartocci, F. Fantozzi, O. Mašek, F. A. Agblevor, Z. Wei, H. Yang, H. Chen, X. Lu, G. Chen, C. Zheng, C. P. Nielsen, and M. B. McElroy, Nat. Commun. **12**(1), 1698 (2021).

[74]A. S. Erses Yay, B. Birinci, S. Açıkalın, and K. Yay, J. Cleaner Prod. **315**, 128087 (2021).

[75]C. vom Eyser, T. C. Schmidt, and J. Tuerk, Chemosphere **153**, 280–286 (2016).

[76]A. Jain, R. Balasubramanian, and M. P. Srinivasan, Chem. Eng. J. **283**, 789–805 (2016).

[77]G. K. Parshetti, Z. Liu, A. Jain, M. P. Srinivasan, and R. Balasubramanian, Fuel **111**, 201–210 (2013).

[78]Y. S. Ok et al., *Biochar: Production, Characterization, and Applications*, 1st ed. (CRC Press, Taylor & Francis Group, 2016).

[79]M. Escala, T. Zumbühl, C. Koller, R. Junge, and R. Krebs, Energy Fuels **27**(1), 454–460 (2013).

[80]A. L. Tasca, M. Puccini, R. Gori, I. Corsi, A. M. R. Galletti, and S. Vitolo, Waste Manage. **93**, 1–13 (2019).

[81]Y. Zhang, J. Qin, and Y. Yi, Sci. Total Environ. **763**, 144550 (2021).

[82]E. Agrafioti, G. Bouras, D. Kalderis, and E. Diamadopoulos, J. Anal. Appl. Pyrolysis **101**, 72–78 (2013).

[83]A. Tomczyk, Z. Sokołowska, and P. Boguta, Rev. Environ. Sci. Biotechnol. **19**(1), 191–215 (2020).

[84]A. Zielińska, P. Oleszczuk, B. Charmas, J. Skubiszewska-Zięba, and S. Pasieczna-Patkowska, J. Anal. Appl. Pyrolysis **112**, 201–213 (2015).

[85]Z. Khanmohammadi, M. Afyuni, and M. R. Mosaddeghi, Waste Manage. Res **33**(3), 275–283 (2015).

[86]S. Aktar, M. A. Hossain, N. Rathnayake, S. Patel, G. Gasco, A. Mendez, C. De Figueiredo, A. Surapaneni, K. Shah, and J. Paz-Ferreiro, J. Anal. Appl. Pyrolysis **164**, 105542 (2022).

[87]M. Gold, M. Cunningham, M. Bleuler, R. Arnheiter, A. Schönborn, C. Niwagaba, and L. Strande, J. Water, Sanit. Hyg. Dev. **8**(4), 707–717 (2018).

[88]O. O. D. Afolabi and M. Sohail, J. Environ. Manage. **187**, 401–415 (2017).

[89]D. Fytili and A. Zabaniotou, Renewable Sustainable Energy Rev. **12**(1), 116–140 (2008).

[90]Y. Lim and U.-D. Lee, Fuel Process. Technol. **128**, 199–210 (2014).

[91]P. Basu, *Biomass Gasification, Pyrolysis, and Torrefaction: Practical Design and Theory*, 2nd ed. (Academic Press is and imprint of Elsevier, Amsterdam, Boston, 2013).

29 August 2023 15:25:40

[92]M. Atienza-Martínez, I. Fonts, J. Ábrego, J. Ceamanos, and G. Gea, Chem. Eng. J. **222**, 534–545 (2013).

[93]Y. W. Huang, M. Q. Chen, and H. F. Luo, Chem. Eng. J. **298**, 154–161 (2016).

[94]J. S. Tumuluru, B. Ghiasi, N. R. Soelberg, and S. Sokhansanj, Front. Energy Res. **9**, 728140 (2021).

[95]F. Thevenon, M. Marchand, M. Grateau, H. Demey, A. Chatroux, A. Pons de Vincent, A. De Ryck, and T. Melkior, Biomass Bioenergy **152**, 106196 (2021).

[96]M. B. Nuagah, P. Boakye, S. Oduro-Kwarteng, and Y. A. Sokama-Neuyam, J. Anal. Appl. Pyrolysis **151**, 104903 (2020).

[97]L. Chen, D. Li, Y. Huang, W. Zhu, Y. Ding, and C. Guo, Water Sci. Technol. **82**(2), 255–265 (2020).

[98]C. Freda, G. Cornacchia, A. Romanelli, V. Valerio, and M. Grieco, Fuel **212**, 88–94 (2018).

[99]B. Ranković, A. Sagatova, I. Vujčić, S. Mašić, Đ. Veljović, V. Pavićević, and Ž. Kamberović, Radiat. Phys. Chem. **177**, 109174 (2020).

[100]M. Siwek and T. Edgecock, Environ. Sci. Pollut. Res. **27**(34), 42424–42448 (2020).

[101]*Perry's Chemical Engineers' Handbook*, 7th ed., edited by R. H. Perry, D. W. Green, and J. O. Maloney (McGraw-Hill, New York, 1997).

[102]R. K. Sinnott, *Coulson & Richardson's Chemical Engineering*, 4th ed. (Elsevier Butterworth-Heinemann, Amsterdam Paris, 2005).

[103]*Technologies for Converting Biomass to Useful Energy: Combustion, Gasification, Pyrolysis, Torrefaction and Fermentation*, edited by E. Dahlquist (CRC Press, Boca Raton, FL, 2013).

[104]M. M. Bello, A. A. Abdul Raman, and M. Purushothaman, J. Cleaner Prod. **141**, 1492–1514 (2017).

[105]M. Kim, Y. Lee, J. Park, C. Ryu, and T.-I. Ohm, Waste Manage. **49**, 204–211 (2016).

[106]P. Andrigo, Catal. Today **52**(2–3), 197–221 (1999).

[107]C.-Y. Wen and L. T. Fan, *Models for Flow Systems and Chemical Reactors* (Dekker, New York, 1975).

[108]P. K. Ghodke, A. K. Sharma, J. K. Pandey, W.-H. Chen, A. Patel, and V. Ashokkumar, J. Environ. Manage. **298**, 113450 (2021).

[109]Y. Qiu, Q. Zhang, Z. Wang, B. Gao, Z. Fan, M. Li, H. Hao, X. Wei, and M. Zhong, Sci. Total Environ. **758**, 143584 (2021).

[110]M. Soroush and C. Kravaris, Ind. Eng. Chem. Res. **32**(5), 866–881 (1993).

[111]J. M. Coulson, J. F. Richardson, in *Chemical Engineering. 3: Chemical & Biochemical Reactors & Process Control*, 3rd ed., edited by J. F. Richardson and D. G. Peacock (Butterworth-Heinemann, Oxford, 2009).

[112]J. Labovský, Z. Švandová, J. Markoš, and L. Jelemenský, Chem. Eng. Sci. **62**(18–20), 4915–4919 (2007).

[113]A. U. Rajapaksha, S. S. Chen, D. C. W. Tsang, M. Zhang, M. Vithanage, S. Mandal, B. Gao, N. S. Bolan, and Y. S. Ok, Chemosphere **148**, 276–291 (2016).

[114]X. Tan, Y. Liu, Y. Gu, Y. Xu, G. Zeng, X. Hu, S. Liu, X. Wang, S. Liu, and J. Li, Bioresour. Technol. **212**, 318–333 (2016).

[115]Z. Yu, W. Qiu, F. Wang, M. Lei, D. Wang, and Z. Song, Chemosphere **168**, 341–349 (2017).

[116]W. Wang, Y. Liu, T. Li, and M. Zhou, Chem. Eng. J. **242**, 1–9 (2014).

[117]D. Bao, Z. Li, R. Tang, C. Wan, C. Zhang, X. Tan, and X. Liu, J. Environ. Manage. **284**, 112113 (2021).

[118]J. Wei, Y. Liu, J. Li, Y. Zhu, H. Yu, and Y. Peng, Chemosphere **236**, 124254 (2019).

[119]H. Jin, S. Capareda, Z. Chang, J. Gao, Y. Xu, and J. Zhang, Bioresour. Technol. **169**, 622–629 (2014).

[120]L. Tang, J. Yu, Y. Pang, G. Zeng, Y. Deng, J. Wang, X. Ren, S. Ye, B. Peng, and H. Feng, Chem. Eng. J. **336**, 160–169 (2018).

[121]Y. Xue, B. Gao, Y. Yao, M. Inyang, M. Zhang, A. R. Zimmerman, and K. S. Ro, Chem. Eng. J. **200–202**, 673–680 (2012).

[122]Y. Sun, B. Zeng, Y. Dai, X. Liang, L. Zhang, R. Ahmad, and X. Su, J. Colloid Interface Sci. **614**, 547–555 (2022).

[123]W.-Q. Zuo, C. Chen, H.-J. Cui, and M.-L. Fu, RSC Adv. **7**(26), 16238–16243 (2017).

[124]Q. Lu, Q. Hu, B. Qiu, D. Pan, G. Song, N. Naik, and Z. Guo, Carbon **177**, 151–159 (2021).

[125]Y. Zhang, S. Liang, R. He, R. Zhao, J. Lv, W. Kang, and J. Zhang, J. Water Process Eng. **46**, 102626 (2022).

[126]D. Guo, R. Shibuya, C. Akiba, S. Saji, T. Kondo, and J. Nakamura, Science **351**(6271), 361–365 (2016).

[127]H. Wang, W. Guo, B. Liu, Q. Wu, H. Luo, Q. Zhao, Q. Si, F. Sseguya, and N. Ren, Water Res. **160**, 405–414 (2019).

[128]J. Yu, L. Tang, Y. Pang, G. Zeng, J. Wang, Y. Deng, Y. Liu, H. Feng, S. Chen, and X. Ren, Chem. Eng. J. **364**, 146–159 (2019).

[129]S. Wang and J. Wang, J. Hazard. Mater. **418**, 126309 (2021).

[130]L. Xing, J. Wei, Y. Zhang, M. Xu, G. Pan, J. Li, J. Li, and Y. Li, Sep. Purif. Technol. **294**, 121160 (2022).

[131]X. Duan, S. Indrawirawan, H. Sun, and S. Wang, Catal. Today **249**, 184–191 (2015).

[132]T. Liu, Y. Li, N. Peng, Q. Lang, Y. Xia, C. Gai, Q. Zheng, and Z. Liu, J. Environ. Manage. **197**, 151–158 (2017).

[133]B. Khiari, M. Jeguirim, L. Limousy, and S. Bennici, Renewable Sustainable Energy Rev. **108**, 253–273 (2019).

[134]T. Liu, Y. Guo, N. Peng, Q. Lang, Y. Xia, C. Gai, and Z. Liu, J. Anal. Appl. Pyrolysis **126**, 298–306 (2017).

[135]L. Liu, X. Liu, D. Wang, H. Lin, and L. Huang, J. Cleaner Prod. **257**, 120562 (2020).

[136]Y. Chen, M. Li, Y. Li, Y. Liu, Y. Chen, H. Li, L. Li, F. Xu, H. Jiang, and L. Chen, Bioresour. Technol. **321**, 124413 (2021).

[137]A. Kumar, K. Saini, and T. Bhaskar, Bioresour. Technol. **299**, 122564 (2020).

[138]*Biokohle*, edited by P. Quicker and K. Weber (Springer Fachmedien Wiesbaden, Wiesbaden, 2016).

[139]C. E. Brewer, V. J. Chuang, C. A. Masiello, H. Gonnermann, X. Gao, B. Dugan, L. E. Driver, P. Panzacchi, K. Zygourakis, and C. A. Davies, Biomass Bioenergy **66**, 176–185 (2014).

[140]C. Li, X. Zhu, H. He, Y. Fang, H. Dong, J. Lü, J. Li, and Y. Li, J. Mol. Liq. **274**, 353–361 (2019).

[141]J. Zhang, J. Shao, Q. Jin, X. Zhang, H. Yang, Y. Chen, S. Zhang, and H. Chen, Sci. Total Environ. **716**, 137016 (2020).

[142]A. Méndez, M. Terradillos, and G. Gascó, J. Anal. Appl. Pyrolysis **102**, 124–130 (2013).

[143]K.-Y. Law, J. Phys. Chem. Lett. **5**(4), 686–688 (2014).

[144]J. Lag, A. Hadas, R. W. Fairbridge, J. C. N. Muñoz, X. P. Pombal, in A. M. Cortizas, G. Almendros, W. Chesworth, M. Camps Arbestain, F. Macías, A. M. Cortizas, W. Chesworth, and W. F. Jaynes, in *Encyclopedia of Soil Science*, edited by W. Chesworth (Springer, Netherlands, Dordrecht, 2008), pp. 329–330.

[145]N. A. Qambrani, M. M. Rahman, S. Won, S. Shim, and C. Ra, Renewable Sustainable Energy Rev. **79**, 255–273 (2017).

[146]P. A. Quinlivan, L. Li, and D. R. U. Knappe, Water Res. **39**(8), 1663–1673 (2005).

[147]*Encyclopedia of Soil Science*, edited by W. Chesworth (Springer, Netherlands, Dordrecht, 2008), pp. 822–822.

[148]M. Gray, M. G. Johnson, M. I. Dragila, and M. Kleber, Biomass Bioenergy **61**, 196–205 (2014).

[149]O. Das and A. K. Sarmah, Sci. Total Environ. **512–513**, 682–685 (2015).

[150]X. Jian, X. Zhuang, B. Li, X. Xu, Z. Wei, Y. Song, and E. Jiang, Environ. Technol. Innovation **10**, 27–35 (2018).

[151]S. Shackley, S. Carter, T. Knowles, E. Middelink, S. Haefele, S. Sohi, A. Cross, and S. Haszeldine, Energy Policy **42**, 49–58 (2012).

[152]M. Ahmad, S. S. Lee, X. Dou, D. Mohan, J.-K. Sung, J. E. Yang, and Y. S. Ok, Bioresour. Technol. **118**, 536–544 (2012).

[153]J. W. Lee, M. Kidder, B. R. Evans, S. Paik, A. C. Buchanan III, C. T. Garten, and R. C. Brown, Environ. Sci. Technol. **44**(20), 7970–7974 (2010).

[154]*Standard Soil Methods for Long-Term Ecological Research*, edited by G. P. Robertson (Oxford University Press, New York, 1999).

[155]B. Liang, J. Lehmann, D. Solomon, J. Kinyangi, J. Grossman, B. O'Neill, J. O. Skjemstad, J. Thies, F. J. Luizão, J. Petersen, and E. G. Neves, Soil Sci. Soc. Am. J. **70**(5), 1719–1730 (2006).

[156]C. S. Helling, G. Chesters, and R. B. Corey, Soil Sci. Soc. Am. J. **28**(4), 517–520 (1964).

[157]A. Mukherjee, A. R. Zimmerman, and W. Harris, Geoderma **163**(3–4), 247–255 (2011).

[158]V. Dhyani and T. Bhaskar, Renewable Energy **129**, 695–716 (2018).

[159]X. Wang, Q. Chi, X. Liu, and Y. Wang, Chemosphere **216**, 698–706 (2019).

29 August 2023 15:25:40

[160]T. Chen, Y. Zhang, H. Wang, W. Lu, Z. Zhou, Y. Zhang, and L. Ren, Bioresour. Technol. **164**, 47–54 (2014).

[161]C. Liang, G. Gascó, S. Fu, A. Méndez, and J. Paz-Ferreiro, Soil Tillage Res. **164**, 3–10 (2016).

[162]K. Crombie and O. Mašek, GCB Bioenergy **7**(2), 349–361 (2015).

[163]H. Sun, W. C. Hockaday, C. A. Masiello, and K. Zygourakis, Ind. Eng. Chem. Res. **51**(9), 3587–3597 (2012).

[164]A. Cross and S. P. Sohi, GCB Bioenergy **5**(2), 215–220 (2013).

[165]P. Srinivasan, A. K. Sarmah, R. Smernik, O. Das, M. Farid, and W. Gao, Sci. Total Environ. **512–513**, 495–505 (2015).

[166]N. Indayaningsih, F. Destyorini, R. I. Purawiardi, D. R. Insiyanda, and H. Widodo, J. Phys.: Conf. Ser. **817**(1), 012006 (2017).

[167]K. Yadav and S. Jagadevan, in *Recent Advances in Pyrolysis*, edited by H. Al-Haj Ibrahim (IntechOpen, 2020).

[168]Z. Wan, Y. Sun, D. C. W. Tsang, I. K. M. Yu, J. Fan, J. H. Clark, Y. Zhou, X. Cao, B. Gao, and Y. S. Ok, Green Chem. **21**(17), 4800–4814 (2019).

[169]M. M. Mian, G. Liu, B. Yousaf, B. Fu, R. Ahmed, Q. Abbas, M. A. M. Munir, and L. Ruijia, J. Environ. Sci. **78**, 29–41 (2019).

[170]S. Guo, X. Xiong, D. Che, H. Liu, and B. Sun, Korean J. Chem. Eng. **38**(1), 55–63 (2021).

[171]M. Kończak, B. Pan, Y. S. Ok, and P. Oleszczuk, Sci. Total Environ. **723**, 137796 (2020).

[172]A. E. Burakov, E. V. Galunin, I. V. Burakova, A. E. Kucherova, S. Agarwal, A. G. Tkachev, and V. K. Gupta, Ecotoxicol. Environ. Saf. **148**, 702–712 (2018).

[173]A. Pratush, A. Kumar, and Z. Hu, Int. Microbiol. **21**(3), 97–106 (2018).

[174]P. M. Gore, L. Khurana, R. Dixit, and K. Balasubramanian, J. Environ. Chem. Eng. **5**(6), 5655–5667 (2017).

[175]P. D. Bhalara, D. Punetha, and K. Balasubramanian, Int. J. Environ. Sci. Technol. **12**(10), 3095–3106 (2015).

[176]P. M. Gore, L. Khurana, S. Siddique, A. Panicker, and B. Kandasubramanian, Environ. Sci. Pollut. Res. **25**(4), 3320–3334 (2018).

[177]R. Gonte and K. Balasubramanian, J. Saudi Chem. Soc. **20**, S579–S590 (2016).

[178]S. Sharma and K. Balasubramanian, RSC Adv. **5**(40), 31732–31741 (2015).

[179]M. Khanale and K. Balasubramanian, J. Environ. Chem. Eng. **4**(1), 434–439 (2016).

[180]P. Rule, K. Balasubramanian, and R. R. Gonte, J. Environ. Radioact. **136**, 22–29 (2014).

[181]P. D. Bhalara, D. Punetha, and K. Balasubramanian, J. Environ. Chem. Eng. **2**(3), 1621–1634 (2014).

[182]A. Nighojkar, R. S. Kothale, and B. Kandasubramanian, J. Hazard. Mater. Adv. **9**, 100210 (2023).

[183]R. B. Amal Raj, R. R. Gonte, and K. Balasubramanian, in *Enhancing Cleanup of Environmental Pollutants*, edited by N. A. Anjum, S. S. Gill, and N. Tuteja (Springer International Publishing, Cham, 2017), pp. 255–295.

[184]A. Subash, M. Naebe, X. Wang, and B. Kandasubramanian, Environ. Sci. **2**(3), 368–396 (2023).

[185]V. U. Kavitha and B. Kandasubramanian, SN Appl. Sci. **2**(6), 1081 (2020).

[186]Y. A. Ghodke, N. Mayilswamy, and B. Kandasubramanian, "Polyamide (PA)- and Polyimide (PI)-based membranes for desalination application," Polym. Bull. (published online).

[187]R. R. Gonte, K. Balasubramanian, and J. D. Mumbrekar, J. Polym. **2013**, 309136.

[188]N. S. Nitesh Singh and K. Balasubramanian, RSC Adv. **4**(53), 27691–27701 (2014).

[189]A. Nighojkar, K. Zimmermann, M. Ateia, B. Barbeau, M. Mohseni, S. Krishnamurthy, F. Dixit, and B. Kandasubramanian, Environ. Sci. **2**, 11–38 (2023).

[190]S. Rastogi and B. Kandasubramanian, Environ. Sci. Pollut. Res. **27**(1), 210–237 (2020).

[191]L. Khurana and K. Balasubramanian, J. Environ. Chem. Eng. **4**(2), 2147–2154 (2016).

[192]S. Sharma, K. Balasubramanian, and R. Arora, Desalin. Water Treat. **57**(20), 9420–9436 (2016).

[193]P. Gore, M. Khraisheh, and B. Kandasubramanian, Environ. Sci. Pollut. Res. **25**(12), 11729–11745 (2018).

[194]A. Subash, M. Naebe, X. Wang, and B. Kandasubramanian, J. Hazard. Mater. **443**, 130168 (2023).

[195]S. Gupta, A. Nighojkar, N. Mayilswamy, and B. Kandasubramanian, J. Polym. Environ. **31**(6), 2243–2272 (2023).

[196]N. Mayilswamy and B. Kandasubramanian, Emergent Mater. **5**(3), 727–753 (2022).

[197]Y. Zhang, O. K. Abass, J. Qin, and Y. Yi, Chemosphere **290**, 133298 (2022).

[198]B. Zhao, X. Xu, F. Zeng, H. Li, and X. Chen, Environ. Sci. Pollut. Res. **25**(20), 19423–19435 (2018).

[199]M. Dudziak, S. Werle, A. Marszałek, S. Sobek, and A. Magdziarz, Energy **261**, 125360 (2022).

[200]R.-N. Mourgela, P. Regkouzas, F.-M. Pellera, and E. Diamadopoulos, Water, Air, Soil Pollut. **231**(5), 206 (2020).

[201]X. Tan, Y. Liu, G. Zeng, X. Wang, X. Hu, Y. Gu, and Z. Yang, Chemosphere **125**, 70–85 (2015).

[202]A. Zhang, X. Li, J. Xing, and G. Xu, J. Environ. Chem. Eng. **8**(4), 104196 (2020).

[203]T. Koottatep, K. Fakkaew, N. Tajai, and C. Polprasert, J. Water, Sanit. Hyg. Dev. **7**(1), 102–110 (2017).

[204]W. Ding, W. Peng, X. Zeng, and X. Tian, Front. Environ. Sci. Eng. **8**(3), 379–385 (2014).

[205]Y. Tong, P. J. McNamara, and B. K. Mayer, Environ. Sci. **5**(5), 821–838 (2019).

[206]G. W. Kajjumba, S. Emik, A. Öngen, H. Kurtulus Özcan, and S. Aydın, in *Advanced Sorption Process Applications*, edited by S. Edebali (IntechOpen, 2019).

[207]Y. Zhou, X. Liu, Y. Xiang, P. Wang, J. Zhang, F. Zhang, J. Wei, L. Luo, M. Lei, and L. Tang, Bioresour. Technol. **245**, 266–273 (2017).

[208]I. Ali, Z. A. Alothman, and A. Alwarthan, J. Mol. Liq. **236**, 205–213 (2017).

[209]G. K. Rajahmundry, C. Garlapati, P. S. Kumar, R. S. Alwi, and D.-V. N. Vo, Chemosphere **276**, 130176 (2021).

[210]J. Ma, B. Zhou, H. Zhang, W. Zhang, and Z. Wang, Chem. Eng. Res. Des. **149**, 209–219 (2019).

[211]Q. Hu and Z. Zhang, J. Mol. Liquids **277**, 646–648 (2019).

[212]M. A. Al-Ghouti and D. A. Da'ana, J. Hazard. Mater. **393**, 122383 (2020).

[213]K. Luo, Q. Yang, Y. Pang, D. Wang, X. Li, M. Lei, and Q. Huang, Chem. Eng. J. **374**, 520–530 (2019).

[214]C.-M. Hung, C.-W. Chen, C.-P. Huang, M.-L. Tsai, C.-H. Wu, Y.-L. Lin, Y.-R. Cheng, and C.-D. Dong, J. Hazard. Mater. **422**, 126922 (2022).

[215]Y.-F. Huang, Y.-Y. Huang, P.-T. Chiueh, and S.-L. Lo, Chemosphere **249**, 126139 (2020).

[216]M. M. Mian, G. Liu, B. Fu, and Y. Song, Appl. Catal., B **255**, 117765 (2019).

[217]M. M. Mian, G. Liu, and H. Zhou, Sci. Total Environ. **744**, 140862 (2020).

[218]B.-C. Huang, J. Jiang, G.-X. Huang, and H.-Q. Yu, J. Mater. Chem. A **6**(19), 8978–8985 (2018).

[219]T. Zang, H. Wang, Y. Liu, L. Dai, S. Zhou, and S. Ai, Chemosphere **261**, 127616 (2020).

[220]D. M. Mitrano and W. Wohlleben, Nat. Commun. **11**(1), 5324 (2020).

[221]M. R. Hossain, M. Jiang, Q. Wei, and L. G. Leff, J. Basic Microbiol. **59**(1), 54–61 (2019).

[222]M. N. Issac and B. Kandasubramanian, Environ. Sci. Pollut. Res. **28**(16), 19544–19562 (2021).

[223]Z. Zhang and Y. Chen, Chem. Eng. J. **382**, 122955 (2020).

[224]M. K. Nguyen, C. Lin, N. T. Q. Hung, D.-V. N. Vo, K. N. Nguyen, B. T. P. Thuy, H. G. Hoang, and H. T. Tran, Sci. Total Environ. **844**, 157066 (2022).

[225]C. Rolsky, V. Kelkar, E. Driver, and R. U. Halden, Curr. Opin. Environ. Sci. Health **14**, 16–22 (2020).

[226]H. Gao, C. Yan, Q. Liu, W. Ding, B. Chen, and Z. Li, Sci. Total Environ. **651**, 484–492 (2019).

[227]Y. Chae and Y.-J. An, Mar. Pollut. Bull. **124**(2), 624–632 (2017).

[228]W. Liu, J. Zhang, H. Liu, X. Guo, X. Zhang, X. Yao, Z. Cao, and T. Zhang, Environ. Int. **146**, 106277 (2021).

[229]Z. Fu, G. Chen, W. Wang, and J. Wang, Environ. Pollut. **266**, 115098 (2020).

[230]H. Tuan Tran, C. Lin, X.-T. Bui, M. Ky Nguyen, N. Dan Thanh Cao, H. Mukhtar, H. Giang Hoang, S. Varjani, H. Hao Ngo, and L. D. Nghiem, Bioresour. Technol. **344**, 126249 (2022).

[231]S. L. Wright and F. J. Kelly, Environ. Sci. Technol. **51**(12), 6634–6647 (2017).

29 August 2023 15:25:40

[232]M. Kedzierski, M. D'Almeida, A. Magueresse, A. Le Grand, H. Duval, G. César, O. Sire, S. Bruzaud, and V. Le Tilly, Mar. Pollut. Bull. **127**, 684–694 (2018).

[233]A. Massos and A. Turner, Environ. Pollut. **227**, 139–145 (2017).

[234]X. Liu, W. Yuan, M. Di, Z. Li, and J. Wang, Chem. Eng. J. **362**, 176–182 (2019).

[235]P. U. Iyare, S. K. Ouki, and T. Bond, Environ. Sci. **6**(10), 2664–2675 (2020).

[236]A. M. Mahon, B. O'Connell, M. G. Healy, I. O'Connor, R. Officer, R. Nash, and L. Morrison, Environ. Sci. Technol. **51**(2), 810–818 (2017).

[237]W. H. Abuwatfa, D. Al-Muqbel, A. Al-Othman, N. Halalsheh, and M. Tawalbeh, Case Stud. Chem. Environ. Eng. **4**, 100151 (2021).

[238]J. Wang, C. Sun, Q.-X. Huang, Y. Chi, and J.-H. Yan, J. Hazard. Mater. **419**, 126486 (2021).

[239]Y. Ma, M. Li, P. Li, L. Yang, L. Wu, F. Gao, X. Qi, and Z. Zhang, Bioresour. Technol. **319**, 124199 (2021).

[240]I. Fonts, G. Gea, M. Azuara, J. Ábrego, and J. Arauzo, Renewable Sustainable Energy Rev. **16**(5), 2781–2805 (2012).

[241]F. R. Amin, Y. Huang, Y. He, R. Zhang, G. Liu, and C. Chen, Clean Technol. Environ. Policy **18**(5), 1457–1473 (2016).

[242]Z. Chen, B. Chen, D. Zhou, and W. Chen, Environ. Sci. Technol. **46**(22), 12476–12483 (2012).

[243]Z. Chen, B. Chen, and C. T. Chiou, Environ. Sci. Technol. **46**(20), 11104–11111 (2012).

[244]R. Zhou, M. Zhang, and S. Shao, Sci. Rep. **12**(1), 13662 (2022).

[245]H. Bamdad, K. Hawboldt, S. MacQuarrie, and S. Papari, Environ. Sci. Pollut. Res. **26**(11), 10902–10915 (2019).

[246]X. Xu, X. Cao, L. Zhao, and T. Sun, Chemosphere **111**, 296–303 (2014).

[247]K. Li, X. Niu, D. Zhang, H. Guo, X. Zhu, H. Yin, Z. Lin, and M. Fu, Environ. Pollut. **306**, 119399 (2022).

[248]F. Dixit, K. Zimmermann, M. Alamoudi, L. Abkar, B. Barbeau, M. Mohseni, B. Kandasubramanian, and K. Smith, Renewable Sustainable Energy Rev. **164**, 112527 (2022).

[249]L. Lu, J. S. Guest, C. A. Peters, X. Zhu, G. H. Rau, and Z. J. Ren, Nat. Sustainability **1**(12), 750–758 (2018).

[250]K. Li, D. Zhang, X. Niu, H. Guo, Y. Yu, Z. Tang, Z. Lin, and M. Fu, Sci. Total Environ. **826**, 154133 (2022).

[251]Y.-C. Chiang and R.-S. Juang, J. Taiwan Inst. Chem. Eng. **71**, 214–234 (2017).

[252]Y. Liu, L. Lonappan, S. K. Brar, and S. Yang, Sci. Total Environ. **645**, 60–70 (2018).

[253]Y. Sun, B. Gao, Y. Yao, J. Fang, M. Zhang, Y. Zhou, H. Chen, and L. Yang, Chem. Eng. J. **240**, 574–578 (2014).

[254]X. Fu, K. Huang, X. Chen, F. Li, and G. Cui, Bioresour. Technol. **175**, 646–650 (2015).

[255]V. K. Garg, S. Suthar, and A. Yadav, Bioresour. Technol. **126**, 437–443 (2012).

[256]C. S. Liew, N. M. Yunus, B. S. Chidi, M. K. Lam, P. S. Goh, M. Mohamad, J. C. Sin, S. M. Lam, J. W. Lim, and S. S. Lam, J. Hazard. Mater. **423**, 126995 (2022).

[257]K. Malińska, M. Zabochnicka-Świątek, R. Cáceres, and O. Marfà, Ecol. Eng. **90**, 35–41 (2016).

[258]K. Malińska, M. Golańska, R. Caceres, A. Rorat, P. Weisser, and E. Ślęzak, Bioresour. Technol. **225**, 206–214 (2017).

[259]J. Lehmann, M. C. Rillig, J. Thies, C. A. Masiello, W. C. Hockaday, and D. Crowley, Soil Biol. Biochem. **43**(9), 1812–1836 (2011).

[260]T. T. Doan, C. Bouvier, Y. Bettarel, T. Bouvier, T. Henry-des-Tureaux, J. L. Janeau, P. Lamballe, B. V. Nguyen, and P. Jouquet, Appl. Soil Ecol. **73**, 78–86 (2014).

[261]I. M. Lubbers, K. J. Van Groenigen, S. J. Fonte, J. Six, L. Brussaard, and J. W. Van Groenigen, Nat. Clim. Change **3**(3), 187–194 (2013).

[262]N. Akdeniz, Waste Manage. **88**, 291–300 (2019).

[263]H. Lu, W. Zhang, Y. Yang, X. Huang, S. Wang, and R. Qiu, Water Res. **46**(3), 854–862 (2012).

[264]X. Zhang, H. Wang, L. He, K. Lu, A. Sarmah, J. Li, N. S. Bolan, J. Pei, and H. Huang, Environ. Sci. Pollut. Res. **20**(12), 8472–8483 (2013).

[265]A. T. C. Sousa and C. C. Figueiredo, Biol. Agric. Hortic. **32**(2), 127–138 (2016).

[266]S. Kuppusamy, P. Thavamani, M. Megharaj, K. Venkateswarlu, and R. Naidu, Environ. Int. **87**, 1–12 (2016).

[267]S. Mehmood, W. Ahmed, J. M. Alatalo, M. Mahmood, M. Imtiaz, A. Ditta, E. F. Ali, H. Abdelrahman, M. Slaný, V. Antoniadis, J. Rinklebe, S. M. Shaheen, and W. Li, Sci. Total Environ. **826**, 154043 (2022).

[268]M. Camps Arbestain, S. Saggar, and J. Leifeld, Agric., Ecosyst. Environ. **191**, 1–4 (2014).

[269]Z. Elkhlifi, M. Kamran, A. Maqbool, A. El-Naggar, J. Ifthikar, A. Parveen, S. Bashir, M. Rizwan, A. Mustafa, S. Irshad, S. Ali, and Z. Chen, Ecotoxicol. Environ. Safety **216**, 112173 (2021).

[270]M. L. Cayuela, L. Van Zwieten, B. P. Singh, S. Jeffery, A. Roig, and M. A. Sánchez-Monedero, Agric., Ecosyst. Environ. **191**, 5–16 (2014).

[271]G. Chen, X. Wang, and R. Zhang, Soil Tillage Res. **186**, 322–332 (2019).

[272]B. P. Singh, A. L. Cowie, and R. J. Smernik, Environ. Sci. Technol. **46**(21), 11770–11778 (2012).

[273]X. Luo, M. Shen, J. Liu, Y. Ma, B. Gong, H. Liu, and Z. Huang, J. Cleaner Prod. **294**, 126372 (2021).

[274]N. Hossain, M. A. Bhuiyan, B. K. Pramanik, S. Nizamuddin, and G. Griffin, J. Cleaner Prod. **255**, 120261 (2020).

[275]J. Pan, B. Gao, P. Duan, K. Guo, X. Xu, and Q. Yue, J. Hazard. Mater. **413**, 125413 (2021).

[276]Q. Li, X.-Y. Guo, X.-H. Xu, Y.-B. Zuo, D.-P. Wei, and Y.-B. Ma, Pedosphere **22**(2), 254–262 (2012).

[277]M. Waqas, S. Khan, H. Qing, B. J. Reid, and C. Chao, Chemosphere **105**, 53–61 (2014).

[278]S. M. Ndirangu, Y. Liu, K. Xu, and S. Song, J. Chem. **2019**, 4506314.

[279]M. E. Lee, P. Jeon, J.-G. Kim, and K. Baek, Korean J. Chem. Eng. **35**(7), 1409–1413 (2018).

[280]M.-H. Lee, Y. S. Ok, and J. Hur, Environ. Pollut. **242**, 1912–1920 (2018).

[281]C. vom Eyser, K. Palmu, T. C. Schmidt, and J. Tuerk, Sci. Total Environ. **537**, 180–186 (2015).

[282]M. Wang, Y. Zhu, L. Cheng, B. Anderson, X. Zhao, D. Wang, and A. Ding, J. Environ. Sci. **63**, 156–173 (2018).

[283]S. Gul, J. K. Whalen, B. W. Thomas, V. Sachdeva, and H. Deng, Agric., Ecosyst. Environ. **206**, 46–59 (2015).

[284]X. Xu, Y. Zhao, J. Sima, L. Zhao, O. Mašek, and X. Cao, Bioresour. Technol. **241**, 887–899 (2017).

[285]A. Zielińska and P. Oleszczuk, Biomass Bioenergy **75**, 235–244 (2015).

29 August 2023 15:25:40